



8th International Conference on Recent Challenges
in Engineering and Technology
(ICRCET-19)

Bangalore, Karnataka
09th - 10th August 2019

Institute For Engineering Research and Publication (IFERP)

www.iferp.in

Publisher: IFERP Explore

©Copyright 2019, IFERP-International Conference, Bangalore, Karnataka

No part of this book can be reproduced in any form or by any means without prior written
Permission of the publisher.

This edition can be exported from India only by publisher

IFERP-Explore

PREFACE

We cordially invite you to attend the ***International Conference on Recent Challenges in Engineering and Technology (ICRCET-19)*** which will be held at ***Springs Hotel, Bangalore, India*** on ***August 09th-10th, 2019***. The main objective of ***ICRCET-19*** is to provide a platform for researchers, engineers, academicians as well as industrial professionals from all over the world to present their research results and development activities in relevant fields of Engineering and Technology. This conference will provide opportunities for the delegates to exchange new ideas and experience face to face, to establish business or research relationship and to find global partners for future collaboration.

These proceedings collect the up-to-date, comprehensive and worldwide state-of-art knowledge on cutting edge development of academia as well as industries. All accepted papers were subjected to strict peer-reviewing by a panel of expert referees. The papers have been selected for these proceedings because of their quality and the relevance to the conference. We hope these proceedings will not only provide the readers a broad overview of the latest research results but also will provide the readers a valuable summary and reference in these fields.

The conference is supported by many universities, research institutes and colleges. Many professors played an important role in the successful holding of the conference, so we would like to take this opportunity to express our sincere gratitude and highest respects to them. They have worked very hard in reviewing papers and making valuable suggestions for the authors to improve their work. We also would like to express our gratitude to the external reviewers, for providing extra help in the review process, and to the authors for contributing their research result to the conference.

Since May 2019, the Organizing Committees have received more than 62 manuscript papers, and the papers cover all the aspects in Engineering and Technology. Finally, after review, about 17 papers were included to the proceedings of ***ICRCET-19***

We would like to extend our appreciation to all participants in the conference for their great contribution to the success of ***ICRCET-19*** We would like to thank the keynote and individual speakers and all participating authors for their hard work and time. We also sincerely appreciate the work by the technical program committee and all reviewers, whose contributions made this conference possible. We would like to extend our thanks to all the referees for their constructive comments on all papers; especially, we would like to thank to organizing committee for their hard work.

Acknowledgement

IFERP is hosting the ***International Conference on Recent Challenges in Engineering and Technology (ICRCET-19)*** this year in month of August. The main objective of ICRCET is to grant the amazing opportunity to learn about groundbreaking developments in modern industry, talk through difficult workplace scenarios with peers who experience the same pain points, and experience enormous growth and development as a professional. There will be no shortage of continuous networking opportunities and informational sessions. The sessions serve as an excellent opportunity to soak up information from widely respected experts. Connecting with fellow professionals and sharing the success stories of your firm is an excellent way to build relations and become known as a thought leader.

I express my hearty gratitude to all my Colleagues, staffs, Professors, reviewers and members of organizing committee for their hearty and dedicated support to make this conference successful. I am also thankful to all our delegates for their pain staking effort to travel such a long distance to attain this conference.



Ankit Rath
Chief Scientific Officer
Institute for Engineering Research and Publication (IFERP)



044-42918383



Email: info@iferp.in
www.iferp.in



Girija Towers, Arumbakkam, Chennai - 600106

Keynote Speaker



Dr. V Pushparajesh,

Associate Professor,
Jain University School of Engineering & Technology,
Bengaluru, Karnataka.

I am delighted to be a part of “International Conference on Recent Challenges in Engineering and Technology (ICRCET-2019)” and to interact with enthusiastic scientists and technologists gathering at Bangalore, Karnataka from August 09th -10th, 2019.

The present-day world is the result of pursuits for novel scientific and technical innovations by the intellectual scientific societies. Burgeoning research has resulted in remarkably enhanced and comfortable human life. However, the urbanization, industrial developments and other anthropogenic activities have resulted in the environmental catastrophe. In spite of breakthrough inventions in engineering and technology, we are facing numerous challenges like climate change, global warming, carbon emission, rising sea level and the environmental deterioration.

New scientific ideas and innovative technology can only help us to cope up with such challenges. The need of hour is that, the contemporary scientist and technologists should find solutions to these problems by continuous progressive efforts, dedication and determination. The interdisciplinary approach combining engineering sciences, basic sciences and social sciences seems to be much effective to address these problems by integrating different novel ideas and technologies.

Further, for the success of new findings and novel technologies, the concerted efforts and trials are needed at global level. This conference is an appropriate platform that can provide an arena to achieve such feats by giving the chance to scientist and technologists to interact, plan and to move together even working at different places.

I hope researchers from different fields will learn from each other and discuss their issues well. I express heartily thanks to organizing committee and wish for the great successful, fruitful and joyous ICRCET-19.

ICRCET-19

International Conference on Recent Challenges in Engineering and Technology

Bangalore, Karnataka, August 09th - 10th, 2019

Organizing Committee

DR.SUDARSHAN RAO K

Professor and HOD
Mechanical Engineering
Shri Madhwa Vadiraja Institute of Technology & Management
Udupi, Karnataka

DR. SHEKHAPPA G. ANKALIKI

Professor and HOD
Electrical and Electronics Engineering
SDM College of Engineering and Technology
Dharwad, Karnataka

DR. BALAKRISHNAN. S

Professor
Computer Science Engineering
Sri Krishna College of Engineering and Technology
Coimbatore, Tamilnadu

DR. NAGAVENI V

Professor
Computer Science Engineering
Acharya Institute of Technology
Bangalore, Karnataka

DR. R. SRINIVASAN

Professor Emeritus
Computer Science Engineering
SRM Institute of Science and Technology
Chennai, Tamilnadu

DR. CHANDRASHEKHAR BHAT

Professor and HOD
Mechanical Engineering
Manipal Institute of Technology
Manipal, Karnataka

DR. U.S.MALLIK

Professor
Mechanical Engineering
Siddaganga Institute of Technology
Tumkur, Karnataka

SHARANABASAPPA C.SAJJAN

Professor and HOD
Mechanical Engineering
K. L. E. Institute of Technology
Hubli, Karnataka

DR. SATHYASHANKARA SHARMA

Professor and HOD
Industrial and Production Engineering
Manipal Institute of Technology
Manipal, Karnataka

DR.ANIL KUMAR. S HAGARGI

Faculty of management
Department of Management Studies and Research
Gulbarga University
Kalburagi, Karnataka

DR. RAJU. B.S

Professor
Mechanical Engineering
REVA University
Bangalore, Karnataka

DR.MANJUNATHA.L.H

Professor
Mechanical Engineering
REVA University
Bangalore, Karnataka

PROF. BALAJI.V

Head of Department
Mechanical Engineering
Sri Sairam College of Engineering
Bangalore, Karnataka

MALINI K V

Professor and HOD
Electrical and Electronics Engineering
Sri Sairam College of Engineering
Bangalore, Karnataka

CONTENTS

SL.NO	TITLES AND AUTHORS	PAGE NO
1.	A Trusted Key Management Protocol (TKMP) For Cluster Based Wireless Networks <ul style="list-style-type: none"> ➤ <i>Jayaprakash R</i> ➤ <i>Radha Balasubramanian</i> 	1 - 6
2.	Design and Implementation of a Low Cost, High Speed, High quality Talking Keyboard for Blind Students <ul style="list-style-type: none"> ➤ <i>K.V.B.Chandrasekhar rao</i> ➤ <i>Yamani.Kotipalli</i> 	7 - 9
3.	Fluidity characteristics of LM6/graphite particulate composite <ul style="list-style-type: none"> ➤ <i>Sharath Kumar R</i> ➤ <i>Dr Sarada B.N</i> ➤ <i>Dr P. L. Srinivasa Murthy</i> ➤ <i>Abhishek</i> 	10 - 16
4.	Power and Performance Analysis Using Multibit Technology <ul style="list-style-type: none"> ➤ <i>Manjunatha Visweswaraiiah</i> ➤ <i>Dr Somashekar K</i> 	17 - 22
5.	Experimental Investigation on Glass Textile Reinforced Mortar Panels <ul style="list-style-type: none"> ➤ <i>Vybhav G V</i> ➤ <i>Dr. Putte Gowda B S</i> ➤ <i>Dr. Vathsala</i> 	23 - 27
6.	A Review on H-Mining-(High Utility Itemsets of Mining) <ul style="list-style-type: none"> ➤ <i>Hare Ram Singh</i> ➤ <i>Dr.Sheo Kumar</i> 	28 - 34
7.	Camera Model Identification <ul style="list-style-type: none"> ➤ <i>Kinjal Patel</i> ➤ <i>Prof.Hetal Gaudani</i> 	35 - 39
8.	The Association between Uterine Electrical Activity and Labor Progress: A Systematic Review <ul style="list-style-type: none"> ➤ <i>Santosh N Vasist</i> ➤ <i>Dr. Parvati Bhat</i> ➤ <i>Dr. Shrutin Ulman</i> ➤ <i>Dr. Harishchandra Hebbar</i> 	40 - 44
9.	A Review on Rate of Heat Transfer in Double Pipe Heat Exchanger Using Fins on Internal Tube Surface <ul style="list-style-type: none"> ➤ <i>Syed Sameer</i> ➤ <i>Dr. SB Prakash</i> ➤ <i>Robinson P</i> 	45 - 48

CONTENTS

SL.NO	TITLES AND AUTHORS	PAGE NO
10.	Aerodynamic Analysis of Wings with Flexible Flaps ➤ <i>Shreya Giri</i> ➤ <i>Suresh P</i> ➤ <i>Vinutha G</i>	49 - 53
11.	Conveyor Interlocking with Equipment, Data Acquisition and Automated Process Control System using RFID and IoT for Axle Assembly Line ➤ <i>Mamatha M</i> ➤ <i>Halesh M. R</i>	54 - 59
12.	Election Canvassing Notification and Candidate Details System Using Web and Mobile App ➤ <i>Devamani N D</i> ➤ <i>Nandini Prasad K. S</i> ➤ <i>Paritosh Tripathi</i>	60 - 63
13.	Fluid Dynamics Simulation of a Heat Sink Made of Al-20Cu Composite Alloy ➤ <i>Mr. Praveen kumar.M.R</i> ➤ <i>Dr.S.Vidyashankar</i> ➤ <i>Dr.Shivappa.D</i> ➤ <i>Dr. Smitha K</i>	64 - 69
14.	Cfd Analysis of Al-30Cu Heat Sink at Different Fluid Velocitiee ➤ <i>Mr. Praveen kumar.M.R</i> ➤ <i>Dr.S.Vidyashankar</i> ➤ <i>Dr.Shivappa.D</i> ➤ <i>Dr. Smitha K</i>	70 - 75
15.	Optimal and Computationally Efficient Priority-Based Routing and Wavelength Allocation Strategy Supporting QoS for High-Speed Transport Networks ➤ <i>Tarun Gupta</i> ➤ <i>Amit Kumar Garg</i>	76 - 80
16.	Real Time Communication between Nodes using LoRaWAN for emergency alert in Elevator ➤ <i>Anupriya</i> ➤ <i>Dr. C Rama Krishna</i> ➤ <i>Ajay Kumar</i>	81
17.	Effect of Exhaust Gas Recirculation on combustion and emission characteristics of direct injection -diesel engine fueled with biodiesel: A review ➤ <i>S.Asha</i> ➤ <i>T.suresh</i>	82

A Trusted Key Management Protocol (TKMP) For Cluster Based Wireless Networks

^[1]Jayaprakash R, ^[2]Radha Balasubramanian

^[1] Assistant Professor in NGM College & Ph. D Research Scholar in STC , Coimbatore, India.

^[2] Assistant Professor, Department of IT, SKASC, Coimbatore, India.

Abstract:-- One of the protected communication techniques in cluster based privacy preserving MANET is providing a Trusted Key Management Protocol (TKMP). A TKMP calculates a trust key exchanging for all the cluster nodes in the communication for security. TKMP allocates a dynamic private and public key exchanging value for trust variable where it will be checked during communications. The total proposed protocol is executed in three stages, for example, Initial-sending, key creation and validation of key and affirmation. In the primary stage, the cluster nodes are offered with the unique identity (ID), and after that, the following stage utilizes the Paillier cryptosystem (PC) holomorphic encryption model, for making the basic key to the message correspondence. Finally, a geometrical model is created in this work with various variables, for example, a hashing capacity, holomorphic encryption, profile succession, irregular number capacities. The proposed TKMP strategy sets up the verified correspondence over the WSN by the authentication process.

Index Terms: Cluster Network, Secured Communication, Key development, Key Validation, Homomorphism Encryption.

1. INTRODUCTION

The Mobile Adhoc Network is a division of Wireless Sensor Network but MANET is ad-hoc in nature. Every node can be initialized, formed, stimulated, disabled and become dead at all time anywhere in the network. In case of MANET which is dynamic and based on the concept of clustering, the functions of the node are not only acting as terminals end and also as a router in-between. Data packets sent by an origin node can attain to a target node through an amount of hops i.e. more than single node capacity be concerned in forwarding messages from origins to targets. MANET succeeds to exclusive privacy preserving properties such as random and dynamic network topology, random mobility and less wireless relations. These properties carry several considerable technical challenges of Quality of Service (QoS) control, routing and security. A hand full of research has been done for the development of the Quality of Service and for the privacy preserving inside the clusters in a MANET. For the security of a cluster to be affordable, all the MANET need to acquire a security necessities in line with the accessibility provision, preserved privacy, truth, a valid verification and the non-redundant[3] .

The cluster based models for the security in case of a MANET are then suffering from various kind of security breaches that can be approached from the external nodes that are malicious and also compromised MANET nodes.[3,4]. For the protection of routing kind of information, the packets are then coded using a particular

key technique [5-7]. The secure cluster based routing protocol had been compatible with some additional reactive routing based protocols was establish to be protected to the attacks that could interrupt the procedure to route discovery. This allows the identification of routes based hotspot for evacuation the deceptive reacts and such secure directing conventions will depend totally on the security relationship among the starting point and the objective hub. The security relationship may likewise be made by assets of utilizing a portion of a blend key that has been founded on that of the open keys of a root hub (O) and furthermore an objective hub (T). The O and the T will utilize a mystery symmetric key which is the (KeyO ,T) that utilizes the open keys of one another.

In the paper, we developed a novel secure routing key management scheme based on Trusted Key Management Protocol(TKMP) is authenticating the public and private key encryption and decryption algorithm is used in protecting the packets or messages from attackers in this phase. In the next section, recent studies for public key development methods are presented and concepts are given. In section 3, our proposed TKMP model is presented where a new trust key model is introduced and verification processes are described. Finally, conclusion remarks are given in the last section.

II. BACKGORUND STUDY

(Azarderakhsh, Reza, ArashReyhani-Masoleh, and Zine-EddineAbid, 2008)[8] stated that the key management in cluster-based wireless sensor networks using both private and public key cryptography. Their objective is to

introduce a platform in which public key cryptography is used to create a secure path among sensor nodes and gateways. Instead of pre-loading a huge amount of keys into the sensor nodes, every node desires a session key from the gateway to set up a secure path with its neighbors after clustering phase. The security examination and performance evaluation showed that the key management method has considerable saving in storage space, broadcast overhead, and perfect resilience against node capture.

(Udaya, D., Suriya Rajkumar, and Rajamani Vayanaperumal, 2013)[9] Examined a security is one of a significant factor to be viewed as truly in remote sensor systems. In WSN, from multiple points of view interruption may happen, in the history decades there is no ideal IDS, with no squandering of assets like time, vitality, cost and number of physical things. The principle target is to guarantee the security and improve the nature of system by applying a Leader based interruption identification framework in the Wireless Sensor Network (WSN). Here, we are concentrating on the assault known as sinkhole assault which is considered as the greatest risk in remote sensor organize which crown jewels the total correspondence and an information misfortune between a couple of hubs as source hub and a goal hub. So as to give a total answer for identify and dodge sinkhole assault a Leader Based Intrusion Detection System (LBIDS) is proposed. Their methodology a pioneer is chosen for each gathering hubs inside the system, area savvy and it do looks at and figures the conduct of every hub, intelligently executes our identification module and screens every hub conduct inside the bunch for any sinkhole assault to happen.

(Xun Yi, Russell Paulet, Elisa Bertino, 2014) [10] Considered the issue that includes executing an encoded focused on commercial framework that creates ads relying upon the substance of a client's email. Since the email is put away in an encoded structure with the client's open key, the email server plays out a homomorphic assessment and processes a scrambled notice to be sent back to the client. The client unscrambles it, plays out an activity relying upon what she sees. On the off chance that the commercial is significant, she may tap on it; else, she just disposes of it. Be that as it may, if the email server knows to this data, to be specific whether the client tapped on the ad or not, it can utilize this as a confined unscrambling prophet to break the security of the client's encryption plan and conceivably considerably recoup her mystery key. Such assaults are omnipresent at whatever point we figure on encoded information, nearly to the point that CCA

security appears to be inescapable. However, it is anything but difficult to see that picked ciphertext (CCA2-secure) homomorphic encryption plans can't exist. In this way, a suitable security definition and developments that accomplish the definition is sought after.

(Q. Jiang, S. Zeadally, J. Ma and D. He, 2017) [11] introduced a lightweight and secure client verification convention dependent on the Rabin cryptosystem, which has the highlights of computational asymmetry. They led a perceived affirmation of the convention utilizing ProVerif so as to display that the strategy finishes the vital security properties. The creators introduced a total heuristic security examination to demonstrate that the convention is secure next to all the potential assaults and gives the ideal security highlights.

(Razaque, Abdul, and Syed S. Rizvi, 2017) [12] expressed that the past secure information collection approaches for remote sensor systems were not proposed for consent, vitality productivity and proper security, leaving them inclined to assaults. The creators presented the protected information accumulation utilizing the entrance control and validation (SDAACA) convention. Utilizing SDAACA convention to see sinkhole and Sybil assaults that are hard to distinguish by existing cryptographic methodologies. The SDAACA convention comprises of two novel calculations: the protected information fracture (SDF) and the hub blend approval (NJA). The SDF calculation secretes the information from the foe by dividing it into little pieces. In the NJA calculation, an approval procedure is started previously enabling any new hub to join the system. The two calculations help improve the Quality of Service (QoS) parameters

(Jaewoo Choi, Jihyun Bang, LeeHyung Kim, MirimAhn, and Taekyoung Kwon, 2017) [13] proposed an area based key administration plot for WSNs, with uncommon thought of insider dangers. In the wake of surveying past area based key administration strategies and examining their benefits and negative marks, they chose area ward key administration (LDK) as an appropriate technique for their investigation. To unravel a correspondence impedance issue in LDK and comparable strategies, they have concocted another key update process that consolidates matrix based area data. They likewise proposed a key foundation procedure utilizing network data. Besides, they developed key update and denial procedures to adequately oppose inside aggressors. For examination, led a thorough reenactment and affirmed that their method can intensify network

while diminishing the trade off proportion when the base number of normal keys required for key foundation is high.

(Ahlawat, Priyanka, and Mayank Dave, 2018) [14] Talked about to diminish the hub catch crash by consolidating a productive antagonistic model for cell model of WSN. The antagonistic model builds up various vulnerabilities introduced in the system, for example, raised hub thickness, task of the sink hub, neighbor weight factor to ascertain the arrangement likelihood of every cell. It at that point depicts the hash chain length for each cell with different rekey period to intensify the system obstruction against hub catch assault. Their technique is contrasted and different past strategies regarding the probability of key trade off and the measure of ways rekeyed. The results affirm its viability in expanding the WSN security.

III. TRUSTED KEY MANAGEMENT PROTOCOL (TKMP)

The proposed TKMP significant goal is to structure and build up a dynamic key administration based protocol dependent on normal and staggered verification in Clusters. The proposed convention includes three units, for example, Cluster Head (CH), Cluster Member (CM), and base station (BS) for the key organization in the system. The general arrangement of the proposed TKMP incorporates the accompanying three stages, for example, Initial-sending, key creation, and key approval and validation. In the primary stage, the bunch part hubs in the system are given the one of a kind personality, and in the key creation stage, lightweight key creation dependent on upgraded homomorphism encryption is utilized to produce the keys.

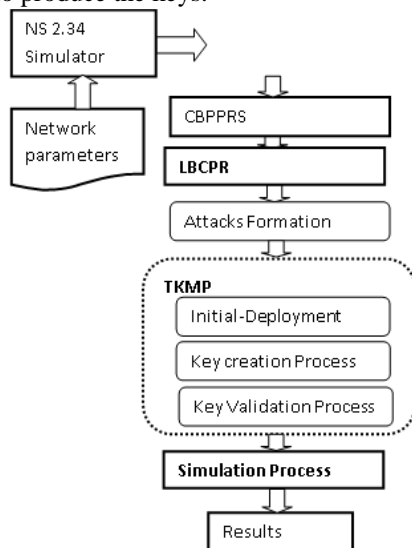


Fig.1: TKMP Process Flow

Ultimately, the key approval and check are finished by determining a geometrical model utilizing a hashing capacity, improved homo-morphic encryption, irregular number capacities. In this way, with the created geometrical model for the key advancement, the proposed TKMP validates the units and accordingly, manages a protected and dynamic key improvement in the bunched Network. The figure 1 portrays the TKMP procedure stream.

A. NETWORK ARCHITECTURE

Network model contains of M number of nodes deployed randomly within network simulation area. All the nodes (N(k)) are dynamic in terms of their creation, location and lifeless. Apart from all the general nodes, the cluster network has two well-configured nodes called as the base station (Bst) and Cluster Head (CH). The behaviors of the whole mobile nodes are observed, record and pass it to Bst is carried out by the CH. The network formation is evaluated in graph model was already we presented (R. Jayaprakash, B. Radha, 2018). The current network includes of Cluster Member (CM) is assigned a unique ID for validation and authorization. Any N(k) can broadcast the packets to any other N(l) in the network without any restrictions (R(k)). All the nodes can modify their location dynamically. In order to provide secure communication, each node is verified using their ID for authenticating and authorizing for communicating with other nodes in the network.

B. CBPPRS and LBCPR

Cluster Based Privacy Preserving Routing Selection (CBPPRS) was at that point we exhibited (R. Jayaprakash, B. Radha, 2018) thinks about the gathering of Cluster heads (CH) in a portable ado system of n intersections/hubs to such an extent that all hubs in this system are inside separation h jumps of a CH, for a known DEFINED – VALUE.

The Load Balancing Cluster Based Privacy Routing (LBCPR) was already we presented (R. Jayaprakash, B. Radha, 2018) load awkwardness in the system and the inclination or bias in getting halfway found hubs for information move. The proposed a novel group based directing measurement, load and a minimization rule to settle on a choice a way that involves versatile hubs with less burden weight on them In LBCPR performs new measurement called burden will reveals to us the evaluated burden a portable hub (mn) is engaged to in a system, its worth will indicate the evaluate of current burden. In this model, connect looking and send react calculations performs bunch burden field precisely.

C. ATTACKER MODEL

In the model for attacker, The following are done

1. The Attacker is able to capture all of the traffic in the area of network concerned.
2. The snooping is so promising in the network and the communications and of the knowledge on the nodes that are near by following the message size , etc
3. Depending on the variation, there seems to be certain possibilities in the attack that drops the packets into the network.

D. TRUSTED KEY MANAGEMENT PROTOCOL (TKMP)

This part depicts the proposed TKMP, for making a verified correspondence interface in cluster Network. The proposed TKMP performs key advancement in three unique stages. The development of TKMP is portrayed in figure 2. As exhibited in the above figure, the TKMP three stages are 1) Intial-Deployment, 2) Key Creation, and 3) Key Validation and Confirmation. The proposed TKMP can be estimated as the advancement to the Paillier cryptosystem (PC), with the end goal that the utilizes the open key for secure correspondence. The means engaged with the proposed TKMP are advised as pursues:

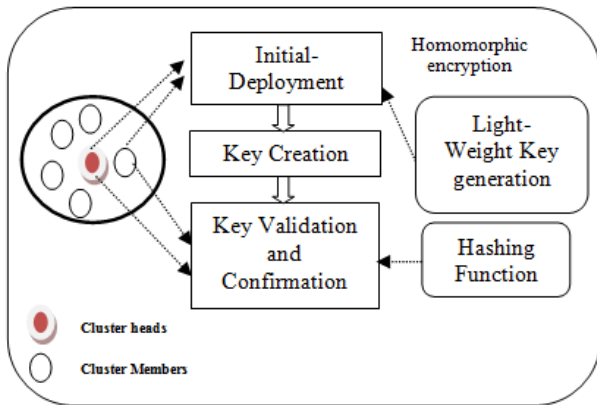


Fig. 1: TKMP Architecture

A) INITIAL-DEPLOYMENT PHASE

The first process in the proposed TKMP is the Intial-arrangement stage, where the portable hubs are given a specific personality (ID). Ordinarily, this stage allots the doable recognizable proof for each group part (CM) hub, BS, and CHs. As the CH is one of the key needs in remote system correspondence, the Initial-arrangement is done after the creation grouping Network portable hubs. Subsequent to bunching the system model, various CHs are shaped.

The Initial phase fills the predefined network key Nkey to every node, CH and BS in the wireless network. The cluster based wireless network has its parameters for every beginning of communication. Most of the network uses the network key of 128 bits for secured transmission. The paper adopts the homomorphic encryption [22] for creating the network key.

B) KEY CREATION PROCESS

After given that the personality for the group hubs, the following most significant stage is to make key for CM, CH and BS. The key creation stage helps with delivering the private and the open keys for the correspondence in the midst of the versatile hubs. This paper acknowledges the PC Encryption Scheme inferred in [22] for making the private and the open keys for the portable hubs. The means received by PC technique for key age are clarified as pursues:

Consider the k^{th} mobile node in cluster network which starts the correspondence and it needs both the open key and the private key for the correspondence reason. Basically, the root hub makes two separate enormous prime numbers p and q . At that point, the creation $C = pq$ is calculated among the random numbers p and q . The private key λ is determined using Carmichael's function,

$$\lambda(n) = lcm(p-1)(q-1) \quad \text{eqn. (1)}$$

The rest factor is calculated as,

$$r_p^{(p-1)/2} = -1(mod p) \quad r_q^{(q-1)/2} = -1(mod p) \quad \text{eqn. (2)}$$

Public Key Generation: For creating the public key, the rest factor r and the product C are used. Thus, the public key consists of (r, C) .

Private Key generation: The private key is constructed based on (p, q) .

The above steps are applied for creating the private and the public keys for the CM, CH and BS. The key created for CM, CH and BS is given as follows:

$$[CM^r_{key}, CM^p_{key}] = PC(p_1, q_1) \quad \text{eqn. (3)}$$

$$[CH^r_{key}, CH^p_{key}] = PC(p_2, q_2) \quad \text{eqn. (4)}$$

$$[BS^r_{key}, BS^p_{key}] = PC(p_3, q_3) \quad \text{eqn. (5)}$$

Equation (3) represents the Cluster Member (CM), equation (4) for Cluster Head (CH) and equation (5) for Cluster Head (CH). Where, (p_1, q_1) , (p_2, q_2) and (p_3, q_3) are group of large distinct prime numbers stated for the CM, CH and BS, respectively.

C) KEY VALIDATION AND CONFIRMATION PROCESS

The last phase in the proposed TKMP is the validation and confirmation of the key. This stage exhibits the progression of communication in the midst of the origin and the objective versatile cluster in the validation of the key and affirmation stage. Preceding exchange verified packets over the correspondence arrange, it is basic to make a secured path for communication among the CM. The secured path for communication is outstanding among the sender and the beneficiary in the key approval stage, in front of moving the parcel. For each datum transmit, the TKMP makes the session key, to find the cipher text.

Begin the data transmit: The packet transmits is started by the origin node and the packet has its individual identity (ID), network key (Nkey), and code.

$$APK_{xy} = \left[\begin{matrix} Enc(Pid) & Enc(Rid) & Enc(Sh_{key}^{xy}) \\ Message & Message & Message \end{matrix} \right] \begin{matrix} Packet_1 \\ Packet_2 \\ Packet_M \end{matrix} \quad eqn. (6)$$

where, *Pid* indicates the packet identity, *Rid* indicates the identity of the receiver node and *Sh_{key}^{xy}* refers to the shared key created among the origin and the target node. The function *Enc()* determines the encryption, which is finished utilizing the improved PC calculation with the help of the session key *session+key*. The session key is one of the noteworthy components in the proposed TKMP. The session key is made temporarily, which lives for the message session done during the information transmit between the hub x and y. The accompanying articulations demonstrate the encryption done through the improved PC technique.

$$Enc[P_{id}] = PC(P_{id}, session^{+key}) \quad eqn. (7)$$

$$Enc[R_{id}] = PC(R_{id}, session^{+key}) \quad eqn. (8)$$

$$Enc[Sh_{id}] = PC(Sh_{key}^{xy}, session^{+key}) \quad eqn. (9)$$

After the achievement of the session key through the sender, the organization is done by the receiver which recognizes the origin which tries to communicate through the secured link of communication. The TKMP executes the parcel move just driving building up the verified information way (connect). For this kind of message, the recipient confirms the specialist of the starting point by making cipher text. Essentially, the collector makes the cipher text C1. The cipher text C1 is accomplished dependent on the center bundle MP. The center bundle MP relies upon the unscrambled data with the session key, and it relies upon the accompanying condition,

$$MP = \left[\begin{matrix} Dec(Enc(Pid)|session^{+key}(received)) \\ (Enc(Rid)|session^{+key}(received)) || Dec(Enc(Pid)|Sh_{key}^{xy}(received)) \end{matrix} \right] \quad eqn. (10)$$

Where, *session⁺(received)* refers to the session key established by the receiver, and *Dec()* specifies the decryption done on packet entities based on the received session key.

Generation of ciphertext *C₁* and *C₂* can be referred as the security layer 1.

$$C_1 = hash(MP) \quad eqn. (11)$$

The ciphertext *C₂* is created based on the ciphertext *C₁*. The next security layer is awarded by the network key, and thus, the ciphertext *C₂* is created as follows,

$$C_2 = [Dec(Enc(C_1)/N_{key}) || CH^p_{key}] \quad eqn. (12)$$

$$C^*_2 = [(Enc(C_1)/N_{key}) || CH^p_{key}] \quad eqn. (13)$$

After creating *C₂*, the receiver replies the sender ask for by transfer the ciphertext *C₂*. Clearly the TKMP acknowledges the parcel during staggered security level, and in this way, diminishes the opportunity of security robbery. The sender confirms the honesty of the collector by indistinguishable the determined cipher text *C₂** with the cipher text built up from the beneficiary *C₂*. Once together the cipher text matches, for example *C₂* = C₂*, the sender announces the beneficiary to be reasonable and accordingly, starts the first information transmit. On the off chance that the figure does not coordinate, the message will be ended, and the session key made for the message gets terminated.

Algorithm 1: TRUSTED KEY MANAGEMENT PROTOCOL (TKMP)

Intialize CH, CM, BS.

Process

Step 1: Allocate *N_{key}* to CM, CH and BS using improved PC algorithm.

Step 2: For each CM, CH and BS and Generate Key Creation using equation 3,4 and 5

End for

Step 3: Execute encryption above the *P_{id}*, *R_{id}*, and Shared key

Step 4: Start packet transmission and updates Active Profile Key using eqn, (6)

Step 5: Calculate Cipher Text using eqn. (11) & (12)

Step 6: Origin Node finds $has(MP^*)$ and C_2^* correspondingly.

Step 7: *if* $C_2^* = C_2$ *then*

start packet transfer

else

State the y_{th} mobile node as the malicious

endif

IV. CONCLUSION

The main objective of this paper is to provide a Trusted Key Management Protocol (TKMP) to improve the quality of secure communication in Cluster based Wireless network. The TKMP is explicitly intended for the grouped system, and it has three phases, in particular Initial-arrangement, key creation and key approval and affirmation. The proposed TKMP performs Paillier cryptosystem (PC) homomorphic encryption is accomplished for disclosure the encryption key. In the interim, the proposed calculation builds up geometrical model created with the verified variables, for example, hashing capacity, homomorphic encryption, profile key succession, irregular number capacities for verified data transmission.

REFERENCES

1. R. Jayaprakash and B. Radha, "CBPPRS: Cluster Based Privacy Preserving Routing Selection in Wireless Networks", *International Journal of Engineering & Technology*, 7 (3.12) (2018) 439-443.
2. R. Jayaprakash and B. Radha, "LBCPR: Load Balancing Cluster Based Privacy Routing In Wireless Networks", *International Conference on Recent Trends in Automation (ICRTA-2018)*.
3. L. Zhou, Z. J. Haas, "Securing ad hoc networks", *IEEE Network*, Vol. 13, No. 6, Nov. 1999, pp: 24 – 30
4. Y. C. Hu, A. Perrig, "A survey of secure wireless ad hoc routing", *IEEE Security & Privacy Magazine*, Vol. 2, No. 3, May-June 2004, pp: 28 - 39
5. Y. C. Hu, A. Perrig, D. B. Johnson, "Ariadne: A Secure On-demand Routing Protocol for Ad Hoc Networks", in the Proc. Of 8th Annual International Conference Mobile Computing and Networking (Mobicom 2002), ACM Press, 20002, pp. 12-23
6. M. G. Zapata, N. Asokan, "Securing ad hoc routing protocols", in the Proc. Of ACM Workshop on wireless security (WiSe), ACM Press, 2002, pp: 1-10
7. K. Sanzgiri et al., "A secure routing protocol for ad hoc networks", 10th IEEE International Conference on Network Protocols, 2002, 12-15 Nov. 2002, pp: 78 - 87
8. Azarderakhsh, Reza, Arash Reyhani-Masoleh, and Zine-Eddine Abid, "A key management scheme for cluster based wireless sensor networks," *Proceedings of IEEE/IFIP International Conference on Embedded and Ubiquitous Computing*, vol. 2, pp. 222-227, 2008.
9. Udaya, D., Suriya Rajkumar, and Rajamani Vayanaperumal, "A leader based monitoring approach for sinkhole attack in wireless sensor network," *J. Comput. Sci.*, 2013, vol. 9, no. 9, pp. 1106–1116.
10. Xun Yi, Russell Paulet, Elisa Bertino, "Homomorphic Encryption and Applications," *Springer Briefs in Computer Science*, 2014
11. Q. Jiang, S. Zeadally, J. Ma and D. He, "Lightweight three-factor authentication and key agreement protocol for internet-integrated wireless sensor networks," in *IEEE Access*, vol. 5, pp. 3376-3392, 2017.
12. Bhajantri, Lokesh. (2018). A Comprehensive Survey on Data Aggregation in Wireless Sensor Networks. *International Journal of Computer Sciences and Engineering*. 6. 798-802. 10.26438/ijcse/v6i7.798802..
13. J. Choi, J. Bang, L. Kim, M. Ahn and T. Kwon, "Location-Based Key Management Strong Against Insider Threats in Wireless Sensor Networks," in *IEEE Systems Journal*, vol. 11, no. 2, pp. 494-502, June 2017. doi: 10.1109/JSYST.2015.2422736
14. Priyanka Ahlawat, Mayank Dave, "An attack model based highly secure key management scheme for wireless sensor networks," *Procedia Computer Science*, Volume 125, 2018, pages 201-207, ISSN 1877-0509, <https://doi.org/10.1016/j.procs.2017.12.028>.

Design and Implementation of a Low Cost, High Speed, High quality Talking Keyboard for Blind Students

^[1] K.V.B.Chandrasekhar rao, ^[2] Yamani.Kotipalli
^[1] Associate professor, ^[2] IIIrd B.Tech.
^[1]sekharscet@gmail.com, ^[2] yaminikotipalli123@gmail.com

Abstract: -- Every day the world is fetching new technologies in the field of Electronics Engineering. But the disabled people, such as blind People are facing many problems while learning and typing their work using computers and they are seeking help from other people to do their work in computer. This work is proposed to help the blind people to do their work by themselves. A low cost talking keyboard is designed using 8051 microcontroller family IC 89S516rd2 which has 64k program memory. Pre recorded audio samples for all the keys in the keyboard are stored in microcontroller. It uses only 60kb space in the program memory of Microcontroller. When a key is pressed the digital samples of the corresponding key are converted into analog signals using DAC. In order to achieve quality in audio signals, proper filtering is done for the respective key signal and the voice can be heard in speakers. As this project is a low cost, simple and easy to carry, it will be very much helpful for the blind people as well as the people who are interested to learn typing.

Index Terms: PS/2 Keyboard, Samples, Microcontroller, Blind people.

1. INTRODUCTION

Now-a-days, Computers are part and parcel in all our lives. The main input device of the computer is keyboard. It is very difficult to operate blind people which are suffered a lot in these days [1]. So, we have implemented a Talking Keyboard with simple technology in sense of Blind People. The main features of this device are low cost, high quality and high speed.

II. EXISTING SYSTEM

There may be available of these type of devices in the market by using different technologies. Some of the devices are Kurzweil reading machine, optacon, braille keyboard etc., [2] [3] They having some disadvantages like lack of portability, high cost etc.,

II. PROPOSED SYSTEM

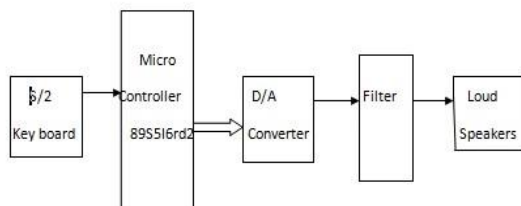


Fig1. Block Diagram of PS/2 Talking Keyboard

The block diagram of our proposed system is shown in Fig 1. Generally, the PS/2 keyboard generates two wire serial frame data [4][5] and clock for its corresponding key. Sample data for each character key is shown in table 1. This serial frame is converted as a parallel in a microcontroller. According to the character data, the corresponding voice samples are send to the 8 bit digital to analog converter. After converting it as a quantized analog signal, it is passed through a low pass filter having cut off frequency 2KHz for getting clear voice signal for a particular key character.

Table 1: PS/2 serial data for different keys

Character	PS2 data	Character	PS2 data	Special function	PS2 data
A	1C	0	45	Control	14
B	32	1	16	Space	29
C	21	2	1E	Tab	0D

The keys in the keyboard are classified into three types alphabets, numerics, special characters and function keys [6]. we have a total memory space for voice samples of 60KB, hence only 10sec of audio samples are to be loaded. Each group total voice times and total samples are given in table 2. Totally 84 keys are in PS/2 keyboard. From Table 2, the voice time for A to Z and 0 to 9 is 6.74sec, and the remaining time 3.26 sec is used for mathematical operation keys and spacebar. For covering

remaining function keys, character voice samples are cascaded for give the voice of that function key.

Table 2 Group voice Time periods and samples

Keyboard keys	Total voice time	Total samples
A to Z(26)	4.655s	27,930
0 to 9(10)	2.085s	12,510
Special function keys	3.26s	19,560

Program Flow chart for Talking Keyboard is given below

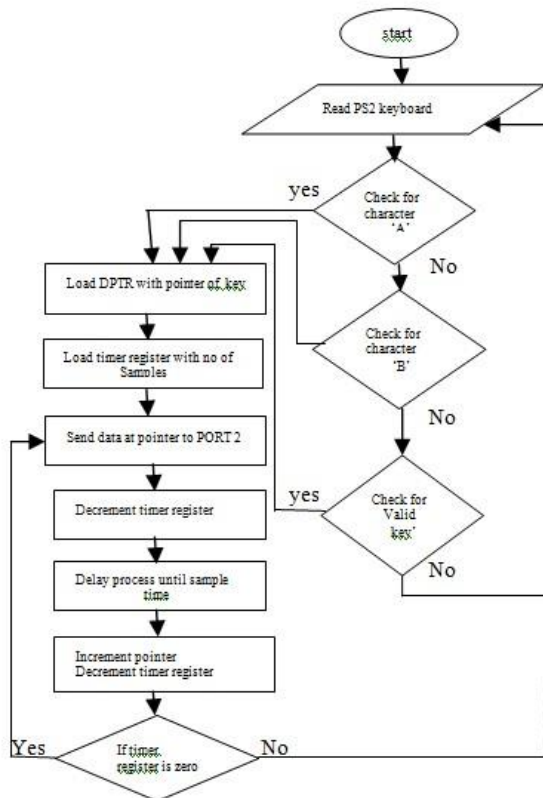


Fig 2 Flow chart of Talking Keyboard

First we enter a character by using PS/2 keyboard, this keyboard send it to the micro controller in a serial frame way. The IC 89s516rd2 microcontroller itself contains the storage space, of 64KB. In that 4KB are utilizes for the programming purpose, Hence 60KB are free which is used to store samples of voice. Then the entered character is decoded by the microcontroller. Later, the corresponding character address is stored in DPTR, at that time timer zero registers is loaded with the maximum number of samples.

After that the microcontroller sends the data pointer to the port 2, Then increases the DPTR and decreases TR0 registers until the TR0 register zero, pointer data is send

to port 2 to resend the corresponding character damples. At that time it takes some delay between sample to sample which is equal to sample time..

We have taken sampling frequency of 6000Hz. Our proposed work is to develop talking keyboard, which gives voice for all keys in the PS/2 keyboard, we use only 10seconds voice for 84 keys. This is achieved by cascading different fundamental voices, corresponding to the function keys in keyboards. To the functional keys F1 to F12 for providing voice microcontroller sends three character voice samples of F and l and 2'

Our proposed work is to develop high speed typing. In our keyboard, the minimum and maximum voice times are 0.1 and 0.33 sec. If the maximum voice time is 0.33sec then we can type, minimum characters per minute is

(60sec/maximum voice time.) i.e., $60/0.33=181$ characters. If average characters per word is 5, then we type the words of (total characters)/(no. of characters per word). i.e., $181/5=36$ words. Therefore using this keyboard we can type minimum 36 words per minute. Similarly, at the voice time of 0.1sec, we can type maximum characters of $60/0.1=600$ characters and words of $600/5=120$. Hence the typing speed is in between 36 to 120 words.

Table3 time and address of the samples

character	Voice time	No. of samples	Starting address	Ending address
A,a	0.2s	1200	1FFF	24AF
B,b	0.17s	1020	24B0	28AC
1	0.16s	960	8A54	8E14
2	0.19s	1140	8E15	9289
Space	0.24	1440	ADE1	B381
+	0.2	1200	C8A0	CD50

The number of samples are calculated using the formula, (Maximum number of samples per character = voice time * sampling frequency). For getting accurate output, we used the digital storage CRO. For identifying and collecting the sample data's for each time interval of 1/6000sec (sampling time). After collecting and tabulating each voice data with respect to sample, they are further plotted as a graph for observing sample wave form equality of actual audio signal which is to be in the digital storage CRO.

By observing the below three waveform, we can justify that the programming and regenerative waves are same as the sampled wave. Hence we say that samples are truly programmed and regenerated in equal time interval. These equal interval samples are converted as true voice signal and get the original audio signal which is to be verified in PC based CRO. When these three waveforms

are correct the output audio will be accurate. We achieved this characteristic in our work. For example character 'A'. the corresponding three waveforms are as follows:



Fig 3. Wave at the time of sampling For A

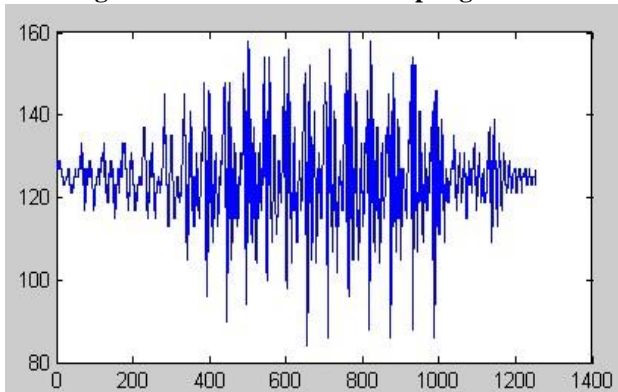


Fig 4 Sample vs Magnitude For A

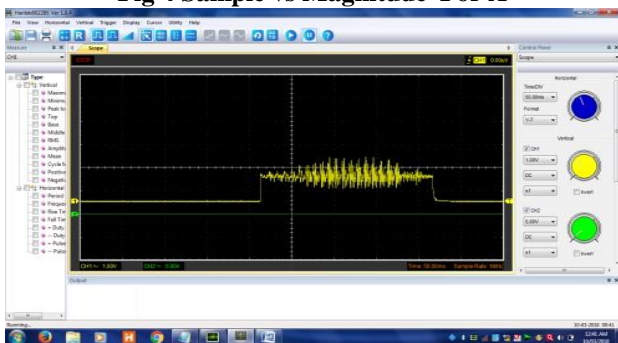


Fig 5 Regenerated Wave For A

III. CONCLUSION

This project proposed a talking keyboard in order to help the blind people to do their work by themselves. The talking keyboard is a low cost because of 8051 family IC89s516rd2. This IC uses only 60kb of memory which is used to store the voice of 84 keys. Even though pre-recorded audio samples have 10 seconds we produce 84 keys audio using voice cascading principle. Using this

keyboard we can type minimum(36) and maximum(120) words per minute. This product is simple and easy to carry, it will be very much helpful for the blind people as well as the people who are interested to learn typing.

IV. REFERENCES

1. R. Hamzah and M. I. M. Fadzil, "Voice4Blind: The talking braille keyboard to assist the visual impaired users in text messaging," in Proceedings - 2016 4th International Conference on User Science and Engineering, i-USER 2016, 2017.
2. F. Block, H. Gellersen, and N. Villar, "Touch-Display Keyboards: Transforming Keyboards into Interactive
3. Surfaces," in Proceedings of the 28th international conference on Human factors in computing systems - CHI '10, 2010.
4. S. Kane and J. Wobbrock, "Usable gestures for blind people: understanding preference and performance," in CHI '11 Proceedings of the 2011 annual conference on Human factors in computing systems, 2011.
5. M. Romero, B. Frey, C. Southern, and G. D. Abowd, "BrailleTouch: Designing a mobile eyes-free soft keyboard," in Mobile HCI 2011 - 13th International Conference on Human-Computer Interaction with Mobile Devices and Services, 2011.
6. A. H. Morad, "GPS talking for blind people," in Journal of Emerging Technologies in Web Intelligence, 2010.
7. M. Hudec and Z. Smutny, "RUDO: A home ambient intelligence system for blind people," Sensors (Switzerland), 2017.

Fluidity characteristics of LM6/graphite particulate composite

^[1] Sharath Kumar R, ^[2] Dr Sarada B.N, ^[3] Dr P. L. Srinivasa Murthy, ^[4] Abhishek

^{[1][4]} Student, ^[2] Assistant Professor, ^[3] Associated Professor.

^{[1][2][3][4]} Department of Mechanical Engineering, Ramaiah Institute of Technology, Bengaluru-560054, Karnataka, India

^[1] mailme.sharathk@gmail.com, ^[2] bnsarada.mech@bmsce.ac.in, ^[3] srinivasgudibanda@gmail.com, ^[4] abhishek199501@gmail.com

Abstract:-- Casting processes involves the flow of molten metal through a gating system and the complete filling of the mould cavity in order to accurately and faithfully reproduce all the contours of the mould. The molten metal is poured into the mould at a particular temperature. This temperature immediately starts dropping when the molten metal enters the mould cavity and begins to flow. The main aim of casting production is to create a casting of excellent quality which carries all intended details and contours from the mould reproduced successfully on it.

To accomplish such a successful casting process, the molten metal is required to possess certain casting characteristics like oxidation, fluidity, shrinkage, hot tear, gas absorption, etc. Amongst these characteristics, fluidity is considered to be an important parameter of the molten metal. Fluidity is the ability of the molten metal to completely fill the mould cavity. It can also be considered as the ability of the molten metal to fill a given cross section of the mould. In simple terms, fluidity can be defined as the mould filling capacity of the molten metal.

Fluidity is influenced by several parameters like pouring temperature of the molten metal, type of mould used for the casting, nature of the metal used, temperature of the mould, coating used on the mould surface, and treatment of the molten metal such as grain refinement and modification. In fact, fluidity is a very complex parameter which cannot be precisely measured. However, there are methods available to qualitatively assess the fluidity of molten metal.

Therefore, it is imperative to determine the fluidity of molten metal under a given set of conditions which will help the practical shop floor staff to obtain an understanding regarding the precautions which must be taken to produce a successful good quality casting.

In this project, attempts will be made to study the fluidity of LM6 (Aluminium 12% silicon) alloy and the composite prepared using graphite particulates in the LM6 base alloy, by pouring the molten metal into two different fluidity test moulds (i.e.: strip and spiral test). These moulds are standardised equipment's which have been designed by taking into consideration several parameters which can influence the flow of molten metal within the mould channels. It is proposed to study the effect of pouring temperature, mould temperature, effect of mould coating material on fluidity of metal.

Index Terms: Fluidity, Strip test, Spiral test.

1. INTRODUCTION

Casting makes use of fusibility property of a material. Fusibility is the ability of a material to undergo phase changes when supplied with energy. The pouring of molten metal into the mould is one of the critical steps in founding, since the behaviour of the liquid and its subsequent solidification and cooling determine whether the cast shape will be properly formed, internally sound and free from defects.

The characteristics of metal/alloy are of great importance in assessing the quality of the same, to understand how they behave during the process of melting, solidification, etc. The following properties are referred to as casting characteristics: shrinkage, fluidity, hot tear, solidification mechanism, oxidation losses, gas solubility, etc. Among these, fluidity plays a vital role in determining casting quality.

Fluidity of molten metal is of significant importance in producing sound castings, particularly thin-walled castings. To meet the industrial demands of complex shaped castings, the knowledge of the parameters affecting fluidity is required in order to have a better control of the production processes. Since fluidity is one of the measures by which the cast ability of metals can be quantified, a definition and a description of cast ability are presented in this study. Fluidity can be defined as that quality of liquid metal that enables it to flow through mould passages and to hence fill all interstices of the mould, providing sharp outlines and a faithful reproduction of design details.

Since fluidity cannot be assessed from individual physical properties, empirical tests have been devised to measure the overall characteristic. These are based on conditions analogous to the casting of metals in the foundry and measure fluidity as the total distance

covered by molten metal in standardised systems of enclosed channels before cessation of flow.

The Strip test indicates the mould filling capacity whereas the Spiral test indicates the flowability of molten metal. The closest approach to complete standardisation is achieved in the vacuum fluidity test devised by Ragone, Adams and Taylor.

Aluminium based alloys are well known for their high strength to their weight ratio, good corrosive resistance and ease of casting into various shapes and sizes. However, their use is limited due to poor wear and low hardness characteristics. These drawbacks can be removed by producing aluminium alloy composites which exhibit the advantages of both constituents.

Composite materials refer to a heterogeneous combination of several materials which provide unique combinations of properties that cannot be realized by the individual constituents acting alone.

Methods of producing composites using simple foundry metallurgy techniques can be developed only by a thorough understanding of their foundry characteristics among which fluidity is of vital importance.

II. LITERATURE REVIEW

O. Bouska [1] has studied on effect of different casting parameters on the relationship between flowability, mould filling capacity and cooling conditions of Al-Si alloys has been determined. In order to achieved better reproducibility of measurements new equipment's for both tests have been developed.

A.K. Birruetal [2] have studied on the fluidity of Al-Zn alloys, such as the standard A713 alloy with and without scrap addition has been investigated. The scrap added was comprised of contaminated alloy turning chips. Fluidity measurements were performed with double spiral fluidity test consisting of gravity casting of double spirals in green sand moulds with good reproducibility. The influence of recycled alloy on fluidity has been compared with that of the virgin alloy and the results showed that the fluidity decreased with the increase in recycled alloy at minimum pouring temperatures. Interestingly, an appreciable improvement in the fluidity was observed at maximum pouring temperature, especially for coated spirals.

MarisaDiSabatino [3] has studied on influence of various parameters on the fluidity of aluminium foundry alloys and, in particular, Al-Si foundry alloys. The effect of casting temperature, and hence melt superheat, was assessed through a series of tests. A linear relationship between casting temperature and fluidity length was observed. The effect of grain refiner on the fluidity of an A356 alloy was systematically investigated. The fluidity

lengths without grain refiner and with three additions of Al-5wt%Ti-1wt%B master alloy were measured. The results showed that grain refinement reduced the grain size throughout the spiral somewhat, particularly at the tip, but there were no statistically significant effects on fluidity.

Rabindra Beheraetal [4] he investigated the effect of weight percentage of Si-Cp on the fluidity and the rate solidification of stir cast MMC's. Many Experiments were carried out over range of particle weigh percentage of 5.0-12.5 wt.% in steps of 2.5wt%.The Spiral castings or three-stepped castings of aluminium alloy (LM6) and the composites reinforced with different mass fractions Si-Cp have produced to study the fluidity of the MMCs and solidification behaviour of the castings by putting many K-type thermocouples at the different sections of the casting. The experimental results indicate the increase in the weight percentage of reinforcement particles, i.e. Si-Cp in aluminium alloy (LM6) MMCs, the fluidity of cast composite metal decrease and the rate of solidification is decreased due to which the total solidification time is enhanced.

Vignesh Retal [5] studied the effect of Squeeze pressure on the Aluminium LM6 fluidity property. Fluidity refers to the property of a metal; the most prevalent fluidity tests is the spiral-shaped mould test, Aluminium LM6 alloy in the molten state was applied into the spiral die cavity by the squeeze pressure. The distance covered by molten metal in spiral channel after the application of pressure is the measure for fluidity. The fluidity keeps increasing up to a particular pressure and drops suddenly. At a pouring temperature of 750°C the maximum fluidity of LM6 alloy during squeeze casting was obtained under the applied pressure of 30 MPa and the fluidity of LM6 alloy during squeeze casting increases with increase in pouring molten metal temperature.

III. EXPERIMENTAL PROCEDURE

Production of LM6 matrix composites by stir casting technique.

Weighting of Aluminium and particulates: Required number of Aluminium ingots are weighed and the required percentage (1%, 2% and 5% by weight of metal) of particulates is also weighed.

Preheating: Preheating of charge materials to evaporate surface moisture can be extended to higher temperatures to volatilize oils, paints or other organic contaminants and to remove water of crystallization from hydrated corrosion products. The crucible is first preheated; this removes any moisture from the furnace and crucible. The aluminium ingots to be used are placed on top of the furnace so that they warm up.

Melting: Melting of LM6 alloy is carried out using Electric arc furnace (3.1) and superheated to a temperature of 8000C.

Mixing of particulates: The particulates are mixed with the molten metal using the vortex method. During mixing, magnesium chips are introduced along with the particulates. The magnesium chips form a coating around the particulates which helps in better adherence of the particulates with the metal, improving their wettability.



Fig.1 9kW electric resistance furnace and stirrer setup

Adding a degassing tablet: Hydrogen is the only gas that is appreciably soluble in aluminium and its alloys. Compounds such as Hexachloroethane are in common use; these compounds dissociate at molten metal temperatures to provide the generation of fluxing gas. Gas fluxing reduces the dissolved hydrogen content of molten aluminium. The use of reactive gases such as chlorine improves the rate of degassing by altering the gas-metal interface to improve diffusion kinetics.

When the aluminium has melted fully and is superheated to the required temperature the furnace is turned off, the crucible is taken out of the furnace and the degassing tablet is added. This removes any impurities in the form of gas.



Fig.2 Degassing in progress

Fluidity tests

Setting up of mould: The preheated moulds are set up such that they are parallel to the floor with the help of the spirit level such that there is no gradient since the strip mould is very sensitive to gradients.



Fig.3 Strip mould



Fig.4 Spiral mould

Pouring of molten composite and solidification: The molten metal mixed with the particulates is poured into the preheated moulds which are maintained at 100oC. The composite is removed from the mould after solidification. Now the composite is allowed to cool and then the strip and spiral lengths are measured.



Fig.5 Pouring of molten metal and demoulding of spiral casting

IV. RESULTS AND DISCUSSIONS

Fluidity of base metal LM6

The following figures show the variation of fluidity lengths with pouring temperature for LM6 alloy during the spiral test. The fluidity length-temperature graphs were analysed to determine the effect of pouring temperature on the fluidity length.

Spiral test



Fig.6 Variation of Aluminium LM6 spiral fluidity length with temperature

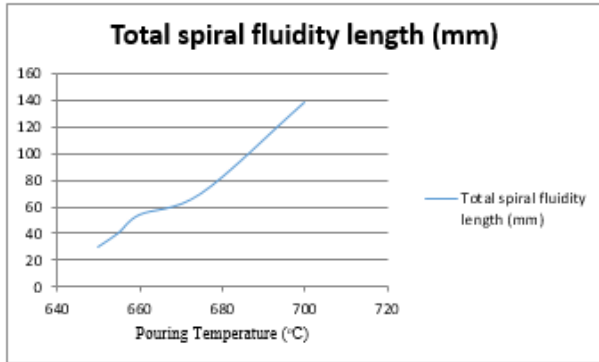


Fig.7 Total spiral fluidity length v/s temperature

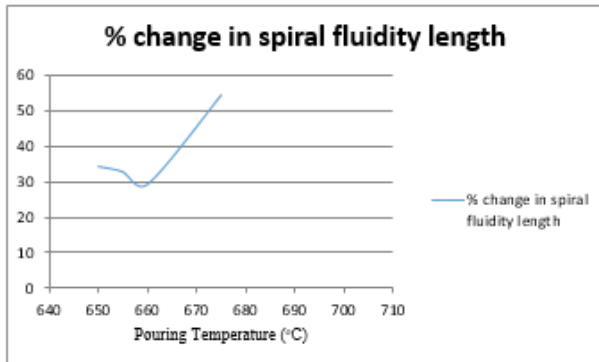


Fig.8 Percentage change in spiral fluidity length v/s temperature

Strip test

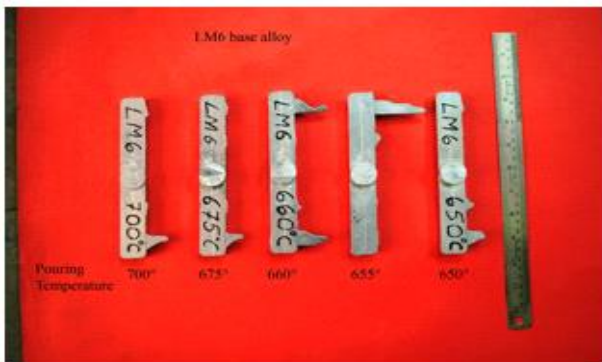


Fig.9 Variation of Aluminium LM6 strip fluidity length with temperature

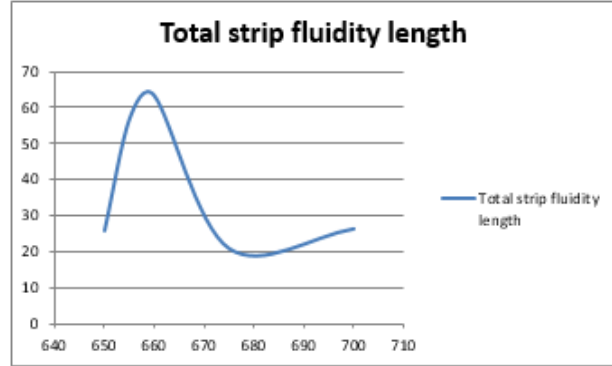


Fig.10 Total strip fluidity v/s temperature

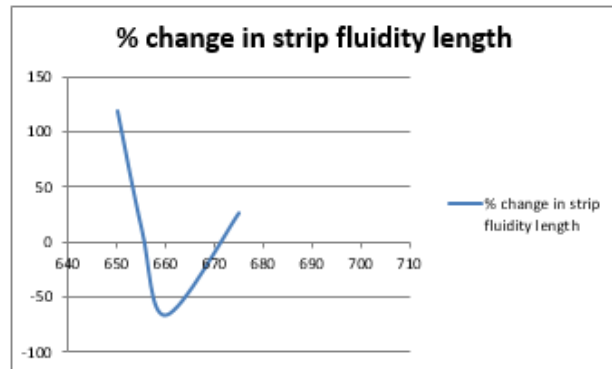


Fig.11 Percentage change in strip fluidity length v/s temperature

Discussion: (a) In case of spiral test the relationship between the fluidity length and temperature is linear and the maximum fluidity length is obtained at 700oC. The linearity is valid in the temperature range chosen in the experiment indicating fluidity increases with temperature.

In case of strip test fluidity increases with temperature till 6600C then decreases, indicates the filling capacity of the alloy. This could be due to easily melting eutectic solidification of the alloy at that temperature.

Fluidity of the composite.

The subsequent figures show the variation of fluidity length with percentage of graphite reinforcement in the composite. The tests were carried out using Spiral and Strip moulds, and the graphs were analysed to determine the effect of particulates on fluidity of a composite material.

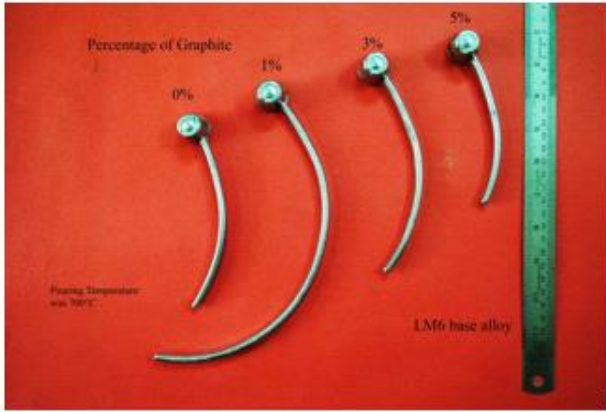


Fig.12 Variation of spiral fluidity length with % graphite

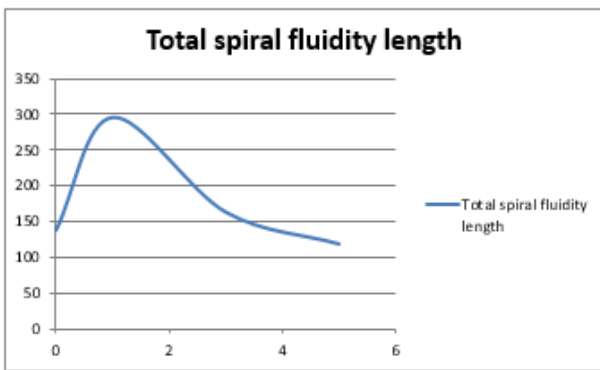


Fig.13 Variation of spiral fluidity length with % graphite



Fig.14 Variation of strip fluidity length with % graphite

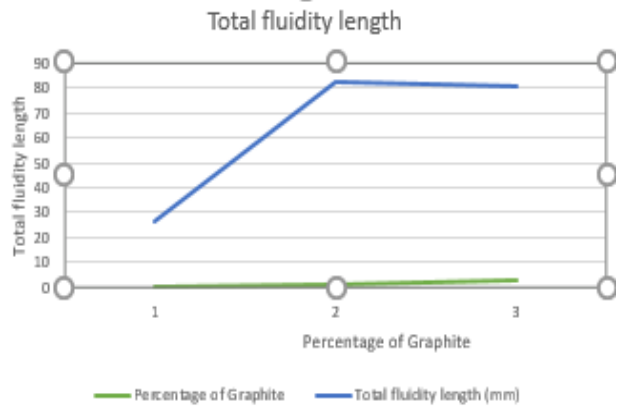


Fig.15 Variation of total strip fluidity length with % graphite

The study indicates that fluidity of the molten composite was highest when it contained 1% by weight of graphite particulates, and subsequently decreased with increase in quantity of particulates. This could be due to decrease in eutectic solidification temperature with increase in reinforcement %.

Effect of mould coating on fluidity at a standardised pouring temperature of 700°C.

The tests were conducted for:

1. China clay coating
2. Graphite coating
3. No coating

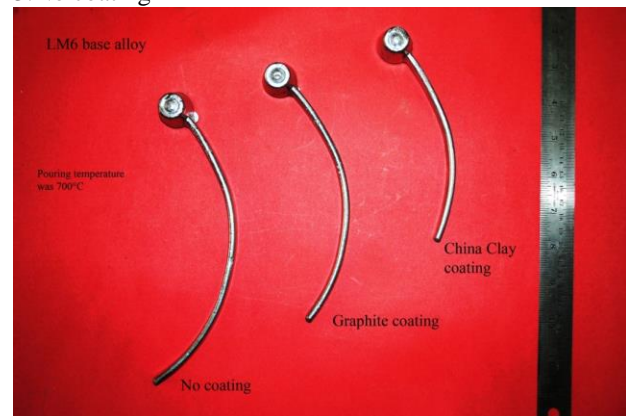


Fig 16 Variation of spiral fluidity length with mould coating

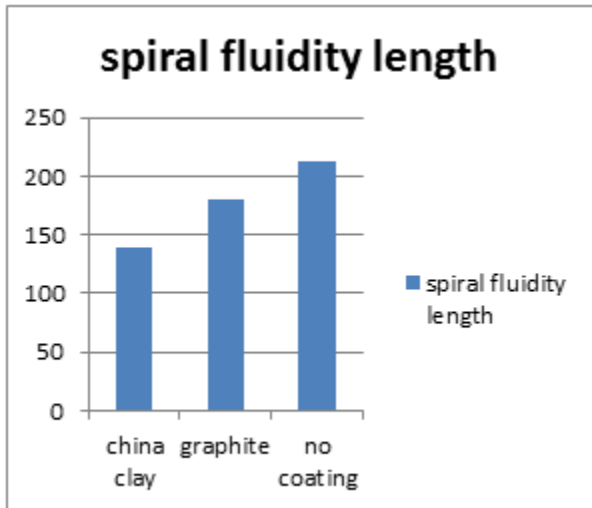


Fig 17 Graphical variation of spiral fluidity length with mould coating

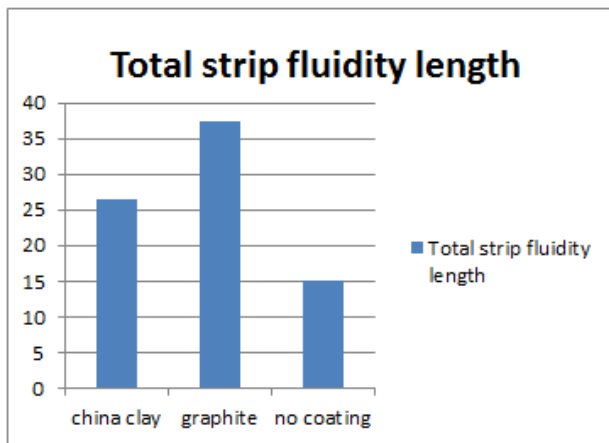


Fig 18 Variation of strip fluidity length with mould coating



Fig19 Graphical variation of total strip fluidity length with mould coating

Surface coating influenced the fluidity of composite material.

Spiral fluidity is maximum when there is no coating. But graphite coating improved the strip fluidity. This could be due to variation in coating thicknesses or surface roughness of the coatings.

Effect of mould coating on surface roughness

The following figures show the variation of roughness parameters with various mould coatings. The graphs were analysed to:

- (a) determine the effect coatings on surface roughness of the strip mould
- (b) study the variation of fluidity length with respect to surface roughness

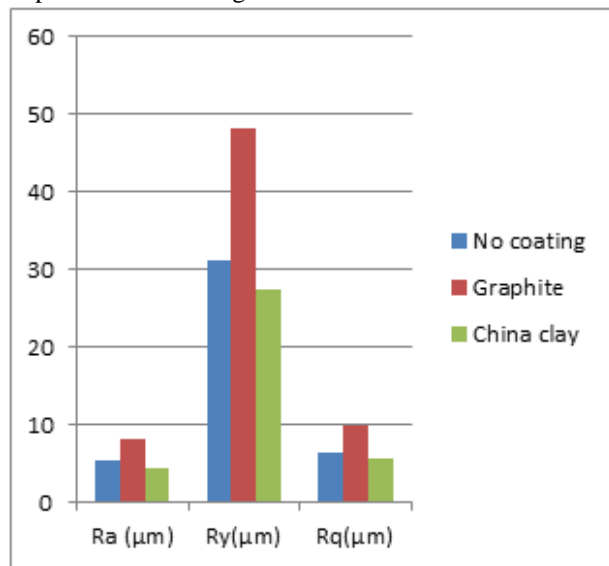


Fig 20 Effect of coating on surface roughness of the strip mould

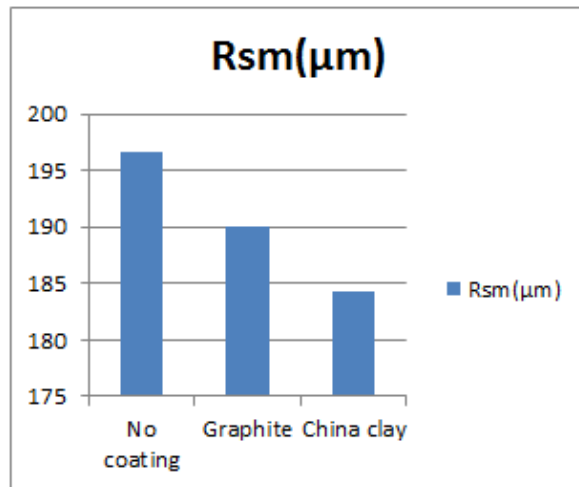


Fig 21 Variation of fluidity length with respect to surface roughness

The study of the figures indicates the following:

(a) There was conclusive evidence of the effect of mould coatings on the surface roughness. The surface roughness increased with graphite coating and reduced with china clay coating compared to the standard uncoated strip mould. There was no conclusive proof of variation in the strip fluidity length due to the changes in surface roughness with various coatings

V. CONCLUSIONS

Results of the investigations carried out to study the influence of various parameters on the fluidity of aluminium alloy and its composite indicate the following:

- The pouring temperature influenced the fluidity to a large extent. Fluidity increased linearly with increase in pouring temperature when all other factors such as composition of alloy, mould temperature, mould coating etc. were kept constant.
- The degree of purity of the alloy had a profound effect on the fluidity length observed. The fluidity length decreased with increase in impurity or other alloying elements. The eutectic alloy is observed to have highest fluidity among the base metals.
- The introduction of graphite particulates to the base alloy resulted in discernible changes in the fluidity. The fluidity length decreased with increasing percentage of the particulates.
- The surface roughness of the mould influenced the fluidity length on molten metal. The fluidity length found to be the highest when no coating was applied.
- For the spiral test, similarities in the percentage change in fluidity were observed for the base alloy and the composite material.

REFERENCES

[1] O. Bouska, The effect of different casting parameters with the relationship between the flowability, the mould filling capacity and the cooling conditions of Al-Si alloys, Germany, in Association of Metallurgical Engineers of Serbia, UDC:669.715'782-147:621.744.3=20

[2] A.K. Birruetal, Fluidity of A713 Cast Alloy with and without Scrap Addition using Double Spiral Fluidity Test: A Comparison, International Journal of Mechanical and Aerospace Engineering 6 2012

[3] Marisa Di Sabatino., Fluidity of aluminium foundry alloys, Norwegian University of Science and Technology (NTNU), September 2005

[4] Rabindra Beheraetal: Effect of Reinforcement Particles on the Fluidity and Solidification Behaviour of the Stir Cast Aluminium Alloy Metal Matrix Composites. American Journal of Materials Science 2012, 2(3): 53-61 DOI: 10.5923/j.materials.20120203.04

Vignesh R et al: Effect of Squeeze Cast Process Parameters on Fluidity of Aluminium LM6 Alloy. International Journal of Advancements in Technology Int J Adv Techno 2016, 7:2 DOI: 10.4172/0976-4860.1000157.

[4]Beeley,P., Foundry Technology, Second edition, 2001, page1-39.

[5] Campbell,J., Castings,The new metallurgy of cast metals, Second edition,2003, page 70-98.

[6]<http://en.wikipedia.org/wiki/Aluminium>

[7]Kaufman, J.G., Mechanical Engineers' Handbook: Materials and Mechanical Design, Volume 1, Third Edition, 2006, page 59-62.

[8]Radhakrishna, K., Manufacturing Process-I, 2006,

[9]ASTM Handbook

Power and Performance Analysis Using Multibit Technology

^[1] Manjunatha Visweswaraiyah, ^[2] Dr Somashekar K
^[1] R&D, Design Compiler, Synopsys India ^[2] Professor, SJBIT, Bengaluru, India.

Abstract:-- The implementation of deep submicron technology has resulted in increased devices on chip making power management a challenging task during design cycle. There are many different techniques developed to reduce the power consumption. Clock-gating, Voltage and frequency scaling, power gating etc. are some of the techniques used to reduce power consumption. Multibit technology is also used widely to help reduce the power. The reduction of power comes with compromise in performance of the integrated circuit. The paper analyses power and performance of face detection chips when multibit is used.

1. INTRODUCTION

The advances in manufacturing technology have enabled tremendous increase in device count on the chip. The increased gates have multiplied the number of nets used for interconnections. The complexity of the chip increases the power consumption. Reduction of power is an important factor or many applications such as hand held devices like mobile phone, notepads etc [1].

The power consumption in a chip can be divided into three major categories as Dynamic Power, Short Circuit Dissipation, and Leakage Power Dissipation. Each of these categories and their components are discussed below in detail.

Leakage Power Dissipation: This component of power dissipation is getting the most attention these days. Not all the components of leakage consumption existed or dominated for quarter micron and above nodes and thus, it contributed a negligible portion of the overall power consumption. However, with the shrinking of MOS due to technology advancements, the quantum mechanical effects started coming into picture and resulted into many of these leakage current components. This is the component of energy dissipation which affects operation of chip largely in the standby operation as other components cease to play during that period.

It has been observed that during Scan and TDF tests, clock signals are supplied simultaneously to numerous flip-flops in Dynamic Energy Consumption: Dynamic Energy consumption is the consumption due to toggling of the cells and nets because of toggle in the input. This is also known as Switching Energy. When a cell changes its state from logical high to logical low or vice versa, various internal capacitors (junction, interconnect and diffusion capacitances) charge or discharge accordingly. Energy is drawn from the supply to charge these capacitors, known as dynamic power.

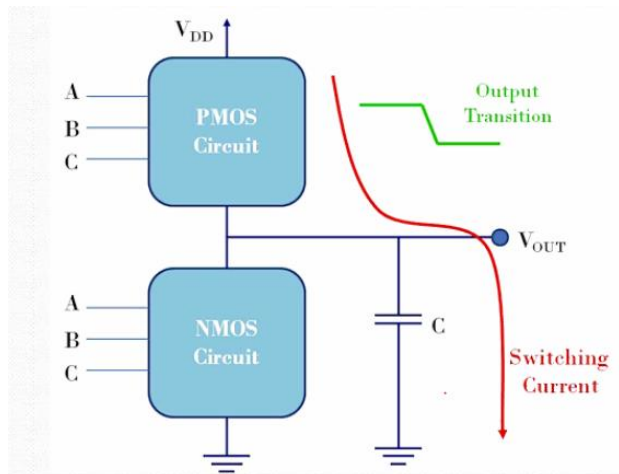


Fig: 1

If all the parasitic capacitances in a CMOS cell are lumped into load capacitance C, then, if the output level changes from V_{DD} to Ground, there is a total energy consumption of CV_{DD}². Half of energy is stored in the load capacitor C and rest half of the energy is dissipated. Similarly, when output changes back to ground, similar energy dissipation of energy takes place. Therefore, this switching energy consumption is directly related to V_{DD} and switching frequency. As a result, reduction of supply voltage is one way of reducing dynamic consumption. However, reduction of V_{DD} causes cells to become slower, therefore, effectively reducing the maximum frequency of the operation. Besides, reduction in frequency causes the same operation to take more time. Average switching energy consumption is:

$$P_{av} = f \cdot C \cdot V^2$$

where, f is the frequency of operation. This power consumption is independent of the rise and fall time of the input and output signals

The other component of switching energy consumption is loss due to dynamic hazards and glitches. Glitches may arise in a circuit due to unbalanced delays in the paths of various inputs coming in or in the path internal to the circuit. Consider the circuit as shown below

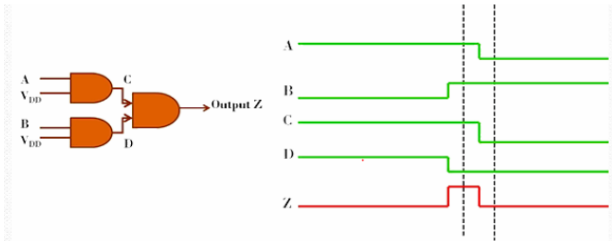


Figure 2: Glitch generation circuit and timing diagram

Consider the case where two of the inputs are at logical one, shown by VDD, and signals A and B transition with some delay, as shown in adjacent timing diagram. Due to unbalanced delays between arrival of A and B, output signal Z is asserted to 1 for a short duration of time. Such transitions are known as glitches/hazards. On the other hand, had A dropped earlier than assertion of B, there would not have been any glitch at the output as one of the input of output AND gate would have toggled to zero before assertion of other input. Therefore, timing is met in such a way that such glitches are either removed or minimized. However, in some cases, this behavior may be intentional to stop race conditions in a circuit. For this purposes, not all the inputs are toggled at the same time. Conditions where such glitches cannot be removed altogether, logic may be placed at the output to absorb such glitches to arrest their propagation to following logic, e.g. adding some buffers in the path to absorb such glitches and balance the timing of the path.

There are many different techniques to reduce power consumption.

Clock-gating: This technique is a very popular Dynamic Power reduction technique. Dynamic power is the sum of transient power consumption (transient) and capacitive load power (cap) consumption. transient represents the amount of power consumed when the device changes logic states, i.e. "0" bit to "1" bit or vice versa. Capacitive load power consumption as its name suggests, represents the power used to charge the load capacitance. Total dynamic power is represented as

$$P_{\text{dynamic}} = P_{\text{cap}} + P_{\text{transient}} = (CL + C) V_{\text{dd}}^2 f N^3$$

where CL is the load capacitance, C is the internal capacitance of the chip, f is the frequency of operation, and N is the number of bits that are switching. As dynamic power consumption is directly linked to toggling of the MOS cells, gating the clock when not

required helps reduce the dynamic current. This technique help preserves the state of the design while only limiting the transient currents. Designers frequently use AND/NOR gates to gate a clock, however, latch based clock gating is the most favored technique as it also saves designs from hazards which can otherwise introduce additional power consumption, inherent in dynamic power consumption.

Variable Frequency Islands [1]: In a big chip, not all the blocks should be clocked at highest possible frequency in order to achieve the desired level of performance. There can be few blocks which inherently work slow (e.g., slow communication blocks like I2C, UART, etc.) and, therefore, can be clocked at slower clock than blocks like core/processor which require high frequency clock for maximum throughput. Therefore, by providing different frequency clocks to different blocks, one can reduce localized dynamic consumption.

Power Gating: There can be applications where certain blocks of the chip might not be required to function in some of the low power modes like sleep, deep-sleep, standby mode, etc. and only a part of the device is required to function. In such cases, it makes sense to power off non-functional blocks so that device does not have to power unused blocks. This not only helps reduce the dynamic consumption but leakage power is also saved for such a power gated block. However, while dealing with such a technique, design has to make sure that signals coming in from power-gated blocks do not affect the functioning blocks while operating in low power. For this purpose, isolation blocks are placed in the path so that functionality corruption does not take place, as can be seen in figure 2. Please note that the isolation signals are not required for signals going out of always-ON domain to other power domains as they are never supposed to go non-deterministic

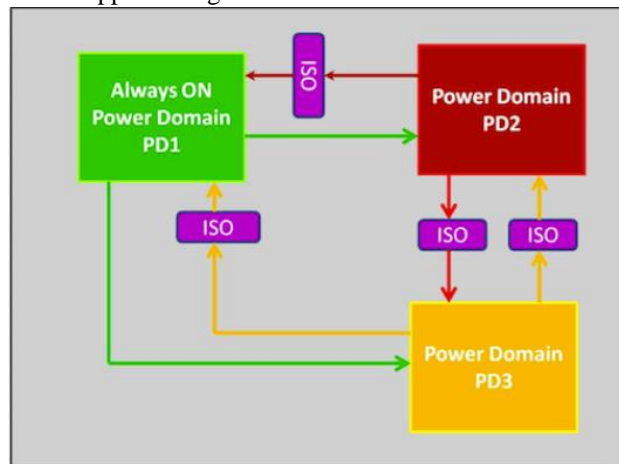


Figure 3: Power Gating

Apart from the above there are other techniques which are process based

Mutli VDD Technique [5]: As we can see from the equation above, there is a quadratic relationship between device voltage VDD and dynamic power consumption. Therefore, one can reduce the dynamic voltage substantially by reducing the supply voltage.

However, voltage reduction has its downside as well. Propagation delay of a cell is as below :

$$T_D = C \cdot V_{DD} / k \cdot (V_{DD} - V_T)^2$$

As one can see from equation above, reduction in the VDD increases the delay of the cell. thus, the operating frequency of the cell reduces when one reduces the supply voltage. Therefore, one must maintain a balance between voltage supply and associated performance. A solution to this challenge can be to create voltage islands in the design where low performance slow peripherals can be powered using lower supply voltage and performance critical blocks can be powered using higher voltage. However, we have to make sure that appropriate voltage level shifters are placed on those signals which talk across the voltage domains

Dynamic Voltage and Frequency Scaling: [3]: Voltage Island technique, also known as Static Voltage Scaling presents few constraints while operating the device. This technique is not adaptive to the application needs and voltage supply to a block cannot be changed once designed. However, Dynamic Voltage Scaling technique liberates designer and customer of such limitations. This technique makes use of a regulator which can be programmed to deliver voltage levels as required. Therefore, various blocks can get configurable voltage and the customer/user can change the voltage settings as per the application settings. This can help save the power dynamically. Various solutions have also been used where the design freed the software to make changes to voltage scaling. The design itself senses the current-load requirement in the device and makes the voltage adjustments accordingly. This technique helps reduce power consumption in a more adaptive manner

Multibit technology [2][3] Multibit cells have more than once cell embedded in a single library cells. The main advantage of using multibit cells areas below

- Reduction in area due to shared transistors and optimized transistor-level layout
- Reduction in the total length of the clock tree net
- Reduction in clock tree buffers and clock tree power

An example of two-bit multibit cell is as below

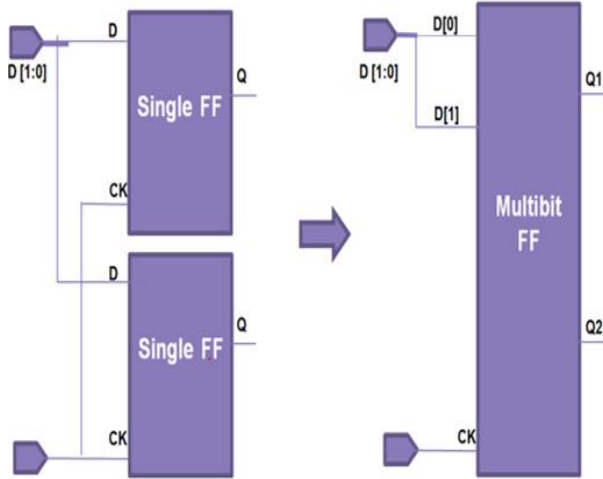


Figure 4: 2 bit multibit cell

The area of the 2-bit cell is less than that of two 1-bit cells due to transistor-level optimization of the cell layout, which might include shared logic, shared power supply connections, and a shared substrate well.

Details of Work Done

The objective of the work is to analyze the power and performance of face detection chips. The face detection chips process real time data and there will be high degree of computation occurring which needs more power. In this work the power and performance analysis of the two designs has been done with and without using multibit cells.

The library is 28nm TSMC having rich flavors of combinational and sequential cells.

The multibit library cells are sequential cells having 2, 4, 8 and 16 bit bus width.

Design1: 900 K instances, 64 macros, Rectangular Floor Plan.

Design2: 835K instances, 15 macros, Rectangular Floor Plan

Tools Used: HDL compiler for RTL elaboration, DFT compiler for Scan insertion and Design Compiler Graphical for physical synthesis

Design Flow:

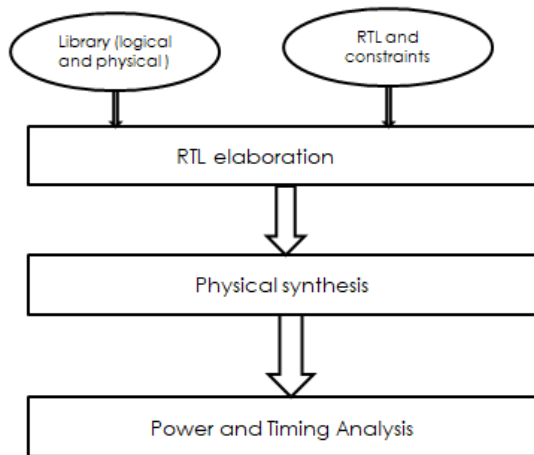


Figure 5: Design flow

The input is the RTL, logical and physical library, Timing constraints and floorplan file which has macro placement information.

The Design flow involved performing first pass of synthesis, then insert the design for testability logic and then perform second pass of synthesis. And then perform analysis of power and timing.

Three different runs conducted on two designs. The details of the runs are as below

Run1: This is called the base flow wherein each design is run through the flow without any multibit mapping of sequential cells

Run2: In this flow the designs are through the same flow as base flow but multibit mapping is enabled. Multibit mapping is through two steps.

In the initial synthesis before scan insertion the bussed registers were mapped to multibit library cells.

In the second pass of multibit mapping which is called physically aware multibit banking is performed before scan insertion, in which the sequential cells which are physically nearer to each other are combined and mapped to multibit library cell as shown in figure 6

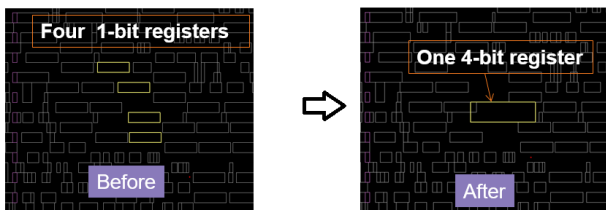


Figure 6: physically aware multibit banking

Run3: In this flow not all the cells are allowed to be mapped to multibit as it may degrade the timing results. The sequential cells on the timing critical path are not allowed to be mapped to multibit. This flow is expected to yield optimal results in terms of timing, area, and power.

Latest version (2018.06) of Design compiler tool from Synopsys is used for physical synthesis.

The above mentioned flows and runs were performed.

Once the runs were performed, timing and area reports were generated along with power numbers.

The congestion map of the design was also generated to compare the effect of multibit mapping on design congestion.

The following tables provide details about the designs selected.

Design 1	Design 2
900 K instance 64 Path groups 12 path groups Frequency: 600 MHz	800 K instance 12 Macros 8 path groups Frequency: 400 MHz

Table 1: Design details

The Quality of Results metrics like total negative slack (TNS), Worst negative slack (WNS), Area, Power is compared between the runs for both the designs.

The multibit banking ratio [2] provide details about the number of sequential cells mapped to multibit cells.

If more number of sequential cells are mapped to multibit, the more power and area is reduced.

In Run2, where full multibit mapping is enabled, the packing ratio results are as below

For Design1: The banking ratio is 90.43% as below

Total number of sequential cells:	71216
Number of single-bit flip-flops:	21058
Number of single-bit latches:	5
Number of multi-bit flip-flops:	50153
Number of multi-bit latches:	0
Total number of single-bit equivalent sequential cells:	221675
(A) Single-bit flip-flops:	21050
(B) Single-bit latches:	5
(C) Multi-bit flip-flops:	200700
(D) Multi-bit latches:	0
Sequential cells banking ratio $((C + D) / (A + B + C + D))$:	91.0%
Flip-Flop cells banking ratio $((C) / (A + C))$:	91.0%

For Design2: The banking ratio is 94.49% as below

Total number of sequential cells:	27117
Number of single-bit flip-flops:	7490
Number of single-bit latches:	0
Number of multi-bit flip-flops:	19627
Number of multi-bit latches:	0
Total number of single-bit equivalent sequential cells:	135894
(A) Single-bit flip-flops:	7490
(B) Single-bit latches:	0
(C) Multi-bit flip-flops:	128404
(D) Multi-bit latches:	0
Sequential cells banking ratio $((C + D) / (A + B + C + D))$:	94.49%
Flip-Flop cells banking ratio $((C) / (A + C))$:	94.49%

In Run3, where timing critical paths are not allowed for multibit mapping, the banking ratio results are as below

For Design1: The banking ratio is 90.43% as below

Total number of sequential cells:	71324
Number of single-bit flip-flops:	21208
Number of single-bit latches:	5
Number of multi-bit flip-flops:	50111
Number of multi-bit latches:	0
Total number of single-bit equivalent sequential cells:	221657
(A) Single-bit flip-flops:	21208
(B) Single-bit latches:	5
(C) Multi-bit flip-flops:	200444
(D) Multi-bit latches:	0
Sequential cells banking ratio $((C + D) / (A + B + C + D))$:	90.43%
Flip-Flop cells banking ratio $((C) / (A + C))$:	90.43%

For Design2: The banking ratio is 94.35% as below

Total number of sequential cells:	27464
Number of single-bit flip-flops:	7679
Number of single-bit latches:	0
Number of multi-bit flip-flops:	19785
Number of multi-bit latches:	0
Total number of single-bit equivalent sequential cells:	135897
(A) Single-bit flip-flops:	7679
(B) Single-bit latches:	0
(C) Multi-bit flip-flops:	128218
(D) Multi-bit latches:	0
Sequential cells banking ratio $((C + D) / (A + B + C + D))$:	94.35%
Flip-Flop cells banking ratio $((C) / (A + C))$:	94.35%

The Quality of Results (QoR) comparison table between the base run Run1 and Run2 (where full multibit mapping is enabled) for Design1 is as below.

	Run1	Run2	% Change
TNS	0.0255	0.0355	10% degradation
WNS	0.13	1.16	23% degradation
AREA	1866796	1819132	2.55% improvement
POWER	1000mW	116 mW	88% improvement

Table2 QoR comparison b/w Run1 and Run 2 for Design1

The Quality of Results (QoR) comparison table between the base run Run1 and Run2 (where full multibit mapping is enabled) for Design2 is as below.

	Run1	Run2	% Change
TNS	0.00164	0.0025	0.04% degradation
WNS	8.01	10.11	25% degradation
AREA	995941	955086	4% improvement
POWER	33 mW	24 mW	27% improvement

Table3: QoR comparison b/w Run1 and Run 2 for Design2

The Quality of Results (QoR) comparison table between the base run Run1 and Run3 (where full multibit mapping is not enabled) for Design1 is as below.

	Run1	Run3	% Change
TNS	0.0255	0.0270	0.02% degradation
WNS	0.13	0.129	No change
AREA	1866796	1829495	4% improvement
POWER	1000mw	600 mW	40% improvement

Table4 QoR comparison b/w Run1 and Run 3 for Design1

The Quality of Results (QoR) comparison table between the base run Run1 and Run3 (where full multibit mapping is not enabled) for Design2 is as below

	Run1	Run3	% Change
TNS	0.00164	0.00170	0.04% degradation
WNS	8.01	9.0	12.5% degradation
AREA	995941	950238	4% improvement
POWER	33 mW	25 mW	24% improvement

Table3: QoR comparison b/w Run1 and Run3 for Design2

The congestion map is also compared between the runs for two designs as below

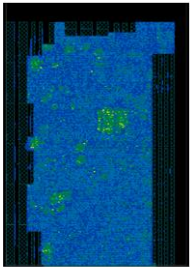
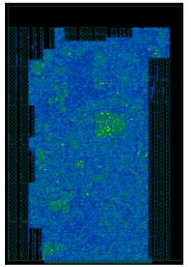
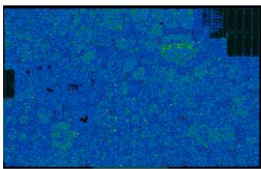
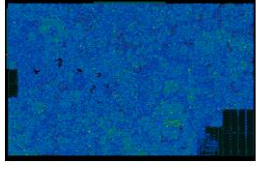
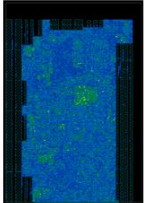
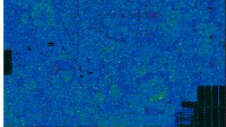
	Run1 (Congestion)	Run2 (Congestion)
Design1	Both Bgg: Overflow = 74131 Max = 6 (4 GRCs) GRCs = 81933 (1.14%) H routing: Overflow = 3020 Max = 3 (4 GRCs) GRCs = 3447 (0.10%) V routing: Overflow = 71330 Max = 6 (4 GRCs) GRCs = 78486 (2.19%) 	Both Dir: Overflow = 60938 Max = 6 (2 GRCs) GRCs = 66021 (0.92%) H routing: Overflow = 1906 Max = 2 (48 GRCs) GRCs = 2439 (0.07%) V routing: Overflow = 59032 Max = 6 (2 GRCs) GRCs = 63582 (1.76%) 
Design2	Both Bgg: Overflow = 78789 Max = 6 (6 GRCs) GRCs = 83664 (2.62%) H routing: Overflow = 76632 Max = 6 (6 GRCs) GRCs = 78686 (5.05%) V routing: Overflow = 2157 Max = 4 (1 GRCs) GRCs = 2978 (0.19%) 	Both Dir: Overflow = 88040 Max = 7 (1 GRCs) GRCs = 53972 (1.02%) H routing: Overflow = 76670 Max = 7 (1 GRCs) GRCs = 80394 (4.16%) V routing: Overflow = 11370 Max = 6 (1 GRCs) GRCs = 13578 (0.87%) 

Table4: Congestion comparison

The congestion for run3 is similar to run2. There are no red spots to make the design non routable and congestion is manageable.

	Design1	Design2
Run3	Both Bgg: Overflow = 48015 Max = 5 (1 GRCs) GRCs = 61975 (0.80%) H routing: Overflow = 1934 Max = 3 (1 GRCs) GRCs = 2296 (0.06%) V routing: Overflow = 4690 Max = 5 (1 GRCs) GRCs = 59679 (1.66%) 	Both Dir: Overflow = 80001 Max = 6 (2 GRCs) GRCs = 94230 (2.02%) H routing: Overflow = 76990 Max = 6 (2 GRCs) GRCs = 80857 (5.19%) V routing: Overflow = 11011 Max = 5 (4 GRCs) GRCs = 13172 (0.86%) 

CONCLUSION AND FUTURE WORK

From the experimental results it is observed that using multibit mapping technology

- The area is improved for both the designs significantly
- There is huge reduction in total power.
- There is no congestion degradation due to mapping to large cells.
- There is slight degradation in worst negative slack (WNS) and it is observed that the degradation is due to multibit cells in the critical path.
- There is sizeable degradation in Total Negative Slack (TNS). The most degradations are due to multibit cells in timing paths.

It is evident that the multibit technology helps to reduce the area and to reduce dynamic power dissipation for the design but there is a negative effect on the timing performance of the design. and dynamic power consumption.

The technology when used intelligently on the design can help provide better area, dynamic power without compromising on the timing Quality of Result. In run3 approach the sequential cells on timing critical path are not allowed to map to multibit cell to ensure timing degradation does not happen The future work can be comprised of taking the design through full flow in physical implementation like detailed placement and clock tree synthesis to compute the clock tree power and to develop a methodology for more intelligent mapping of multibit cells.

REFERENCES

[1] P. Girard, "Survey of Low-Power Testing of LVSII Circuits", in proc. IEEE Design and Test of Computers, May - June 2002,
 [2] Synopsys Design Compiler User Guide
 [3] Synopsys IC Compiler II User Guide
 [4] Wai Tung Ng, O Trescases "Power management for Modern VLSI loads using dynamic voltage scaling" in proc Proceedings. 7th International Conference on Solid-State and Integrated Circuits Technology, 2004.
 [5] Martn D.F.Wong "Low power design with multi-Vdd and voltage islands" 2007 7th International Conference on ASIC", in proc. IEEE Int. Test Conf., Nov. 2005, pp. 266-273.

Experimental Investigation on Glass Textile Reinforced Mortar Panels

^[1] Vybhav G V, ^[2] Dr. Putte Gowda B S, ^[3] Dr. Vathsala

^[1] PG Scholar, ^[2] Associate professor.

^{[1][2][3]} Department of Civil Engineering, B.I.T Bengaluru, Karnataka

^[1] vybhav10@gmail.com, ^[2] puttuji123@gmail.com, ^[3] vathsalagowda@gmail.com

Abstract:-- The alternative building material industry is seeing a boom as the infrastructure development, energy efficient low-cost housing and green building concept has increased in construction industry. Among the advanced alternative material, the ferrocement is one of the promising low-cost green material. The ferrocement consist of closely spaced multiple layer of wire mesh embedded in cement mortar. The main disadvantage is the chance of corrosion of wire mesh. Replacement of steel wire mesh with some other suitable material is a major concern. The glass textile fibre is readily available material and the glass textile reinforced mortar is an emerging technology that differ from the conventional ferrocement, where the textile fabric along with cement mortar used as standard material, it can be used as a substitute of wire mesh in composite structure. This study describes the results of testing glass textile reinforced panels reinforced with two and four layers and comparing them with conventional ferrocement panels. The main objective of the experimental test is to explore the possibility of replacing the wire mesh by TRM in ferrocement. Among the advanced alternative materials, the ferrocement is one of the promising low cost, green material. The experimental program is planned to study the behavior of ferrocement panel replaced with TRM. The investigation shows the TRM is effective and definitely a better alternative to the wire mesh and gives better understanding and knowledge of TRM.

Keywords: Textile reinforced matrix, ferrocement, Flexural Strength, Ultimate Strength, Layers and Panels.

1. INTRODUCTION

The union of reinforcement material and matrix is described as a composite material. The composite materials properties are better than the individual components properties. For strength and stiffness of the composite material the main load-bearing component is reinforcement. Fibre particles and flakes are included in reinforcement arrangement. Additionally, matrix protects it from chemical and physical damage and keeps the reinforcement in a given orientation. It is additionally in charge of the corresponding distribution of applied load between reinforcement element. Traditional materials like ceramics, polymers and metals are composite materials are generally employed do not satisfy the specific requirements of certain application. They may be designed to get a wide range of properties by altering ratios of process parameters and the type, constituent materials, their orientations and so on. Composite materials have low weight with high mechanical property which bring them as an ideal material for aerospace and automotive applications. Toughness, high fatigue resistance, thermal conductivity and corrosion resistance are other advantages of composites. High processing cost which avoid their wide-scale usage are the main disadvantage of composite. Fibre reinforcement basically contains continuous fibers and textile fabrics. Textile reinforced composite contains textile form as the

reinforcement and a polymer for the matrix phase. 2D or 3D knitted fabric, woven fabric, braids, non woven, multiaxial fabric, stitched fabric can be used as textile material. This textile formation has their own fibre architecture and combination of properties like stiffness, toughness, strength and flexibility are interpret to a performance of composite to an extent. Unlike textile architectures give huge future for designing the composite properties.

II. OBJECTIVES

1. To study the flexural behavior of the glass textile reinforced cementitious matrix panel in comparison with conventional ferrocement
2. Conduct the comparative study to explore the possibilities of using glass textile reinforced matrix as an alternative to ferrocement.

III. EXPERIMENTAL WORK

The experimental program is planned and preliminary investigations were conducted on the materials as per IS standards. The specimens were prepared and tested

Table I: Details of the panels

SL no	Designation	Panels Details	No of specimens
1	2LFP	Ferrocement panels 2 layers wire mesh	6
2	2LGTRM	2 layers glass textile reinforced mortar panel	3
3	4LGTRM	4 layers glass textile reinforced mortar panel	6



Fig 1 (a): Preparation of reinforcement

A. Mix proportion

The cement mortar mix design is for grade MM 7.5 obtained as per IS: 2250-1981 guidelines. The proportion adopted as per mix design is 1:3 based on strength and workability water cement ratio was selected as per IS 5512- 1983, the matrix proportion is 1:3 with w/c ratio of 0.56 as it gives 125% of spread.

Table II: Compressive strength test results of mortar cubes

Sl. No	Proportion	days	Compressive strength (N/mm ²)	Avg. comp strength (N/mm ²)
1	1:3	7	17.12	17.16
2			17.39	
3			16.98	
4		28	23.07	24.13
5			21.26	
6			28.08	



Fig 1 (b): Casting of panel specimens

B. Casting of Panel Specimens

Totally 15 panels were casted and tested, the specimen's size was selected to suit the capacity of the test equipment available in laboratory. All panels were 750 X 450 mm with 40mm thick. The clear cover of 5mm was provided on all faces.

C. Flexural Strength Test

The assumed loading was two-point loading. The load is transferred to panel using two 25mm rods, to have a pure bending in the panels. The load was applied using the control valve in the UTM with constant increment up to the ultimate load or failure load. The initial load applied was 40kg and 80kg respectively for longer span and shorter span. To calculate the deflection of the panel dial gauge readings were noted at every interval of load. The deflection at the center point of the panel was measured by using dial gauge. The load was incremented

manually, the load increment is 40kg for longer span and 80kg shorter span and the readings of dial gauge were taken at each interval. The measured deflection results were tabulated. The load at the corresponding load to the first crack was noted down. At increment of every load the propagation of old cracks and appearance of any fresh crack were clearly marked. The respective load levels were marked. The crack pattern was painted using pen marker and the photographs of each of the panels were taken after failure. the duration of testing for each panel was around 1 hour.



Fig 2: Flexural testing of panels

IV. RESULTS AND DISCUSSION

After testing of all the panels, first crack load, ultimate load and max deflection were noted and tabulated in table below.

Table III: Test results for longer span

Panel Designation	Load At First-Crack (kN/m ²)	Ultimate-Load (kN/m ²)	Deflection (mm)
4LGTRM-1LS	11.18	12.75	4.73
4LGTRM-2LS	10.20	11.96	4.128
4LGTRM-3LS	11.37	13.37	5.01
2LGTRM-1LS	7.12	8.83	2.931
2LGTRM-2LS	6.67	7.85	3.387

2LGTRM-3LS	6.67	8.24	3.458
2LFP-1LS	6.13	9.18	3.657
2LFP-2LS	7.65	9.57	5.28
2LFP-3LS	5.88	7.45	3.21

Table IV: Test results for shorter span

Panel Notation	Load At First-Crack (kN/m ²)	Ultimate-Load (kN/m ²)	Deflection (mm)
4LGTRM-1SS	20.01	23.15	3.642
4LGTRM-2SS	17.65	18.33	3.325
4LGTRM-3SS	18.44	20.01	3.698
2LFP-1SS	10.20	12.00	3.021
2LFP-2SS	10.98	12.00	3.358
2LFP-3SS	9.42	11.77	2.998

A. Combined load vs deflection curve

To understand the behavior of glass textile reinforced panel in flexure, the average behavior of combined load vs deflection curve was drawn for both longer span and for shorter span and presented in figure3 (a) and 3 (b) from the curve it is observed that the conventional ferrocement panel and glass textile reinforced mortar showed similar behavior up to cracking load i.e. the curve shows linear variation. But the glass textile reinforced panels showed more stiffness than conventional ferrocement panel. The glass textile reinforced panels show more ductile behavior than conventional ferrocement panel. The glass textile reinforced panels with 2 layers and 4 layers carry more load than that of the conventional ferrocement panel.

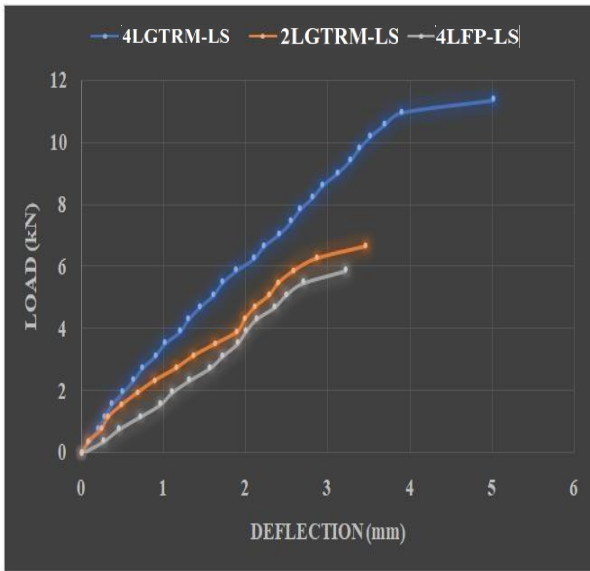


Fig 3 (a): Combined Load vs Deflection curve of glass textile reinforced panel and ferrocement panel in longer span.

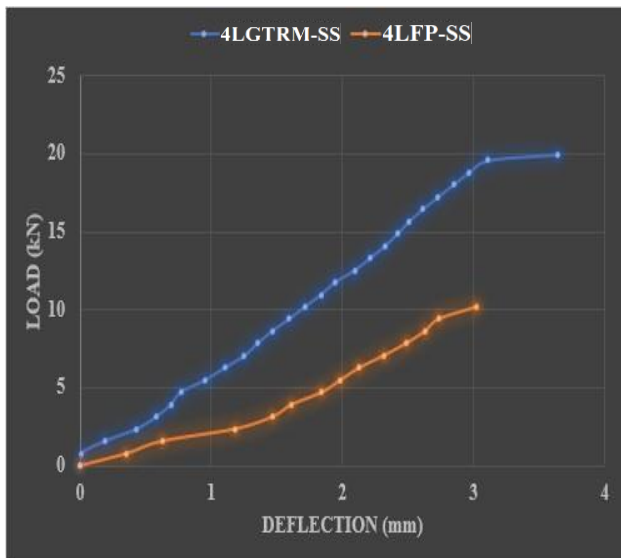


Fig 3 (b): Combined Load vs Deflection curve of glass textile reinforced panel and ferrocement panel in shorter span.

B. Crack pattern

Cracks were observed and marked and photograph are presented in Fig 4 (a) and 4 (b).



Fig 4 (a): Crack pattern of two point loading flexural test in longer span

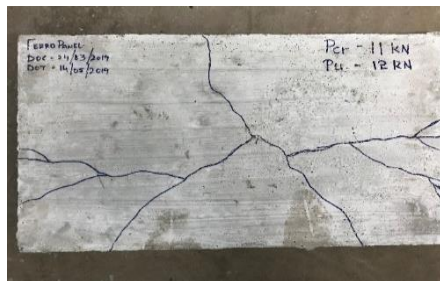
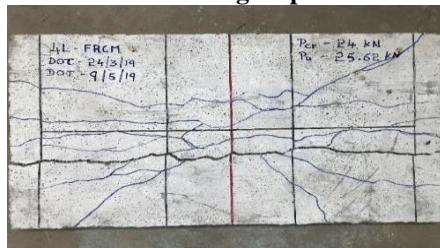


Fig 4 (b): Crack pattern of two point loading flexural test in shorter span

V. CONCLUSIONS

Based on the experimental investigation conducted on ferrocement and glass textile reinforced mortar panels following conclusions can be made

1. Fabrication and construction of glass textile reinforced panels are easier compared to conventional ferrocement panels.
2. The cracking load as well as breaking load increases as the number of glass textile reinforcement layer is increased, further research needed to decide the optimum value.
3. The load carrying capacity of the glass textile reinforced mortar panel substantially increased. The increase in cracking load is around 40.7% when tested along longer span and 46.5% for shorter span when compared with conventional ferrocement panel.
4. The ultimate load carrying capacity of glass textile reinforced mortar panel is higher than conventional ferrocement panel it is about 35% more when tested along longer span and 42% along shorter span.
5. The crack pattern shows when tested along longer span it behaves as one-way slab and when tested along shorter span behaves as two-way slab.
6. The glass textile reinforced panels are corrosion free and a serious limitation of ferrocement is that the steel reinforcement in the existing mortar system is highly prone to corrosion.

REFERENCES

- [1] Niteen Deshpande, Mohan Shirsath “Comparative study between bamboo reinforced and conventional ferrocement panels”, IJRPET: international journal of research publications in engineering and technology. Vol-02, Issue-07. July 2016 ISSN 2229-55188.
- [2] Lampros N. Koutas; Ph. D; and Dionysios. A. Bournas; “Flexural Strengthening of Two-Way RC Slabs with Textile-Reinforced Mortar: Experimental Investigation and Design Equations”, J. Compos. Constr., 2017, 21(1): 04016065(ASCE).
- [3] Zhong-Feng Zhu¹, Wen-Wei Wang, Kent A. Harries and Yu-Zhou “Uniaxial Tensile Stress–Strain Behaviour of Carbon-Fiber Grid–Reinforced Engineered Cementitious Composites”, J. Compos. Constr., 2018, 22(6): 04018057. ASCE.
- [4] Randhir J. Phalke¹, Darshan G. Gaidhankar², “Flexural behaviour of ferrocement slab panels using welded square mesh by incorporating steel fibers.” IJRET: International Journal of Research in Engineering and Technology

- [5] S Jaganathan and P Sudharsanamurthy “An experimental study of geogrid in ferrocement panels”, International Journal of Emerging Trends in Science and Technology. Vol-03, Issue-03. March 2016 ISSN 2348-9480.
- [6] Ibrahim G. Shaaban, Yousry B. Shaheen, Essam L. Elsayed, Osama A. Kamal, Peter A. Adesina “Flexural characteristics of lightweight ferrocement beams with various types of core materials and mesh reinforcement”, Construction and Building Materials 171 (2018) 802–816. Elsevier.
- [7] S. Jeeva Chithambaram and Sanjay Kumar “Flexural behavior of bamboo based ferrocement slab panels with fly ash”, Construction and Building Materials 134 (2017) 641–648. Elsevier.
- [8] Usman Ebead, Kshitij C. Shrestha, Muhammad S. Afzal, Ahmed El Refai, and Antonio Nanni, “Effectiveness of Fabric Reinforced Cementitious Matrix in Strengthening Reinforced Concrete Beams”, J. Compos. Constr., 2016, 04016084 (ASCE).
- [9] ACI 549.1R-93. Guide for the Design Construction, and Repair of Ferrocement, ACI Committee.
- [10] ACI 549R-97. Report on Ferrocement, ACI committee
- [11] Concrete Technology - M L Gambhir.

A Review on H-Mining-(High Utility Itemsets of Mining)

^[1] Hare Ram Singh, ^[2] Dr. Sheo Kumar

^[1] Research scholar, JJTU, Jhunjhunu, Rajasthan,

^[2] Professor & HOD, Dept of CSE, CMREC, Hyderabad

^[2] sheo2008@gmail.com

Abstract:-- High utility pattern mining is a rising information science task, which comprises of finding patterns having a high significance in databases. The utility of a pattern can be estimated regarding different target criteria's, for example, its benefit, recurrence, and weight. Among the different sorts of high utility patterns that can be found in databases, high utility itemsets are the most considered. A high utility itemset is a lot of qualities that shows up in a database and has a high significance to the client, as estimated by an utility capacity. High utility itemset mining sums up the issue of successive itemset mining by thinking about thing amounts and loads. A well known use of high utility itemset mining is to find all arrangements of things bought together by clients that return a high benefit. This paper gives a prologue to high utility itemsets mining, audits the best in class calculations

Keywords: high-utility itemset mining, frequent pattern mining, itemsets, pattern mining.

1. INTRODUCTION

The objective of data mining is to concentrate patterns or train models from databases to comprehend the past or foresee what's to come. Different kinds of data mining algorithms have been proposed to investigate data [1, 38]. A few algorithms produce models that work as secret elements. For instance, a few sorts of neural networks are intended to perform forecasts all around precisely however can't be effectively deciphered by people. To extricate learning from data that can be comprehended by people, pattern mining algorithms are structured [27, 28]. The objective is to find patterns in data that are intriguing, helpful, as well as sudden. A bit of leeway of pattern mining more than a few other data mining methodologies is that finding patterns is a sort of solo learning as it doesn't require marked data. Patterns can be legitimately extricated from crude data, and after that be utilized to get data and bolster basic leadership. Pattern mining algorithms have been intended to separate different kinds of patterns, each giving diverse data to the client, and for extricating patterns from various sorts of data. Prevalent kinds of patterns are sequential patterns [27], itemsets [28], bunches, patterns, anomalies, and graph structures [38].

Research on pattern mining algorithms has begun during the 1990s with algorithms to find successive patterns in databases [2]. The primary calculation for continuous pattern mining is Apriori [3]. It is intended to find visit itemsets in client exchange databases. An exchange database is a lot of records (transactions) demonstrating

the things acquired by clients at various occasions. A successive itemset is a gathering of qualities (things) that is every now and again acquired by clients (shows up in numerous transactions) of an exchange database. For instance, a successive itemset in a database might be that numerous clients purchase the thing noodles with the thing zesty sauce. Such patterns are effectively reasonable by people and can be utilized to help basic leadership. For example, the pattern {noodles, fiery sauce} can be utilized to take advertising choices, for example, co-advancing noodles with zesty sauce. The disclosure of successive itemsets is a well-examined data mining task, and has applications in various areas. It very well may be seen as the general undertaking of dissecting a database to discover co-happening esteems (things) in a lot of database records (transactions) [10, 16, 20, 37, 61]. To address this constraint of successive itemset mining, a rising examination zone is the disclosure of high utility patterns in databases [31, 52, 56, 58, 59 and 62]. The objective of utility mining is to find patterns that have a high utility (a high significance to the client), where the utility of a pattern is communicated as far as an utility capacity. A utility capacity can be characterized as far as criteria, for example, the benefit produced by the clearance of a thing or the time spent on site pages. Different sorts of high utility patterns have been examined. This section overviews explore on the most mainstream type, which is high utility itemsets [83]. Mining high utility itemsets can be viewed as a speculation of the issue of successive itemset mining where the information is an exchange database where everything has a weight speaking to its significance, and where things can have non paired amounts in

transactions. This general issue plan permits demonstrating different errands, for example, finding all itemsets (sets of things) that return a high benefit in an exchange database, discovering sets of site pages where clients invest a lot of energy, or discovering every single successive pattern as in customary regular pattern mining. High utility itemset mining is a functioning examination region. This section gives a complete overview of the field.

2. PROBLEM DEFINITIONS

This segment presents the issue of high utility itemset mining [31, 52, 56, 58, 59]. And afterward clarifies how it is summed up. Key Algorithms of high utility itemset mining are introduced.

2.1 High Utility Itemset Mining.

The issue of continuous itemset mining comprises of removing patterns from an exchange database.

The issue of continuous itemset mining has been read for over two decades. Various algorithms have been proposed to find incessant patterns proficiently, including Apriori [2], FP-Growth [39], Eclat [41], LCM [51] and H-Mine [52]. Albeit visit itemset mining has numerous applications, a solid presumption of regular itemset mining is that continuous patterns are helpful or intriguing to the client, which isn't in every case genuine. To address this significant impediment of conventional regular pattern mining, it has been summed up as high utility itemset mining, where things are commented on with numerical qualities and patterns are chosen dependent on a client characterized utility capacity.

2.2 High Utility Itemset Mining

The assignment of high utility itemset mining [31, 52, 56, 58, 59] comprises of finding patterns in a summed up kind of exchange database called quantitative exchange database, where extra data is given, that is the amounts of things in transactions, and loads showing the overall significance of everything to the client.

2.2.1 High-Utility Itemsets Mining algorithms

These algorithms find patterns having a high utility (significance) in various types of data.

a) Algorithms for mining high utility itemsets in a transaction database having profit information

i. The EFIM algorithm

Acquainted a few new thoughts with all the more proficiently find high-utility itemsets EFIM depends on two new upper-limits named reexamined sub-tree utility and nearby utility to all the more adequately prune the

pursuit space. It additionally presents a novel cluster based utility checking method named Fast Utility Counting to compute these upper-limits in direct reality. Besides, to diminish the expense of database examines, EFIM proposes proficient database projection and exchange blending methods named High-utility Database Projection (HDP) and High-utility Transaction Merging (HTM), likewise performed in straight time.

ii. The FHM algorithm

A tale procedure dependent on the investigation of thing co-occurrences to lessen the quantity of join tasks The FHM (Fast High-Utility Miner) diminishes the quantity of join tasks by up to 95 % and is up to multiple times quicker than the best in class calculation HUI-Miner.

iii. The HUI-Miner algorithm

HUI- HUI-Miner utilizes a novel structure, called utility-list, to store both the utility data about an itemsets and the heuristic data for pruning the inquiry space of HUI-Miner. By maintaining a strategic distance from the costly generation and utility computation of various up-and-comer itemsets, HUI-Miner can proficiently mine high utility itemsets from the utility records constructed from a mined database.

iv. The UFH algorithm

HUI-Miner utilizes a novel structure, called utility-list, to store both the utility data about an itemsets and the heuristic data for pruning the inquiry space of HUI-Miner. By maintaining a strategic distance from the costly generation and utility computation of various up-and-comer itemsets, HUI-Miner can proficiently mine high utility itemsets from the utility records constructed from a mined database.

v. The IHUP algorithm

Incremental and interactive data mining give the capacity to utilize past data structures and mining brings about request to decrease superfluous estimations when a database is refreshed, or when the base threshold is changed. The three novel tree structures to proficiently perform incremental and interactive HUP mining, the primary tree structure, Incremental HUP Lexicographic Tree (IHUPL-Tree), is organized according to a thing's lexicographic request. It can catch the incremental data with no rebuilding task. The second tree structure is the IHUP Transaction Frequency Tree (IHUPTF-Tree), which acquires a compact size by organizing items according to their transaction frequency (descending order). To diminish the mining time, the third tree, IHUP-Transaction-Weighted Utilization Tree

(IHUPTWU-Tree) is planned dependent on the TWU estimation of items in descending order.

The following algorithms also used for discovering patterns having a high utility (importance) in different kinds of data.

vi).The Two-Phase algorithm vii).The UP-Growth algorithm viii).The UP-Hist algorithm ix).The d2HUP algorithm x).The HUP-Miner algorithm xi).The mHUIMiner algorithm xii).The HMiner algorithm xiii).The ULB-Miner algorithm xiv).The UP-Growth+ algorithm

b) Algorithm for efficiently mining high-utility itemsets with length constraints in a transaction database

o The FHM+ Algorithm

FHM+ for mining HUIs, while considering length constraints. To discover HUIs efficiently with length constraints, FHM+ introduces the concept of Length UpperBound Reduction (LUR), and two novel upper-bounds on the utility of itemsets.

c) Algorithm for mining correlated high-utility itemsets in a transaction database

o The FCHM_bond algorithm and The FCHM_allconfidence algorithm, to use the bond measure FCHM (Fast Correlated high-utility itemset Miner), to efficiently discover correlated high-utility itemsets using the bond measure, FCHM is up to two orders of magnitude faster than FHM, and can discover more than five orders of magnitude less patterns by only mining correlated HUIs.

d) Algorithm for mining high-utility itemsets in a transaction database containing negative unit profit values

o The FHN Algorithm (Fast High-utility Miner)

Discovers HUIs without generating candidates and introduces several strategies to handle items with negative unit profits efficiently. Experimental results with six real-life datasets shows that FHN is up to 500 times faster and can use up to 250 times less memory than the state-of-the-art algorithm HUIINIV-Mine

o The HUIINIV-Mine Algorithm

HUIINIV (High Utility Itemsets with Negative Item Values)-Mine, for efficiently and effectively mining high utility itemsets from large databases with consideration of negative item values

e) Algorithm for mining on-shelf high-utility itemsets in a transaction database containing information about time periods of items

o The FOSHU Algorithm

Incremental and interactive data mining give the capacity to utilize past data structures and mining brings about request to decrease superfluous estimations when a

database is refreshed, or when the base threshold is changed. The three novel tree structures to proficiently perform incremental and interactive HUP mining, the primary tree structure, Incremental HUP Lexicographic Tree (IHUPL-Tree), is organized according to a thing's lexicographic request. It can catch the incremental data with no rebuilding task. The second tree structure is the IHUP Transaction Frequency Tree (IHUPTF-Tree), which acquires a compact size by organizing items according to their transaction frequency (descending order). To diminish the mining time, the third tree, IHUP-Transaction-Weighted Utilization Tree (IHUPTWU-Tree) is planned dependent on the TWU estimation of items in descending order.

The Algorithms listed bellow, classified according to type of search on database, techniques used and etc., with name and small description, which are very useful in HUIs.

f) Algorithm for mining frequent high-utility itemsets in a transaction database

1.The TS-HOUN Algorithm 2.The FHMFreq Algorithm, a variation of the FHM Algorithm

g) Algorithm for incremental high-utility itemset mining in a transaction database

1.The EIHI Algorithm 2.The HUI-LIST-INS Algorithm

h) Algorithm for mining concise representations of high-utility itemsets in a transaction database

1.The HUG-Miner Algorithm for mining high-utility generators 2.The GHUI-Miner Algorithm for mining generators of high-utility itemsets 3.The MinFHM Algorithm for mining minimal high-utility itemsets 4.The EFIM-Closed Algorithm for mining closed high-utility itemsets 5.The CHUI-Miner Algorithm for mining closed high-utility itemsets 6.The CHUD Algorithm for mining closed high-utility itemsets 7.The CHUI-Miner(Max) Algorithm for mining maximal high utility itemsets 8.Algorithm for mining the skyline high-utility itemsets in a transaction database 9.The SkyMine Algorithm

i) Algorithm for mining the top-k high-utility itemsets in a transaction database

1.The TKU Algorithm, obtained from UP-Miner under GPL license 2.The TKO-Basic Algorithm

j) Algorithms for mining the top-k high utility itemsets from a data stream with a window

The FHMDS and FHMDS-Naive Algorithms

k) Algorithm for mining frequent skyline utility patterns in a transaction database

The SFUPMinerUemax Algorithms

l) Algorithm for mining quantitative high utility itemsets in a transaction database:

The VHUQI Algorithm

m) Algorithm for mining high-utility sequential rules in a sequence database

The HUSRM Algorithm

n) Algorithm for mining high-utility sequential patterns in a sequence database

The USPAN Algorithm

o) Algorithm for mining high-utility probability sequential patterns in a sequence database

1.The PHUSPM Algorithm 2. The UHUSPM Algorithm

p) Algorithm for mining high-utility itemsets in a transaction database using evolutionary Algorithms

1.The HUIM-GA Algorithm 2.The HUIM-BPSO Algorithm 3.The HUIM-GA-tree Algorithm 4.The HUIM-BPSO-tree Algorithm 5.The HUIF-PSO Algorithm 6.The HUIF-GA Algorithm 7.The HUIF-BA Algorithm

q) Algorithm for mining high average-utility itemsets in a transaction database

1.The HAU-Miner Algorithm for mining high average-utility itemsets 2.The EHAUPM Algorithm for mining high average-utility itemsets 3.The HAU-MMAU Algorithm for mining high average-utility itemsets with multiple thresholds 4.The MEMU Algorithm for mining high average-utility itemsets with multiple thresholds

r) Algorithms for mining high utility episodes in a sequence of complex events (a transaction database)

1.The TUP Algorithm for mining frequent periodic patterns in a sequence of transactions (a transaction database) 2.The UP-SPAN Algorithm for mining periodic high-utility patterns (periodic patterns that yield a high profit) in a sequence of transactions (a transaction database) containing utility information

s) Algorithms for mining periodic high-utility patterns (periodic patterns that yield a high profit) in a sequence of transactions (a transaction database) containing utility information

The PHM Algorithm

t) Algorithms for discovering irregular high utility itemsets (non periodic patterns) in a transaction database with utility information

The PHM_irregular Algorithm, which is a simple variation of the PHM Algorithm

u) Algorithm for discovering local high utility itemsets in a database with utility information and timestamps

The LHUI-Miner Algorithm

v) Algorithm for discovering peak high utility itemsets in a database with utility information and timestamps

The PHUI-Miner Algorithm

2.3 A Comparison of High Utility Itemset Mining Algorithms

This segment has given an outline of some well known high utility itemset mining algorithms. The Table no 1 gives a comparison of their attributes regarding sort of inquiry (breadth-first hunt or depth-first pursuit), the quantity of phases (one or two), database portrayal (horizontal or vertical), and the most comparative frequent itemset mining algorithm.

Table no 1: Algorithms for high utility itemset mining

Algorithm	Search type	No of phases	DB representation	Extends
Two-Phase	breadth-first	Two	Horizontal	Apriori
PB	breadth-first	Two	Horizontal	Apriori
IHUP	depth-first	Two	Horizontal(prefix tree)	FP-Growth
UPGrowth(+)	depth-first	Two	Horizontal (prefix-tree)	FP-Growth
HUP-Growth	depth-first	Two	Horizontal (prefix-tree)	FP-Growth
MU-Growth	depth-first	Two	Horizontal (prefix-tree)	FP-Growth
D2HUP	depth-first	One	Vertical (hyper structure)	H-Mine
HUI-Miner	depth-first	One	Vertical (utility-lists)	Eclat
FHM	depth-first	One	Vertical (utility-lists)	Eclat
mHUIMiner	depth-first	One	Vertical (utility-lists)	Eclat
HUI-Miner*	depth-first	One	Vertical (utility-lists*)	Eclat
ULB-Miner	depth-first	One	Vertical (buffered utility-lists)	Eclat
EFIM	depth-first	One	Horizontal (with merging)	LCM

3. RESEARCH OPPORTUNITIES

Despite the fact that the issue of high utility itemset mining has been read for more than 10 years, and various papers have been distributed on this subject, there are various research opportunities. We have distinguished four kinds of opportunities:

Novel applications: The first research opportunities are to apply existing pattern mining algorithms in new courses as far as application spaces. Since pattern mining algorithms are very broad, they can be connected in a huge number of spaces. Specifically, the utilization of pattern mining strategies in developing examination territories, for example, informal community investigation, the Internet of Things, sensor networks gives a few novel conceivable outcomes regarding applications.

Enhancing the performance of pattern mining algorithms: Since pattern mining can be very tedious, particularly on thick databases, huge databases, or databases containing many long transactions, much research is continued growing more effective algorithms This is an important issue particularly for new augmentations of the high utility itemset mining issue, for example, on-rack high utility itemset mining or occasional high-utility itemset mining, which have been less explored. Numerous opportunities additionally lies in conveyed, GPU, multi-

core or parallel algorithm advancement to build speed and versatility of the algorithms.

Extending pattern mining to consider more complex data: Another exploration opportunity is to grow high utility pattern mining algorithms that can be connected on complex kinds of data.

Extending pattern mining to discover more complex and meaningful types of patterns: Identified with the above opportunity, another important issue to discover more complex sorts of patterns. Additionally, another exploration opportunity is to work on the assessment of patterns utilizing for instance novel measures, since it is likewise key to guarantee that the most fascinating or helpful patterns are found.

4. OPEN-SOURCE IMPLEMENTATIONS

Usage of high utility pattern mining algorithms are offered in the SPMF data mining library (<http://www.philippe-fournier-viger.com/spmf/>) [21, 25]. It offers more than 180 algorithms for mining patterns, for example, high utility patterns, itemsets, sequential patterns, sequential principles, occasional patterns, and affiliation rules. It is a multi-platform library created in Java and discharged under the GPL3 permit. It is intended to be effectively incorporated in other Java software programs, and can be kept running as standalone software utilizing its command-line or graphical UI. Standard datasets for seat stamping high utility itemset and pattern mining algorithms can be found on the SPMF site at <http://www.philippe-fournier-viger.com/spmf/index.php?link=datasets.php>.

5. CONCLUSION

High-utility itemset mining is a functioning field of research having various applications. This paper has displayed the issue of high-utility itemset mining, examined the principle strategies for exploring the inquiry space of itemsets, utilized by high-utility itemset mining algorithms. At that point, the paper has talked about research opportunities and open-source software.

6. REFERENCES

[1]. Aggarwal,R, C.C.: Springer, Heidelberg (2015) Data mining: the textbook.
[2]. Srikant, R Agrawal, R., pp. 487–499. Morgan Kaufmann (1994) : Fast algorithms for mining association rules. In: Proc. 20th int. conf. very large data bases,
[3]. Tanbeer, S.K., Jeong, B.S.,Ahmed, C.F.,: ETRI journal 32(5), 676–686 (2010). A novel approach for

mining high-utility sequential patterns in sequence databases.

[4]. Jeong, B.S., Choi, H.J.Ahmed, C.F., Tanbeer, S.K.: Information Sciences. 181(21), 4878–4894 (2011) A framework for mining interesting high utility patterns with a strong frequency affinity.
[5]. Jeong, B.-S., Lee, Y.-K Ahmed, C.F., Tanbeer, S.K.,: IEEE Trans. Knowl. Data Eng. 21(12), 1708–1721 (2009) Efficient Tree Structures for High-utility Pattern Mining in Incremental Databases.
[6]. Karagoz, P, Alkan, O.K.,: Crom and huspext: IEEE Trans. Knowl. Data Eng. 27(10), 2645–2657 (2015): Improving efficiency of high utility sequential pattern extraction.
[7]. Goyal, V Bansal, R., and Dawar, S.. In: Proc. Intern. Conf. on Big Data Analytics, 84–98. Springer (2015) : An efficient algorithm for mining high-utility itemsets with discount notion.
[8]. Yu,J, B, Rissanen, Barron, A. J.. IEEE Transactions on Information Theory. 44(6), 2743–2760 (1998) : The minimum description length principle in coding and modeling.
[9]. Ben Yahia and Bouasker, S., S. In: Proc. 30th Symp. on Applied Computing, pp. 851-856. ACM (2015) : Key correlation mining by simultaneous monotone and anti-monotone constraints checking.
[10]. Dimitropoulos, X., Brauckhoff, D., Salamatian, K Wagner, A., IEEE/ACM Transactions on Networking, 20(6), 1788– 1799 (2012) : Anomaly extraction in backbone networks using association rules.
[11]. Chan, R., Yang, Q., Shen, Y. In: Proc. of 3rd IEEE Int’l Conf. on Data Mining, pp. 19–26. IEEE (2003) : Mining High Utility Itemsets.
[12]. Chi, T.T., Fournier-Viger, P. In: Fournier-Viger et al. (eds). High-Utility Pattern Mining: Theory, Algorithms and Applications, to appear. Springer (2018) : A Survey of High Utility Sequential Patten Mining.
[13]. Chu, C., Tseng, V.S. Liang, T. Applied Mathematics and Computation 215(2), 767–778 (2009) : An Efficient Algorithm for Mining High Utility Itemsets with Negative Item Values in large databases.
[14]. Dam, T.-L., Li, K., Fournier-Viger, P., Duong, H. Frontiers of Computer Science, doi: <https://doi.org/10.1007/s11704-016-6245-4>. Springer (2018) : CLS-Miner: Efficient and Ef-fective Closed High utility Itemset Mining.
[15]. Dam, T.-L., Li, K., Fournier-Viger, P., Duong, H. Knowledge and Information Systems 52(2), 621–655 (2017) : An efficient algorithm for mining top-k on-shelf high utility itemsets.
[16]. Duan, Y., Fu, X., Luo, B., Wang, Z., Shi, J., Du, X.: Detective In: Proc. 2015 IEEE International Conf. on Communications, pp. 5691–5696. IEEE (2015) :

Automatically identify and analyze malware processes in forensic scenarios via DLLs.

[17]. Duong, Q.H., Fournier-Viger, P., Ramampiaro, H., Norvag, K. Dam, T.-L. *Applied Intelligence* 48(7), 1859–1877 (2017): Efficient High Utility Itemset Mining using Buffered Utility-Lists.

[18]. Duong, Q.-H., Liao, B., Fournier-Viger, P., Dam, T.-L. *Knowledge-Based Systems* 104, 106–122 (2016) : An efficient algorithm for mining the top-k high utility itemsets, using novel threshold raising and pruning strategies.

[19]. Duong, H., Ramampiaro, H., Norvag, K., Fournier-Viger, P., Dam, T.-L. *Knowledge-Based Systems* 157(1), 34–51 (2018) : High Utility Drift Detection in Quantitative Data Streams.

[20]. Fernando, B., Elisa F., Tinne T. In: *Proc. 12th European Conf. on Computer Vision*, pp. 214–227. Springer (2012) : Effective use of frequent itemset mining for image classification.

[21]. Fournier-Viger, P., Gomariz, A., Gueniche, T., Soltani, A., Wu, C.W., Tseng, V.S. *Journal of Machine Learning Research*, 15,3389–3393 (2014) : SPMF: a Java Open-Source Pattern Mining Library,

[22]. Fournier-Viger, P., Lin, J.C.-W., Duong, Q.-H., Dam, T.-L. In: *Proc. 29th Intern. Conf. on Industrial, Engineering and Other Applications of Applied Intelligent Systems*, pp. 115–127. Springer (2016) : FHM+: Faster High-Utility Item-set Mining using Length Upper-Bound Reduction.

[23]. Fournier-Viger, P., Lin, J.C.-W., Gomariz, A., Soltani, A., Deng, Z., Lam, H.T. In: *Proc. 19th European Conf. on Principles of Data Mining and Knowledge Discovery*, pp. 36–40. Springer (2016) : The SPMF Open-Source Data Mining Library Version 2.

[24]. Fournier-Viger, P., Lin, C.W., Wu, C.-W., Tseng, V.S., Faghihi, U.: Mining Minimal High-Utility Itemsets. *Proc. 27th International Conf. on Database and Expert Systems Applications*, pp. 88-101. Springer (2016)

[25]. Fournier-Viger, P., Wu, C.W., Tseng, V.S.: Novel Concise Representations of High Utility Itemsets using Generator Patterns. In: *Proc. 10th Intern. Conf. on Advanced Data Mining and Applications*, pp. 30–43. Springer (2014)

[26]. Fournier-Viger, P., Zida, S. Lin, C.W., Wu, C.-W., Tseng, V. S.: EFIM-Closed: Fast and Memory Efficient Discovery of Closed High-Utility Itemsets. In: *Proc. 12th Intern. Conf. on Machine Learning and Data Mining*, pp. 199–213. Springer (2016)

[27]. Gan, W., Lin, J.C.-W., Fournier-Viger, P., Chao, H.C.: More efficient algorithms for mining high-utility itemsets with multiple minimum utility thresholds.

In: *Proc. 26th International Conf. on Database and Expert Systems Applications*, pp. 71–87. Springer (2016)

[28]. Glatz, E., Mavromatidis, S., Ager, B., Dimitropoulos, X.: Visualizing big network traffic data using frequent pattern mining and hypergraphs. *Computing* 96(1),27–38 (2014)

[29]. Han, J., Pei, J., Kamber, M.: *Data mining: concepts and techniques*. Elsevier, Amsterdam (2011)

[30]. Hegland, M.: The apriori algorithm—a tutorial. *Mathematics and computation in imaging science and information processing*. 11, 209–62 (2005)

[31]. Hong, T.P., Lee, C.H., Wang, S.L.: Mining High Average-Utility Itemsets. In: *Proc. of IEEE Int'l Conf. on Systems, Man, and Cybernetics*, pp. 2526-2530. IEEE (2009)

[32]. Krishnamoorthy, S.: Efficient mining of high utility itemsets with multiple minimum utility thresholds. *Engineering Applications of Artificial Intelligence* 69, 112–126 (2018)

[33]. Lan, G.-C., Hong, T.-P. Tseng, V.S.: Discovery of high utility itemsets from on-shelf time periods of products. *Expert Systems with Applications* 38, 5851–5857 (2011)

[34]. Lan, G.-C., Hong, T.-P., Tseng, V.S.: Efficiently mining high average-utility itemsets with an improved upper-bound strategy. *International Journal of Information Technology and Decision Making* 11(5), 1009–1030 (2012)

[35]. Lin, J.C.-W., Ren, S., Fournier-Viger, P., Hong, T.-P.: EHAUPM: Efficient High Average-Utility Pattern Mining with Tighter Upper-Bounds. *IEEE Access* 5, 12927–12940. IEEE (2017)

[36]. Lin, Y.C., Wu, C.W., Tseng, V.S.: Mining high utility itemsets in big data. In: *Proc. Pacific-Asia Conf. on Knowledge Discovery and Data Mining*, pp. 649–661. Springer (2015)

[37]. Liu, J., Wang, K., Fung, B.: Direct discovery of high utility itemsets without candidate generation, In: *Proc. 12th IEEE Intern. Conf. Data Mining*, pp. 984–989. IEEE (2012)

[38]. Lucchese, C., Orlando, S., Perego, R.: Fast and Memory Efficient Mining of Frequent Closed Itemsets. *IEEE Trans. Knowl. Data Eng.* 18(1),21–36 (2006)

[39]. Mukherjee, A., Liu, B., Glance, N.: Spotting fake reviewer groups in consumer reviews. In: *Proc. 21st international conference on World Wide Web*, pp. 191–200. ACM (2012)

[40]. Naulaerts, S., Meysman, P., Bittremieux, W., Vu, T.N., Berghe, W.V., Goethals, B, Laukens, K.: A primer to frequent itemset mining for bioinformatics. *Briefings in bioinformatics* 16(2), 216–231 (2015)

- [41]. Omiecinski, E.R.: Alternative interest measures for mining associations in databases. *IEEE Trans. Knowl. Data Eng.* 15(1), 57–69 (2003)
- [42]. Pei, J., Han, J., Lu, H., Nishio, S., Tang, S., Yang, D.: H-mine: Hyper-structure mining of frequent patterns in large databases. In: *Proc. 2001 IEEE Intern. Conf. Data Mining*, pp. 441–IEEE (2001)
- [43]. Peng, A.X., Koh, Y.S., Riddle, P.: mHUIMiner: A Fast High Utility Itemset Mining Algorithm for Sparse Datasets. In: *Pacific-Asia Conf. on Knowledge Discovery and Data Mining*, pp. 196–(2017)
- [44]. Qu, J.-F., Liu, M., Fournier-Viger, P.: Efficient algorithms for high utility itemset mining without candidate generation. In: Fournier-Viger et al. (eds). *High-Utility Pattern Mining: Theory, Algorithms and Applications*, to appear. Springer (2018)
- [45]. Ryang, H., Yun, U.: Top-k high utility pattern mining with effective threshold raising Strategies. *Knowl.-Based Syst.* 76, 109–126 (2015)
- [46]. Shie, B.-E., Yu, P.S., Tseng, V.S.: Efficient algorithms for mining maximal high utility itemsets from data streams with different models. *Expert Syst. Appl.* 39(17), 12947–12960 (2012)
- [47]. Song, W., Huang, C.: Discovering High Utility Itemsets Based on the Artificial Bee Colony Algorithm. In: *Proc. the 22nd Pacific-Asia Conf. Knowledge Discovery and Data Mining*, pp. 3–14. Springer (2018)
- [48]. Truong, T., Duong, H., Le, B., Fournier-Viger, P.: Efficient Vertical Mining of High Average-Utility Itemsets based on Novel Upper-Bounds. *IEEE Trans. Knowl. Data Eng.* DOI:10.1109/TKDE.2018.2833478 (2018)
- [49]. Tseng, V.S., Shie, B.-E., Wu, C.-W., Yu, P. S.: Efficient algorithms for mining high utility itemsets from transactional databases. *IEEE Trans. Knowl. Data Eng.* 25(8), 1772–1786 (2013)
- [50]. Tseng, V., Wu, C., Fournier-Viger, P., Yu, P.S. *IEEE Trans. Knowl. Data Eng.* 28(1), 54–67 (2016) : Efficient Algorithms for Mining Top-K High Utility Itemsets.
- [51]. Uno, T., Kiyomi, M., Arimura, H.: LCM ver. 2 In: *Proc. ICDM'04 Workshop on Frequent Itemset Mining Implementations*. CEUR (2004) : Efficient mining algorithms for frequent/closed/maximal itemsets.
- [52]. Yao, H., Hamilton, H. J. *Data and Knowledge Engineering* 59(3), 603–626 (2006) : Mining itemset utilities from transaction databases.
- [53]. Yao, H., Hamilton, H.J., Geng, L. In: *Proc. of ACM SIGKDD Workshop on Utility-Based Data Mining*, pp. 28-37. ACM (2006) : A Unified Framework for Utility-based Measures for Mining Itemsets.
- [54]. Yin, J., Zheng, Z. and Cao, L.: USpan *Proc. of the 18th ACM SIGKDD international conference on Knowledge discovery and data mining*, pp. 660–668. ACM (2012) : an efficient algorithm for mining high utility sequential patterns.
- [55]. Yun, U., D. Kim. *Future Generation Computer Systems* 68, 346-360 (2016) : Mining of high average-utility itemsets using novel list structure and pruning strategy.
- [56]. Yun, U., Ryang, H. *Applied Intelligence* 42(2), 323–352 (2015) :Incremental high utility pattern mining with static and dynamic databases.
- [57]. Yun, U., Ryang, H., Ryu, K.H. *Expert Syst. Appl.* 41(8),3861–3878 (2014) : High utility itemset mining with techniques for reducing overestimated utilities and pruning candidates.
- [58]. Yu, C.-V., Fournier-Viger, Tseng, V.-S ,P., Gu, J.-Y. in: *Proc. 2015 Conf. on Technologies and Applications of Artificial Intelligence*, pp. 187–194. IEEE (2015) : Mining Closed+ High Utility Itemsets without Candidate Generation.
- [59]. Fournier-Viger, P.,Wu, C.-W., Tseng, V.S, Yu., P.S., *Proc. 11th IEEE Intern. Conf. on Data Mining*, pp. 824– 833. IEEE (2011) : Efficient Mining of a Concise and Lossless Representation of High Utility Itemsets.
- [60]. Zaki, J.M. *IEEE Trans. Knowl. Data Eng.* 12(3), 372–390 (2000) : Scalable Algorithms for Association Mining.
- [61]. Zhang, L., , Su, Y, Cheng, F., Fu, G.,Qiu, J.. *Applied Soft Computing* 62, 974–986 (2018) : A multi-objective evolutionary approach for mining frequent and high utility itemsets.
- [62]. Tseng, V.S ,Zida, S., P., Wu, C.W., Lin, J.C.-W., and Fournier-Viger,. In: *Proc. 11th Intern. Conf. on Machine Learning and Data Mining*, pp. 157–171. Springer (2015) : Efficient Mining of High Utility Sequential Rules.
- [63]. Tseng, V.S ,Zida, S., P., Wu, C.W., Lin, J.C.-W., and Fournier-Viger,. In: *Proc. 14th Mexican Intern. Conf. Artificial Intelligence*, pp. 530–546. Springer (2015) : EFIM: A Highly Efficient Algorithm for High-Utility Itemset Mining.

Camera Model Identification

^[1] Kinjal Patel, ^[2] Prof.Hetal Gaudani

^[1] Department of Computer Engineering, G.H.Patel College Of Engineering and Technology, Bakrol, Anand, Gujarat

^[2] Assistant Professor, Department of Computer Engineering, G.H.Patel College Of Engineering and Technology Bakrol-, Anand, Gujarat.

^[1]kinjal445@gmail.com

Abstract:-- The Camera model is used to shoot a picture for solving wide series of forensic problems ,from copyright infrac- tion to owner's equity. In today's digital age , the manipulation of image is very simple by digital processing tools and they are widely available. An interesting problem in digital forensics is ,given a digital image , would it be possible to identify the camera model which was used to take the picture. Our goal is to classify camera model used in particular image. To identify camera model we will use intrinsic hardware artifacts and software artifacts which could be used by various machine learning algorithm(Logistic Regression, Support Vector Machine, K-Nearest Neighbors, Random Forest, Perceptron) to identify correct source camera of a image. we will carried out the experiment on dresden image dataset and try to get reasonable accuracy in distinguishing pictures.

Keywords: Camera Model Identification , Machine learn- ing algorithms, Forgery Detection, Image Source Identifica- tion, Digital Image Forensics.

1. INTRODUCTION

Everybody is keen on demonstrating that a specific picture is taken by his/her camera, so as to guarantee the property. Additionally ,when all is said in done an image was taken by specific camera, however it is vital component for choices in court and It can't depend on Meta data(EXIF labels) which can be effectively manipulated.It is noticed that in 2015 more than 1.8 billion pictures distributed on the web every day [12], and this pattern is going increasingly more every day. Source Iden- tification significantly depending on the Photo Response Non- Uniformity(PRNU) design , it is steady in time, it is begun by the inevitable flaws occurring amid the sensor producing process. Since each image is taken by specific camera has hints of PRNU Pattern, It can be dependable and conceivable distinguishing proof, Image Falsification identification and furthermore improving acknowledgment calculations.

As Indicated by the study PRNU approach isn't increasingly helpful in light of the fact that an extensive number of pictures taken by that camera is vital and furthermore it is outlandish without participation of the camera proprietor. Moreover, PRNU based systems are extraordinarily tedious and it can't be effectively connected to an extensive dataset of pictures. The yield picture is gotten by applying a few number of complex calculations; every one is described by parameters. For instance, Demoaicing and JPEG pressure, in this quantization lattice can be characterized by the client.

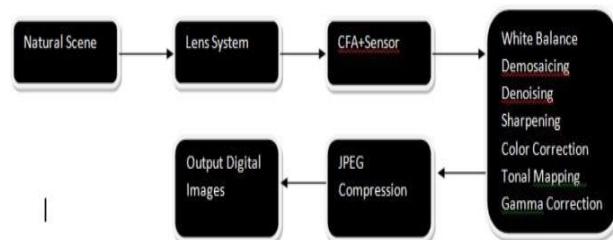


Fig. 1. Image Processing Pipeline in Digital Camera.

Figure 1. offers a rundown of a run of the mill picture process pipeline in computerized cameras. everything about stages generally upheld by plant made of different camera models. Past analysts have some expertise in beyond any doubt stages amid this pipeline like focal point abandons, Color Filter Array(CFA),Demosaicing, JPEG Compression , Denoising, Sharpening, white equalization and gamma amendment , and so on. Some mull over very one phases or entire pipeline.

Pragmatic trial settings for camera demonstrate recognizable proof need in more than one camera from every show with the top goal to evacuate the unclearness of whether or not the highlights, on that the classifiers square measure factory-made, catch camera show attributes or individual camera qualities [11-13]. within every model, testing footage ought not come back from an identical individual cameras that square measure related to getting ready. In any case, the bigger a part of the past appearance into simply utilize one camera to talk to a camera show thanks to the constraints of camera sources.

Parallel likeness measures (BSM) determined from 3 least essential piece planes was used in [10] for camera display ID.

close by another 2 sorts of capabilities (HOWS and IQM).

In this paper, we tend to propose to local paired examples (LBP) as connected math alternatives. Considering 8-neighbor dim dimension refinement for each picture component around a circle, fifty nine local paired example square measure sepa- rated, severally, from spacial area of red and unpracticed shad- ing channels, their expectation mistake second clusters, and along these lines the first dimension inclining swell subband of each picture. shifted AI calculation's Classifier's model square measure designed for grouping of eighteen camera models from 'Dresden Image Database'. Contrasted with the leads with writings, the identification exactness revealed amid this paper isway higher.

The rest of the paper is structured as follows. In Section two, the LBP options that we have a tendency to use, a way to extract options. In Section3, experimental works square measure given and a few discussions square measure created. Conclusions square measure drawn in Section four.

II. PROPOSED METHOD

In this section, we have a tendency to 1st provides a transient description of uniform native binary patterns planned in[15].Our planned featureextractionframework can th en be introduced. we have a tendency to 1st provides a transient description of uniform native binary patterns planned in [15].

Our planned feature extraction framework can then be introduced.

A. Local Binary Patterns[Feature Extraction Framework]

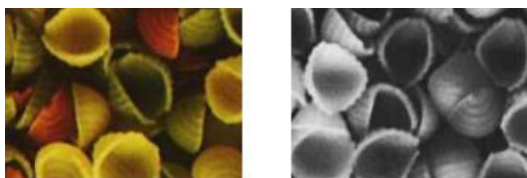


Fig. 2. A color texture and gray-scale version of image.

Surface examination ways are developedwithgray-scale pic- tures, naturally for all time reasons. People will essentially catch the surfaces on a surface, even with no shading informa- tion. Figure.2 demonstrates a photo of

tricolor nutritious glue and its dark scale adaptation. the sole factor that can't be told, upheld the dim scale information, is that the shade of the nutri- tious glue — the vibe itself is that the equivalent. The human tangible framework is prepared to translate much colorless scenes for example in low enlightenment levels. Shading acts even as a sign for more extravagant understandings. Indeed, even once shading information is misshaped, for example because of innate oddity, the tactile framework still works. Naturally, this implies at least for our tangible system,color and surface ar separate marvels. all the equivalent, the usage of joint colortexture alternatives has been a favored way to deal with paint surface examination

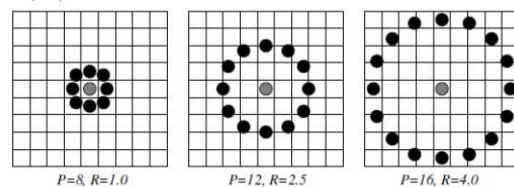


Fig. 3. Circularly trigonal neighbor sets. Samples that don't specifically match the picture element grid ar obtained via interpolation.

$$LBP_{P,R}(x_c, y_c) = \sum_{p=0}^{P-1} s(g_p - g_c)2^p. \tag{1}$$

wherever R is that the sweep of a circularly trigonal neigh- borhood utilized for local paired patterns calculation P is that the assortment of tests round the circle. In this paper, we set R =1, P =8 . c g and p g speak to dark dimensions of the center picture component and its neighbor pixels, severally. In pursue, Equation 2.1 means the signs of the variations in a very neighborhood ar taken as a P-bit binary variety, leading to 2^P distinct values for the LBP code. The native gray-scale distribution, i.e. texture, will therefore be close to delineated with a 2^P -bin distinct distribution of LBP codes:

$$T_{-}t(LBPP,R(xc, yc)). \tag{2}$$

Give us a chance to accept we are given a N M picture test (xc 2 0, . . . ,N 1, yc 2 0, . . . ,M 1).

In figuring the LBPP,R circulation (highlight vector) for this picture, the focal part is considered on the grounds that an adequately extensive neighborhood can't be utilized on the outskirts. The LBP code is determined for every pixel in the trimmed segment of the picture, and the circulation of the codes is utilized as a component vector, signified by S:igure 4. (Left) Constellation of neighborhood. (Right) Ex- amples of 'uniform' and 'non-uniform' neighborhood double

patterns.[11]

As indicated by Equations , graylevel contrast is first determined between focus pixel and its eight neigh-bors. The distinction will at that point be double quantized and coded, producing nearby twofold examples, which, basically, structure a 8-dimensional histogram with an aggregate of 28 of 256 canisters.

TABLE I
EXPERIMENTAL DATASET

List of Camera Models	# of cameras
Sony NEX-7	275
Motorola Moto X	275
Motorola Nexus 6	275
Motorola DROID MAXX	275
LG Nexus 5x	275
Apple iPhone 6	275
Apple Iphone 4s	275
HTC One M7	275
Samsung Galaxy S4	275
Samsung Galaxy Note 4	275

III. EXPERIMENTS AND DISCUSSIONS

A. Dataset for Experiments

We picked a comparable 10 camera models from 'Dresden Image Dataset' as used in [10]. The amount of camera contraptions for each model degrees from 2 to 5. The amount of pictures per exhibit is 275. All of the photos are prompt camera JPEG yields which are gotten with various camera settings. Nuances are given in Table 1.

Pictures in the test set were caught with a similar 10 camera models. For instance, if the pictures in the train information for the iPhone 6 were taken with Ben Hamner's gadget (Camera 1), the pictures in the test information were taken with Ben Hamner's subsequent gadget (Camera 2), since he lost the main gadget in the Bay while kite-surfing. None of the pictures in the test information were taken with a similar gadget as in the train information.

While the train data includes full images, the test data contains only single 512 x 512 pixel blocks cropped from the center of a single image taken with the device. No two image blocks come from the same original image.

B. Experimental Settings

In the majority of our analyses, Various Machine Learning Algorithm is prepared and utilized as the classifiers for testing. From the entire dataset, we haphazardly select one camera for each model, and utilize every one of the pictures taken by the chose cameras for testing. Pictures from the remainder of the cameras structure the preparation information. This

arbitrary determination methodology is iterated multiple times for each analysis. Including pictures from more than one camera of each model (aside from those have just 2 cameras) for preparing can significantly lessen the opportunity of overtraining[9]. Utilizing the cameras that are not associated with the preparation strategies for testing makes the investigations progressively handy [13]. entire dataset, we haphazardly select one camera for each model, and utilize every one of the pictures taken by the chose cameras for testing. Pictures from the remainder of the cameras structure the preparation information. This arbitrary determination methodology is iterated multiple times for each analysis. Including pictures from more than one camera of each model (aside from those have just 2

cameras) for preparing can significantly lessen the opportunity of overtraining[9]. Utilizing the cameras that are not associated with the preparation strategies for testing makes the investigations progressively handy [13].

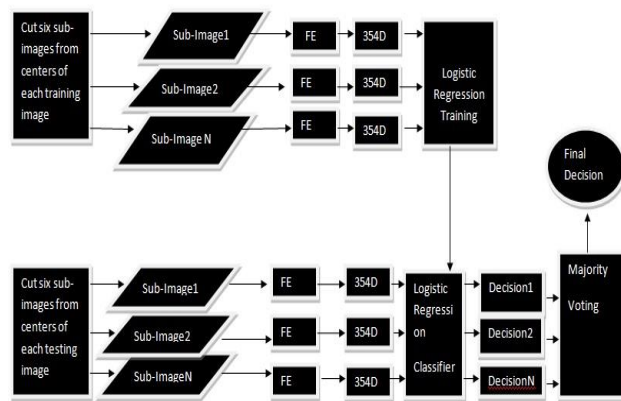


Fig. 5. Diagram of training and testing phases.
FE=Feature Extraction.

C. Results and Discussions

The proposed was tested on dataset of 10000 images with the 10 cross fold validation technique. This approach involves randomly dividing the set of observations into 10 groups, or folds, of approximately equal size. The first fold is treated as a validation set, and the method is fit on the remaining k -1 folds.

A confusion matrix is a table that is often used to describe the performance of a classification model (or "classifier") on a set of test data for which the true values are known.

As we can see in the below figure , I achieved highest accuracy in random forest algorithm that will be considered as an over fitting problem so the accuracy of SVM and Logistic regression gives good outcome.

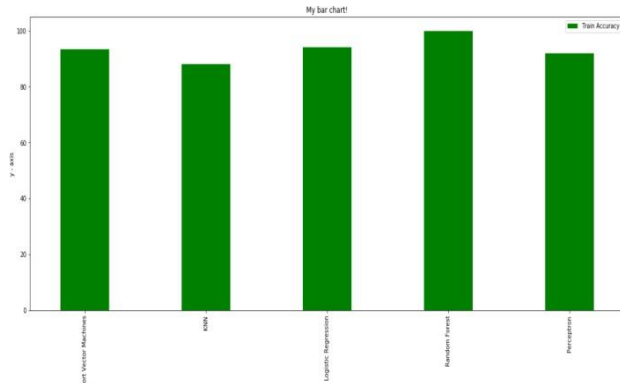


Fig 6. Bar Chart Graph of all algorithm

	Train Accuracy
Support Vector Machines	93.33
KNN	88.00
Logistic Regression	94.00
Random Forest	100.00
Perceptron	92.00

Fig 7. Accuracy of all proposed algorithms

REFERENCES

[1] Mehdi Kharrazi , Husrev T Sencur ', Nasir Memon ', " BLIND SOURCE CAMERA IDENTIFICATION",IEEE,0- 7803-8554-3/04/
 [2] J. Adams, K. Parulski, and K. Spaulding, "Color processing in digital cameras," Micm,IEEE, vol. 18, pp.20-30, Nov.-Dec 1998.
 [3] Z. Deng, A. Gijsenij, and J. Zhang, "Source camera identification using auto-white balance approximation," in Proc. 13th IEEE Int. Conf.Comput. Vis., Barcelona, Spain, Nov. 2011, pp. 57–64.
 [4] Amerini I, Becarelli R, Bertini B, Caldelli R (2015) Acquisition source identification through a blind image clas- sification. IET Image Process 9(4):329–337.
 [5] Avcibas, I, Memon N, Sankur B (2003) Steganaly- sis using image quality metrics. IEEE Trans Image Process 12(2):221–229.
 [6] Bayram S, Sencar H, Memon N (2006) Improvements on source camera-model identification based on CFA. In: Advances in Digital Forensics II, IFIP international conference on digital Forensics, pp 289–299.
 [7] Z. Deng, A. Gijsenij, and J. Zhang, "Source camera identification using auto-white balance approximation," in Proc. 13th IEEE Int. Conf.Comput. Vis., Barcelona, Spain, Nov. 2011, pp. 57–64.

[8] Camera Imaging Products Association, Exchangeable Image File Format for Digital Still Cameras: Exif Version 2.3, CIPA DC-008-2010
 [9] I. J. Cox, M. L. Miller, and J. A. Bloom, Digital Watermarking. San Francisco, CA, USA: Morgan Kaufmann, 2002.
 [10] Camera Imaging Products Association, Exchangeable Image File Format for Digital Still Cameras: Exif Version 2.3, CIPA DC-008-2010
 [11] G. Xu and Y. Q. Shi, "Camera model identification using local binary patterns," in International Conference on Multimedia and Expo (ICME), 2012 IEEE. 2012, pp. 392–397 [12] M. Chen, J. Fridrich, M. Goljan, and J. Lukas, "De- termining Image Origin and Integrity Using Sensor Noise," Information Forensics and Security, IEEE Transactions on, vol. 3,pp. 74-90, 2008
 [13] A. E. Dirik, H. T. Sencar, and N. Memon, "Digital Sin- gle Lens Reflex Camera Identification From Traces of Sensor Dust," Information Forensics and Security, IEEE Transactions on, vol. 3, pp. 539-552, 2008.
 [14] S. Bayram, H. Sencar, N. Memon, and I. Avcibas, "Source camera identification based on CFA interpolation," in Image Processing, 2005. ICIP 2005. IEEE International Conference on, 2005, pp. III-69-72.
 [15] Y. Long and Y. Huang, "Image Based Source Cam- era Identification using Demosaicking," in Multimedia Signal Processing, 2006 IEEE 8th Workshop on, 2006, pp. 419-424.
 [16] A. Swaminathan, W. Min, and K. J. R. Liu, "Non- intrusive component forensics of visual sensors using output images," Information Forensics and Security, IEEE Transac- tions on, vol. 2, pp. 91-106, 2007.
 [17] F. Marra, D. Gagnaniello, L. Verdoliva, On the vul- nerability of deep learning to adversarial attacks for camera model identification, Signal Processing:Image Communication (2018), <https://doi.org/10.1016/j.image.2018.04.007>.
 [18] Z. Deng, A. Gijsenij, and J. Zhang, "Source camera identification using auto-white balance approximation," in Proc. 13th IEEE Int. Conf.Comput. Vis., Barcelona, Spain, Nov. 2011, pp. 57–64.
 [19] Camera Imaging Products Association, Exchangeable Image File Format for Digital Still Cameras: Exif Version 2.3, CIPA DC-008-2010 JEITA CP-3451B Standard,2010. [20] E. Kee, M. K. Johnson,

and H. Farid, "Digital Image Authentication from JPEG Headers," *Information Forensics and Security, IEEE Transactions on*, vol. 6, pp. 1066-1075, 2011.

[21] M. C. Stamm and K. J. R. Liu, "Forensic detection of image manipulation using statistical intrinsic fingerprints," *IEEE Trans. Inf. Forensics Security*, vol. 5, no. 3, pp. 492–506, Sep. 2010.

[22] G. Xu, S. Gao, Y. Q. Shi, R. Hu, and W. Su, "Camera- Model Identification Using Markovian Transition Probability Matrix," in *Digital Watermarking*. vol. 5703, ed: Springer Berlin / Heidelberg, 2009, pp. 294-307.

[23] T. Gloe, K. Borowka, and A. Winkler, "Feature-Based Camera Model Identification Works in Practice," in *Information Hiding*. vol. 5806, ed: Springer Berlin / Heidelberg, 2009, pp. 262-276.

[24] M. J. Weinberger, G. Seroussi, and G. Sapiro, "LOCO-I: a low complexity, contextbased, lossless image compression algorithm," in *Data Compression Conference*.

[25] R. Lienhart and J. Maydt. An extended set of haar-like features for rapid object detection. *Proc. of ICIP*, 1:900:903, 2002.

[26] A. Hadid, M. Pietikainen and T. Ahonen. A Discriminative Feature Space for Detecting and Recognizing Faces. *Proc of CVPR* 2004.

The Association between Uterine Electrical Activity and Labor Progress: A Systematic Review

^[1] Santosh N Vasist, ^[2] Dr. Parvati Bhat, ^[3] Dr. Shrutin Ulman, ^[4] Dr. Harishchandra Hebbar

^[1] Research scholar, Manipal School of Information Sciences, MAHE

^[2] Professor, Melaka Manipal Medical College, MAHE, ^[3] Principal scientist, Philips Healthcare

^[4] Professor, Manipal School of Information Sciences, MAHE

Abstract: Prolonged or arrested progress of labor is one of the major contributors for non-elective cesarean deliveries. Electrical activity in the myometrium of the uterus muscle is widely accepted to be associated with uterine contractions. The analysis of these electrical signals (called Electrohysterography or EHG) can reveal crucial information regarding uterine activity, which could provide an early indication of labor dystocia.

The review is a systematic search of literature using PubMed and EMBASE database. The objective of this review was to identify the parameters of the EHG signal that can possibly predict prolonged or arrested progress of labor and to structure the current knowledge of EHG and labor progress. This article, to our knowledge, is the first review article which attempts at evaluating various EHG parameters and their association with dystocia.

The review suggests; the propagation patterns of contractions and its frequency analysis among others could be analyzed from EHG signals. EHG has been shown to estimate the spatio-temporal evolution of a contraction, however it fails in predicting arrested progress of labor. Frequency analysis and energy distribution patterns has been partially successful in predicting arrested progress of labor. Synchronization of uterine contractions could be a potential predictor, but needs more studies to confirm the same.

Keywords: Electro Hysterography, Electromyography, Uterine Contraction, Labor, Dystocia, And Arrested Labor

INTRODUCTION

Labor is considered to be the preparatory phase for delivery, and is marked by the presence of regular painful uterine contractions and progressive cervical effacement and dilatation. Labor is said to be prolonged if the duration of labor is more than 20 hours including the latent and the active phase. Arrested progress of labor occurs when the rate of cervical dilatation is less than 1 cm/hr [1]. If unattended, these conditions may lead to many critical complications both for the baby as well as the mother. This is the leading cause of non-elective cesarean deliveries [2]. In 2014, cesarean deliveries was 40.5% in some countries and was 18.6% globally [3]. This is a cause of concern because of the short-term (excessive bleeding, infections), long-term risks (hernia) and the cost associated with it. Prolonged or arrested progress of labor becomes a critical issue in developing countries and low resource settings as it may require shifting the patient to a higher care center to perform the cesarean section.

Three factors are crucial for the normal progress of labor; power (uterine contractions), passenger (baby) and passage (maternal pelvis). The only unpredictable factor of the trio is the uterine contractions. Monitoring uterine activity during labor could thus possibly aid early detection of progress of labor. However, existing

techniques and technologies such as Tocodynamometer (TOCO) and Intra uterine pressure catheter (IUPC) are only capable of measuring the average pressure of the uterus and have not improved outcomes [4]. Electrohysterography (EHG), the measure of the electrical activity in the uterus muscle has gained traction with the recent advancements in Digital signal processing (DSP). EHG has been shown to have better correlation to contractions than a Toco [5]. EHG is capable of detecting not just overall uterine activity but coordination, direction, propagation velocity of the contraction [6]–[8] to name a few, which may be crucial in early detection of prolonged or arrested progress of labor.

UTERINE ELECTRICAL ACTIVITY

The uterus is active during the menstrual cycle; however, it largely remains in a state of inactivity during most part of pregnancy. This absence of activity is crucial as it allows the development of the fetus. The contractile activity of the uterus although not significant during early pregnancy, increases as the pregnancy approaches its end, which can be viewed as a preparatory phase for labor.

Although, studies suggest the possibility of a mechanical process as the signaling system for the contractions [9], it is widely accepted that uterine contractions appear and

spread as a result of the electrical activity in the myometrial cells of the uterus [10], [11]. This phenomenon of initiating a contraction through electrical activity is similar to other muscle tissues. These electrical signals are referred to as action-potentials or spikes. The myometrium is made up of a huge number of smooth muscle cells, close to about 200 billion in number [11]. Electrical activity in the myometrium is a result of the de-polarization and re-polarization of the smooth muscle cells. De-polarization of one cell leads to the activation of a neighboring non de-polarized cell, in turn initiating a wave of activation in a specific direction.

The uterus unlike other muscles is able to contract without nervous or hormonal inputs [13]. The depolarization phase of the action potential is caused by an inward current carried by the Ca^{2+} and Na^{+} ions in the uterus muscle. The repolarization phase in the action potential is caused by an outward current carried by K^{+} ions [11]. Uterine contractions are stimulated or suppressed by modifying the electrical properties of the myometrial cells.

Myometrial cells are electrically connected through gap-junctions, which offer low resistance pathway for the propagation of action-potentials [14]. During early pregnancy, it is believed that poor electrical coupling, or in other words the low number of gap-junctions is one of the main reasons for the poor electrical activity and in turn lack of powerful uterine contractions [10]. Studies have shown that an increase in the gap-junctions associated with the myometrial cells, improves the propagation of the electrical activity at term. If the action-potential spreads to many myometrial cells, in quick succession, the series of spikes is called as a burst of electrical activity [15]. Such electrical bursts are responsible for efficient uterine contractions. The frequency of action potentials within a burst is a direct measure of the rate of repolarization and depolarization [16].

The uterine myometrial cells can function as both pacemaker and pacerollower, i.e., it can generate action potentials on its own or it can be excited by the action potentials of a neighboring cell [10]. A spike of action potential initiates a contraction and spreads progressively across cells to sustain the contraction. Propagation of a spike can occur in any direction and is highly unpredictable. The conduction velocity of action potentials in the human uterus have been measured to be in the range of 1-5 cms-1 by various studies [6]. It has also been observed that the spread of action potential is faster longitudinally than circumferential directions.

STUDY DESIGN & METHOD

The objective of this systematic review was to identify the parameters of the EHG signal that can possibly predict prolonged and/or arrested labor and structure the current knowledge of EHG and labor progress, so as to inspire further research in this area.

PubMed and EMBASE databases were systematically searched using the keywords electro hystero-graphy, electromyography, uterine contraction, labor, dystocia, and arrested labor, filtered to include articles only in English language. The selection criteria were defined to include studies which involved subjects in term labor and EHG signals analysis pertaining to the progress of labor from recordings using abdominal surface electrodes. Certain referenced articles from the selected works, which focused on predicting or identifying preterm labor were also included in this review, as parameters analyzed in these studies could also be relevant in predicting progress of labor. The selected articles were agreed upon by all authors to be suitable to this review.

GENERAL CHARACTERISTICS OF THE SELECTED STUDIES

Four of the selected studies [8], [17]–[19] had detection of labor arrest as one of the primary objectives. Even though the number of electrodes used to record EHG sensors varied from 4 to 20 amongst the studies, the placement of electrodes was centered around the umbilicus and was symmetrical about it. All the studies down sampled the EHG data to the range of 4 to 20 Hz, to avoid aliasing while filtering the EHG data for analysis. The EHG signals recorded varied widely ranging from no labor contractions as early as 30 weeks of gestation to contractions in active phase of labor.

FREQUENCY ANALYSIS

The rise in Power Spectral Density Peak Frequency (PSD PF) has been widely accepted as a reliable method of predicting preterm labor. The PSD PF has been observed to increase significantly in preterm subjects who were in labor as compared to non-laboring subjects [20]. This rise is explained to be the reflection of increased contraction strength and propagation distance. So, going by the same theory, one would expect the normal progress of labor at term to exhibit higher PSD PF than cases with protracted or arrested labor. However Vasak [18] noted when labor was spontaneous, arrested labor cases exhibit PSD PF levels which are significantly higher than subjects with normal progress of labor. They also observed a considerable increase in the same post oxytocin augmentation. This contrary result may be due to the prolonged exposure to oxytocin leading to lactic acidosis (muscle fatigue in simple words). It could also

be due to the fact that arrested labor could have a certain degree of lactic acidosis without oxytocin augmentation as well. Meaning, although the process responsible for initiation and coordination of uterine contractions is functioning normally, the muscle simply fails to contract due to fatigue.

The same group later [19] observed no differences between labor outcomes, when the labor was induced. They, in fact observed that in subjects with induced labor who delivered vaginally without oxytocin augmentation the PSD PF decreased with increase in cervical dilatation. The results hint at a possible influence of labor augmentation on the conduction and propagation properties of the uterine electrical activity, and needs further exploration.

Vrhovec [21] used two separate EHG databases and observed that the median frequency of EHG bursts during the active phase of labor was significantly lower than the latent phase for subjects diagnosed with dystocia as compared to subjects with normal progress of labor. Median frequency (MDF) is that which divides the total power area in to two equal halves, so a lower median frequency would mean higher concentration of power towards the lower frequency band. The higher frequency activity of the EHG burst in the 0.1 to 3 Hz band is attributed to spikes in the electrical activity. Studies focusing on spike analysis and labor progress may throw more light on this topic.

SYNCHRONIZATION

Jiang [22] also studied the energy distribution pattern across the frequency band, and the transformed values of those patterns were used to identify dis-synchronization in contractions. They observed that out of 225 contractions of subjects in labor, 87 were synchronous and 138 were semi synchronous, with zero asynchronous contractions. In contrast, out of 33 contractions of subjects who had failed induction of labor, 3 were semi synchronous, 30 were asynchronous with none of them being synchronous.

Takagi [23] also studied the synchronization of uterine contraction at different locations on the abdominal surface. They observed that subjects with asynchronous pattern had a slower cervical dilatation rate of 1.15 ± 0.93 cm/hr as compared to 2.58 ± 0.72 cm/hr of subjects who had synchronous pattern of uterine contractions. They also noted that asynchronous patterns tended to be localized and failed to spread effectively across the uterus as the contractions evolved.

ORIGIN AND DIRECTION OF PROPAGATION

It is well known that a descending pressure gradient from fundus to cervix is also important along with adequate pressure for complete cervical dilatation. Any uterine muscle cell can act as a pacemaker and there is no concrete evidence about Cajal-like interstitial cells' activity in pace-making. Lange [24] however observed that in the 35 contractions that they analyzed, 63% of uterine contractions originated in the upper half of the uterus. Euliano [8] observed that throughout the evolution and spread of the contraction, there was a distinct lack of the center of uterine activity (CUA) near the fundal region in arrested progress of labor cases. In simpler words, they observed lack of fundal dominance in a contraction to be associated with arrested progress of labor.

However, the same group Edwards [17] in a later study with a much larger sample, found no relation between fundal dominance and progress of labor. Mikkelsen [25] too found no preferred direction of propagation of uterine contractions. Lange [24] too had reported to have not observed any preferred direction of propagation for contractions. The contradictory results calls for more studies on this with larger number of subjects for better understanding and treatment strategies for labor progression. The relationship between oxytocin augmentation and propagation patterns, which is currently unknown also needs to be explored. It would be interesting to see if any differences exist in the speed of propagation of the electrical activity between normal progress of labor and cases with prolonged or arrested progress. Although many studies have evaluated this parameter to identify preterm labor, we did not find any study that attempts to use it to study progress of labor.

CONCLUSION

Although all the studies used EHG data as the primary source of information for their research, the parameters used to quantify and comprehend are widely varying in their nature and behavior. The parameters analyzed and the techniques employed in all the above-mentioned studies were examined for their possible association with labor progress. Our review suggests that EHG signal analysis could reveal crucial information about the uterine activity during labor and potentially predict the irregularities in labor. It also seems to be the better suited technology to monitor uterine activity, at least in the near foreseeable times.

EHG as a diagnostic tool to predict the progress of labor however still remains to be an elusive wish. PSD PF has

been only partially successful in predicting progress of labor, failing in case of labor induction or augmentation. The role of fundal dominance did offer a glimmer of hope; however recent results have taken us back to where we started. The association between synchronization and labor progress although promising, has been explored in the late 80s and sadly not much work in the recent times linking the two have been carried out. More studies exploring uterine contractions and labor progress is the need of the hour.

In spite of being unable to predict progress of labor, EHG as of today is proven to have better correlation to uterine activity than TOCO [5]. It does not fail in case of obese subjects unlike TOCO. EHG could prove to be an indispensable tool in labor monitoring soon. There are however numerous challenges in achieving this.

- Standardization of EHG practices (location of electrodes, number of electrodes, frequency band of EHG, etc.), parameters (origin and direction of contractions, PSD PF, etc.) and their thresholds seems to be the most prominent.
- Exploration of currently unknown parameters (for example: conduction patterns and their association with genetics) from the EHG signals which could affect labor and its progress should continue.
- EHG has been proven to reveal more information regarding uterine activity than the current gold standard, IUPC. Surface EHG is confined to a portion of the abdomen and hence reveals only partial information of uterine activity. This highlights the need for superior methods (for example: magnetomyography - MMG or invasive micro/nano EHG electrodes) to establish the ground truth about the complete uterine electrical activity.

REFERENCES:

- [1] A. A. Boatín et al., "Dysfunctional labor: Case definition & guidelines for data collection, analysis, and presentation of immunization safety data," *Vaccine*, vol. 35, no. 48Part A, pp. 6538–6545, Dec. 2017.
- [2] J. Zhang et al., "Contemporary cesarean delivery practice in the United States," *American Journal of Obstetrics and Gynecology*, vol. 203, no. 4, pp. 326.e1-326.e10, Oct. 2010.
- [3] A. P. Betrán, J. Ye, A.-B. Moller, J. Zhang, A. M. Gülmezoglu, and M. R. Torloni, "The Increasing Trend in Caesarean Section Rates: Global, Regional and National Estimates: 1990-2014," *PLOS ONE*, vol. 11, no. 2, p. e0148343, Feb. 2016.
- [4] "Outcomes after Internal versus External Tocodynamometry for Monitoring Labor | NEJM." [Online]. Available: <https://www.nejm.org/doi/full/10.1056/NEJMoa0902748>. [Accessed: 07-Jun-2019].
- [5] T. Y. EULIANO et al., "Monitoring uterine activity during labor: a comparison of three methods," *Am J Obstet Gynecol*, vol. 208, no. 1, pp. 66.e1-66.e6, Jan. 2013.
- [6] "Propagation of electrical activity in uterine muscle during pregnancy: a review - Rabotti - 2015 - Acta Physiologica - Wiley Online Library." [Online]. Available: <https://onlinelibrary.wiley.com/doi/abs/10.1111/apha.12424>. [Accessed: 07-Jun-2019].
- [7] R. E. Garfield, W. L. Maner, L. B. MacKay, D. Schlembach, and G. R. Saade, "Comparing uterine electromyography activity of antepartum patients versus term labor patients," *American Journal of Obstetrics and Gynecology*, vol. 193, no. 1, pp. 23–29, Jul. 2005.
- [8] T. Y. Euliano, D. Marossero, M. T. Nguyen, N. R. Euliano, J. Principe, and R. K. Edwards, "Spatiotemporal electrohysterography patterns in normal and arrested labor," *Am. J. Obstet. Gynecol.*, vol. 200, no. 1, pp. 54.e1–7, Jan. 2009.
- [9] R. C. Young, "Myocytes, Myometrium, and Uterine Contractions," *Annals of the New York Academy of Sciences*, no. 1101, pp. 72–84, 2007.
- [10] R. E. Garfield and W. L. Maner, "Physiology and Electrical Activity of Uterine Contractions," *Semin Cell Dev Biol*, vol. 18, no. 3, pp. 289–295, Jun. 2007.
- [11] C. Y. Kao, "Electrophysiological Properties of Uterine Smooth Muscle," in *Biology of the Uterus*, R. M. Wynn and W. P. Jollie, Eds. Boston, MA: Springer US, 1989, pp. 403–454.
- [12] R. K. Riemer and M. A. Heymann, "Regulation of uterine smooth muscle function during gestation," *Pediatr. Res.*, vol. 44, no. 5, pp. 615–627, Nov. 1998.
- [13] R. K. Riemer and M. A. Heymann, "Regulation of Uterine Smooth Muscle Function during Gestation," *Pediatric Research*, vol. 44, no. 5, pp. 615–627, Nov. 1998.
- [14] A. Shmygol, A. M. Blanks, G. Bru-Mercier, J. E. Gullam, and S. Thornton, "Control of uterine Ca²⁺ by membrane voltage: toward understanding the excitation-contraction coupling in human myometrium," *Ann. N. Y. Acad. Sci.*, vol. 1101, pp. 97–109, Apr. 2007.
- [15] D. Devedeux, C. Marque, S. Mansour, G. Germain, and J. Duchêne, "Uterine electromyography: A critical review," *American Journal of Obstetrics and Gynecology*, vol. 169, no. 6, pp. 1636–1653, Dec. 1993.
- [16] E. Bytautiene, Y. P. Vedernikov, G. R. Saade, R. Romero, and R. E. Garfield, "Effect of histamine on phasic and tonic contractions of isolated uterine tissue from pregnant women," *American Journal of Obstetrics*

and Gynecology, vol. 188, no. 3, pp. 774–778, Mar. 2003.

[17] R. K. Edwards et al., “Evaluating Fundal Dominant Contractions on Spatiotemporal Electrohysterography as a Marker for Effective Labor Contractions,” *Amer J Perinatol*, no. EFirst, ///.

[18] B. Vasak et al., “Uterine electromyography for identification of first-stage labor arrest in term nulliparous women with spontaneous onset of labor,” *Am. J. Obstet. Gynecol.*, vol. 209, no. 3, pp. 232.e1–8, Sep. 2013.

[19] “Identification of first-stage labor arrest by electromyography in term nulliparous women after induction of labor - Vasak - 2017 - *Acta Obstetricia et Gynecologica Scandinavica* - Wiley Online Library.” [Online]. Available:

<https://obgyn.onlinelibrary.wiley.com/doi/full/10.1111/aogs.13127>. [Accessed: 07-Jun-2019].

[20] M. P. G. C. Vinken, C. Rabotti, M. Mischi, and S. G. Oei, “Accuracy of frequency-related parameters of the electrohysterogram for predicting preterm delivery: a review of the literature,” *Obstet Gynecol Surv*, vol. 64, no. 8, pp. 529–541, Aug. 2009.

[21] J. Vrhovec, “An uterine electromyographic activity as a measure of labor progression,” in *Applications of EMG in clinical and sports medicine*, vol. 2, intechopen, 2012, pp. 243–268.

[22] W. Jiang, G. Li, and L. Lin, “Uterine electromyogram topography to represent synchronization of uterine contractions,” *International Journal of Gynecology & Obstetrics*, vol. 97, no. 2, pp. 120–124, May 2007.

[23] “A Topographic Investigation of the Site of Origin and Subsequent Propagation of Uterine Contractions in Spontaneous Labor and Their Clinical Significance - Takagi - 1986 - *Asia-Oceania Journal of Obstetrics and Gynaecology* - Wiley Online Library.” .

[24] L. Lange, A. Vaeggemose, P. Kidmose, E. Mikkelsen, N. Uldbjerg, and P. Johansen, “Velocity and Directionality of the Electrohysterographic Signal Propagation,” *PLoS One*, vol. 9, no. 1, Jan. 2014.

[25] E. Mikkelsen, P. Johansen, A. Fuglsang-Frederiksen, and N. Uldbjerg, “Electrohysterography of labor contractions: propagation velocity and direction.. *Acta Obstet Gynecol Scand* 2013; 92: 1070– 1078.” .

A Review on Rate of Heat Transfer in Double Pipe Heat Exchanger Using Fins on Internal Tube Surface

^[1] Syed Sameer, ^[2] Dr. SB Prakash, ^[3] Robinson P

^[1] Ph.D Scholar, Department of Thermal Power Engineering, VTU-RRC-Mysuru.

^[2] Professor & Head, Department of Thermal Power Engineering, VTU-PG Studies, Mysuru.

^[3] Assistant Professor, School of Mechanical Engineering, REVA University, Bengaluru.

^[1]syedsameer30@gmail.com

Abstract:-- Through the initiation of new technology and energy saving encouragements, appreciable efforts has been devoted in developing new methods for increasing effectiveness of the heat exchanger. Among the various attempts dedicated on evolving energy efficient heat transfer medium, the incorporation of surface irregularities on the heat transfer surface is captivating its consideration because it augments the thermo-hydraulic performance of the heat exchanger to the considerable level. However, the thermal performance enhancement and pressure drop increment comes side by side with heat transfer enhancement technique. But in some applications, it is highly appropriate to provide surface roughness where space concern is more vigorous to power loss as a result of pressure drop, namely on aerospace industry and nuclear reactors. In order to check the feasibility of the analytical technique, experimental research of a double-pipe pin fin heat exchanger were carried out.

A smooth tube of 25 mm diameter and two enhanced tubes of same diameter with V corrugations on the inner surface of inner tube having surface height, $e=0.3$ mm and $e=0.6$ mm and pitch, $p=1.3$ mm are used to get heat transfer and friction factor parameters and also Reynolds number is taken in the range 16700 to 22300. The percentage of heat transfer enhancement for tube with surface height $e=0.3$ mm is found to be 67% to 52% and also for a tube surface height $e=0.6$ mm is 89% to 64% in the Reynolds number regime of 16700 to 22300 compared to plane tube. The friction factor ratio of tube with $e=0.3$ mm is obtained in the range of 5.02 to 5.23 and for a tube with $e=0.6$ mm, it came to be 5.89 to 6.2 in the range of frictional Reynolds number of 5610 to 7480.

Keywords: Double Pipe Heat Exchanger, Corrugation, Reynolds Number

1.INTRODUCTION

Heat exchanger is a device that facilitates the exchange of heat between two fluids that are at different temperature while keeping them from mixing with each other. Heat exchangers are heat transfer equipment's which have several industrial and engineering applications. The design procedure of heat exchangers is quite complicated, as it needs exact analysis rate of heat transfer and pressure drop approximations apart from issues such as long term performance and the economic aspect of the equipment. The foremost task in designing a heat exchanger is to make the equipment compressed and achieve high heat transfer rate using minimum pumping power [1].

Energy and materials cost convertible considerations have led to yield more efficient heat exchanger equipment. Improvement of the heat transfer process is desired in heat exchangers to enable reductions in weightage and size, to increase the rate of heat transfer or to reduce the mean temperature difference between the fluids and thus to improve the overall process efficiency [2]. The study of advance in heat transfer performance is

denoted as heat transfer enhancement or augmentation or intensification [3].

Augmentation methods can be classified either as passive methods which require no direct application of external power, or as active methods, which require external power. The effectiveness of both categories of procedures is strongly needy on the mode of heat transfer, which may range from single -phase free convection to dispersed -flow film boiling. Enhanced heat transfer surface or enhanced tube is a type of the passive technique for enhancing the thermal performance of the heat exchangers with a few increase of the friction penalty [4]. Corrugated tube is one of the important improved tube in various engineering applications. For example, for heat exchanger, diet industry, paint making industry, navel and medicines production. The overall heat -transfer coefficient has been remarkably improved because of the turbulent flow impact on the internal surface and external surface of the tube caused by the corrugation [5].

2. EXPERIMENTAL SETUP

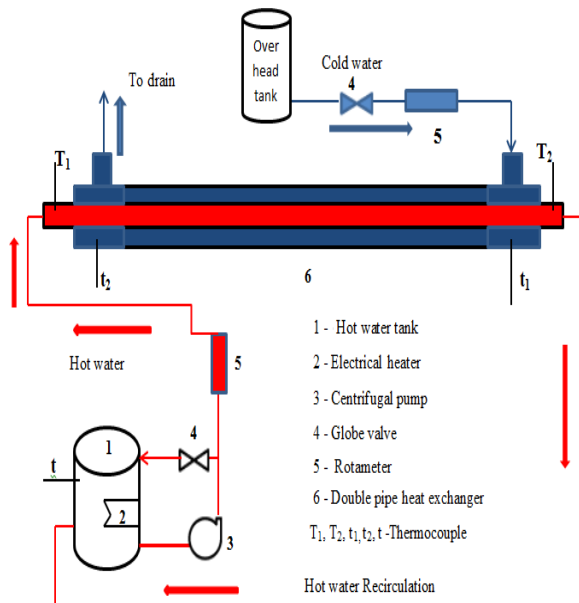


Fig. 1: Schematic Layout of the Experimental Setup

The figure 1 illuminates the schematic layout of the experimental setup. The experimental setup consists of double pipe heat exchanger, Rota meter, Centrifugal pump, U -Tube manometer, Thermocouples, Temperature display unit, overhead tank which is used for supplying cold water, hot water tank with submersion heater and a control unit.

The practical test section which is one of the constituents of the experimental arrangement is a double pipe heat exchanger arranged in a counter current flow configuration. It consists of inner tube made up of Aluminium with outer diameter of 25 mm and length of 1500 mm and the reason to use Aluminium is its lower price compared to copper. The external tube is made of CPVC pipe with external diameter of 40 mm and length of 1400 mm and the advantage to use plastic material is to -fold; primarily, it works as insulator and confirms the decrease of heat loss and furthermore, there is no need of insulation layer if the cold water temperature is low enough. Total of 3 tubes were tested; one smooth tube for the reference motive and the remaining two were enhanced tubes [6].

Two calibrated flow meters: Rota meter were used in the setup, placed in the cold fluid and the hot fluid side correspondingly with the flow gauging range of 20 - 1080 LPH in each side. The rate of flow is controlled manually in each side. The cold fluid is providing from the overhead tank with the help of gravity. The hot water was provided from the hot water tank at an estimated temperature of 50 -520C with the help of

the centrifugal pump. The hot water was produced with the aid of the submerged Nichrome heater. The U-Tube manometer was located in order to estimate the pressure drop in the cold fluid and the hot fluid side arrangements respectively. The K - Type Thermocouple with a temperature measuring range: 0 – 2000C, were placed six in number, one at the hot water tank, one for atmospheric temperature, two at the inlet and outlet of the hot fluid side cross section and the left over two at the inlet and outlet of the cold fluid side [7].

3. RESULTS AND DISCUSSIONS

This section deliberates and relates the results obtained on the smooth tube and the enhanced tube in the turbulent flow region. The smooth tube of outer diameter 25 mm is used for the experimental work and the parameters obtained for smooth tube are taken as reference values. The experiment is conducted on two enhanced tubes having V shaped internal corrugations by height $e = 0.3$ mm and $e = 0.6$ mm and of same pitch value of $P = 1.3$ mm.

3.1 RATE OF HEAT TRANSFER

The average rate of heat transfer through the heat exchanger is drawn in compare to the Reynolds number of the cold fluid as shown in the figure 2.

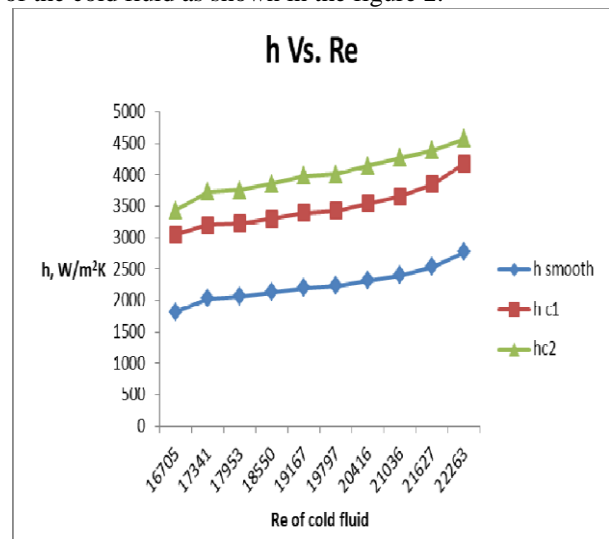


Fig. 2: Average Heat Transfer Rate vs. Reynolds Number of Cold Fluid

The three sets of data for average heat transfer rate Q_s , Q_{c1} , Q_{c2} namely, one for smooth, two for enhanced tubes, $e = 0.3$ mm and $e = 0.6$ mm simultaneously are plotted. The average heat transfer rate for smooth tube increases from 2.8 kW to 3.6 kW, in the range of Re 16700 to 22300 because of the

increased overall heat transfer coefficient with flow. The higher Reynolds number consequences in higher Nusselt number and also greater convective heat transfer coefficient leading to higher overall heat transfer coefficient. The tube with $e = 0.3$ mm consisted of heat transfer rate increment from 4.1 kW to 4.57 kW for the given range of Re . The result indicated highly augmentation in rate of heat transfer in enhanced tube as compared to smooth tube. As the roughness in the heat transfer surface increases, the thinning of the boundary layer causes enhanced transport properties leading to rapid increment in the heat transfer coefficient and thus higher heat transfer rate. The heat transfer rate for tube with $e = 0.6$ mm ranges from 4.4 kW to 4.7 kW. The heat transfer increment range is 0.8 kW, 0.47 kW and 0.3 kW simultaneously for smooth tube and two rough tubes of $e = 0.3$ mm and 0.6 mm.

3.2 CONVECTIVE HEAT TRANSFER COEFFICIENT

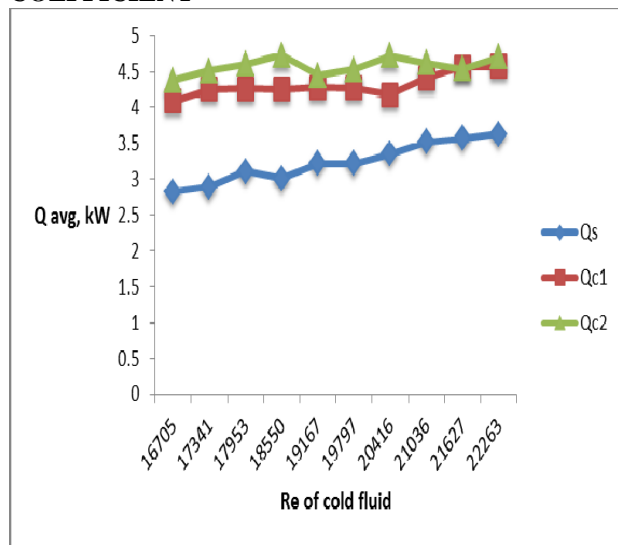


Fig. 3: Relationship between Convective Heat Transfer Coefficient and Re of Cold Fluid

The figure. 3 demonstrate the scheme of convective heat transfer coefficient versus Re of the cold fluid. The use of corrugations on the inner tube of double pipe heat exchanger enhances the convective heat transfer coefficient in an attractive way. It is noted that the heat transfer coefficient for enhanced tube with $e = 0.3$ mm increases from 68 % to 51% in a Reynolds number range of 1670, $e = 0.6$ mm, the coefficient of heat transfer rises from 90 % to 65% in a given range of Re . It can be deduced that for 0 to 22300 and the maximum enhancement occurred at the lower value of

Re . Greater irregularity leading to greater heat transfer coefficient. Also it can be understood that the proportion of raise of convective heat transfer coefficient for a given roughness falls with increasing Re .

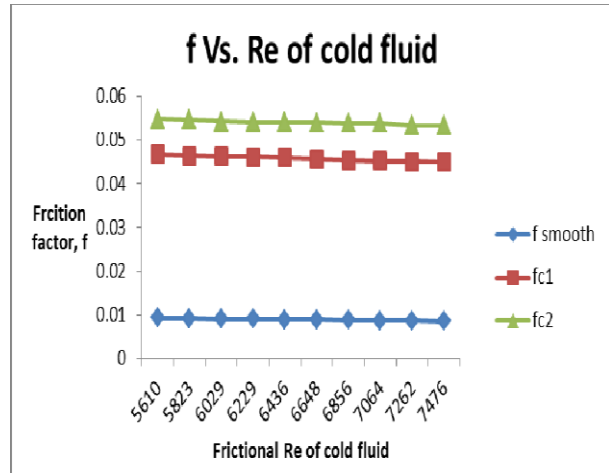


Fig. 4: Relationship between Frictional Re and Friction Factor f.

3.3 FRICTION FACTOR RESULTS

The pressure drop across the annulus of the double pipe heat exchanger is measured with the help of the Mercury U -Tube manometer. The measurement of manometric head results in pressure drop and friction factor calculation. The friction factor of the boosted tube and the smooth tube is presented in the figure 4. For smooth tube the friction factor as displayed by the graph lies in the range of 0.0093 to 0.0086 with the Frictional Reynolds Number varying from 5610 to 7476. Thus friction factor value is decreased as Re goes higher. For the given improved tube of $e = 0.3$ mm the friction factor is extremely increased in the range of 0.0467 to 0.0449. Adding to this, for the tube having $e = 0.6$ mm, the friction factor lies in the range of 0.055 to 0.053. The higher the Re , higher is the inertia force which dominates the frictional force and the flow experiences little of shear force and hence gradually the friction provided by roughness diminishes slowly.

4. CONCLUSION

The main objective of this research was to study the influence of surface corrugations to heat transfer in a heat exchanger. Following conclusions are derived from the review of experimental study :

- ★ The corrugated tubes increases the film coefficient because of turbulence in the flow and hence enhances the heat transfer rate.

- ✦ The average heat transfer rate for smooth tube, tube with $e = 0.3$ mm and tube with $e = 0.6$ mm are found to be in the range 2.8 kW to 3.6 kW, 4.1 kW to 4.57 kW and 4.4 kW to 4.7 kW correspondingly in the Reynolds number range of 16700–22300. It shows very high rate of heat transfer for enhanced tubes as compared to smooth tube.
- ✦ The convective heat transfer coefficient enhancement for tube with surface height $e = 0.3$ mm is set up to be 68% and with surface height $e = 0.6$ mm is set up to be 75% higher than plane tube for Reynolds number range of 16700 to 22300.
- ✦ The augmentation in the heat transfer coefficient at lower value of Reynolds number is found to be greater. Therefore, the heat transfer augmentation ratio is decreases with increase in Reynolds number. For a tube with $e = 0.3$ mm, the ratio is highest with a value of 1.68 at Re of 16700 and lowest with a value of 1.51 at Re of 22300.
- ✦ The friction factor increases with increase in the roughness value then tends to remain constant at higher regime of Reynolds number.

flow liquid through circular tubes using twisted angles and tapes”, NIT Rourkela, 2008.

[7] Gaurav Johar, Virendra Hasda, “ Experimental Studies on heat transfer augmentation using modified reduced width twisted tapes (RWTT) as inserts for the tube side flow of liquids”, NIT Rourkela, 2010.

REFERENCES

- [1] Hamed Sadighi Dijazi, Samad Jafarmadar, Farokh Mobadersani, “ Experimental Studies on heat transfer and pressure drop characteristics for new arrangements of corrugated tubes in a double pipe heat exchanger”, International Journal of Thermal Sciences 96(2015) 211 -220.
- [2] Pradeep Kumar, Vijay Kumar, Sunil Nain,” Experimental Study on Heat Enhancement of Helix exchanger with grooved tubes”,IJLTET,Vol.3 Issue 4 March 2014.
- [3] S. Pethkool, S. Eiamsa-ard, S. Kwankaomeng, P. Promvong,,” Turbulent heat transfer enhancement in a heat exchanger using helically corrugated tube”, International Communications in HMT 38(2011) 340 - 347, Dec 2010.
- [4] Lu Linping, Liang Ying, 2012, “Comparative Experimental Study on Performance of Corrugated Tube Heat Exchanger” Materials Research Vols 560 -561 pp 156-160, 2012.
- [5] Vinous M. Hameed and Alia H Akhbala,“ Investigation on Heat Transfer on Smooth and Enhanced tube in Heat Exchanger”, International Journal of Current Engineering and Technology, Vol.5 No.3 June 2015.
- [6] Ranjit Gouda, Amit Bikram Das, “Some experimental studies on heat transfer augmentation for

Aerodynamic Analysis of Wings with Flexible Flaps

^[1] Shreya Giri, ^[2] Suresh P, ^[3] Vinutha G

^{[1][2][3]} Department of Aeronautical Engineering, Dayananda Sagar College of Engineering, Kumaraswamy Layout, Bengaluru, Karnataka, India

Abstract:-- Flaps are prominent-lift devices and have been used throughout the history of aviation. Deploying the wing flaps elevates the camber of the wing hence leading to the increase of upper limit lift co-efficient. There are many diverse designs of flaps used, with the particular choice depending on the dimensions, speed and complication of the aircraft. Plain, slotted and fowler flaps are the familiar types including Kruger flap usually positioned on the wing's leading edge. However, traditional flaps when deployed create gaps in the edge of wing, which generate turbulent airflow and hence decreases the aerodynamic efficiency of the aircraft. The present study of flexible flap, a kind of passive flap augment the design of the control surfaces. In the present experimental study, two different materials of different thickness are used as flexible flaps with aspect ratio of 6.2 on a wing of aspect ratio of 2.05. The results obtained showed around 12 % improvement in the aerodynamic characteristics. It is evident that such surfaces can lead to quicker landings and less turbulent flights.

Keywords: aerodynamic characteristics, flexible flaps, maximum lift co-efficient, turbulent air flow, aerodynamic efficiency.

1. INTRODUCTION

Flaps are being used since they were invented in order to descent the lowest speed at which the aircraft can be securely hovered and it is used to rise the angle of descent for landing. Deploying the wing flaps increases the camber of the wing hence leading to the upsurge of maximum lift co-efficient.

However, the traditional flaps when deployed create gaps in the edge of wing, which increases a lot of noise and generate turbulent airflow. This drastically decreases the efficiency of the plane. They also require complex mechanisms, which add weight and complexity. Hence, they give rise to the flexible wing concept that includes replacing old traditional flaps with shape changing flexible flaps.

1.1. INSPIRATION FOR FLEXIBLE FLAPS

The landing birds transposed themselves for landing; secondary undercover feathers from the upper surface of the wing would deviate from the usual position and form recirculation pockets. Passive or inactive flow devices inspiration came from this observation. The relocation of the wing increases its angle of attack initiating flow separation along the upper wing. The upturned flow in the interior of the turbulent separation area configures sufficient difference in pressure to force the covert (undercover) feathers upwards and create smoother upper wing outline, conveying the airflow above the wing and dipping flow separation.

1.2. PROBLEM DEFINITION

The problem taken is to study the effectiveness of a flap made of flexible material that can replace traditional flaps on a conventional aircraft wing replacing the deployable flaps and to assess the aerodynamic characteristics of the wing.

1.3. OBJECTIVE

- 1.) To select an airfoil based on the aerodynamic efficiency and better stall characteristics of the airfoil.
- 2.) To conduct benchmark analysis and validation using Six Component Force Balance equipment for flat plate at different AOA.
- 3.) To fabricate a scaled model of typical conventional wing for low Reynolds' number application.
- 4.) To conduct experimental wind tunnel test for wing with and without flexible flaps at various AOA.
- 5.) To compare and analyze the wing with the flaps and without them at various AOA.
- 6.) To study the effects of flexible flaps, influence on aerodynamic characteristics of the wing when compared to traditional flaps.

2. THEORY OF FLEXIBLE FLAPS

2.1. FLEXIBLE FLAPS

Flexible flaps/Self-movable flaps are the inactive lift improvement device that do not require any external control, and is self-adjusting depending on the condition of the flow. The flow around the wing section is responsible for opening and closing of the flaps. These kinds of flexible flaps have evidenced to reduce the

approach speed or for high angle of attack (AOA) vehicles to keep flow attached during maneuvers, (the latter may require active control of flaps). Until an equilibrium condition, under passive control, the flap arranges when the pressure force under the flap exceeds that beyond the flap; this causes the flap to rise. On the other hand, active control devices used to attain analogous effects necessitate electronics, power mechanisms and additional equipment to regulate the mechanism. This significantly increases the weight and complexity of the vehicle and in several circumstances enlarges the risk of mechanism failure. It includes removal of additional devices; not only improving price considerations, it also reduces the weight, but improves lift in poor conditions making these flaps appealing. Contrasting the active flow control devices like periodic suction and blowing or driven flap oscillation, the self-activated movable flaps also called flexible flaps, deliver a modest and economical tool for intensified lift, and these active control devices have made it very advantageous for smaller aircraft deprived of the power or weight allowance. At low incidence, the flap continues to attach to the airfoil exterior and this will not have any effect on the aerodynamics. However, with increasing angle of attack, based on the aerodynamic forces and flap weight, the flap lifts and self-adjusts to a position when flow separation in occurs in the region of trailing edge. The mean flow itself activates the opening and closing of the mechanism. Compared to active flow control devices like periodic suction and blowing or driven flap oscillations, the current method forms a modest and economical tool that assures to expand the operation of technical high-lift devices.

2.2. COMPARISON OF TRADITIONAL AND FLEXIBLE FLAPS

Table 1: Comparison of Traditional and Flexible Flaps

Sl.no.	Traditional flaps	Flexible flaps
1	Fixed shape	Shape changes according to the flow
2	Pilot controlled	Automatic control

3	Complex mechanisms increases the weight	Drastic reduction in weight due to absence of complex mechanisms.
4	Less lift at high AOA	Comparatively more lift at high AOA

2.3. ADVANTAGES

- 1.) Flexible flaps prevent sudden drop in lift generation during stall.
- 2.) Help in operative shape alteration of the airfoil that interrupts the flow separation and thus leads to the increase in the lift and the stall margin.
- 3.) Drastic reduction in weight due to absence of complex mechanisms.
- 4.) Flexible flap is a modest and economical tool that assures to enhance the performance of practical high lift device.

2.4. DISADVANTAGES

- 1.) The upturned flow would trigger the flap to tip forward completely. This consequence of the flap would disappear at very high AOA.
- 2.) There is a trivial reduction in lift, because the angle of the airfoil skeleton line at the trailing edge is subsided and in effect, AOA of the airfoil declines.
- 3.) Application of flexible flaps is inadequate to subsonic flows and the outline of the non-swept wing.

2.5. SELECTION OF FLEXIBLE FLAP MATERIALS

Based on the literature survey, Plastic sheets, Carbon fiber strips, Thin Cellulose Acetate sheet, Flexible plastic material, Aluminum sheet, Vinyl plastic are the materials that can be used for the flaps. Market survey was conducted on above materials after which we selected Vinyl plastic rubber of 0.5 mm and PVC Sheet of different thicknesses such as 0.5 mm and 0.8 mm as preferred materials for the further testing. The aspect ratio of the flaps was maintained at 6.2 for efficient testing and results.

3. EXPERIMENTAL ANALYSIS OF WING WITH S1223

3.1. ANALYSIS OF S1223 WING MODEL WITHOUT FLAP

The wing model was manufactured out of wood according to the tunnel specifications from the chosen S1223 airfoil. The wing model had a span of 480 mm,

the chord length was 190 mm with an aspect ratio of 2.05, which would help the experiments to be carried with ease and achieve error-free results. The data obtained after conducting the experiments in the wind tunnel is as shown in Table 2. The model without flap was tested at a Reynolds' number of around 1,75,000 with a flow velocity of around 12.2 m/s. The tests on the flat plate were approved in the conditions mentioned above for AOA stretching from -8 to 12 degrees and the interpretations from the force balance component is noted down and the coefficient of lift, co-efficient of drag and co-efficient of moments were computed to obtain the polar curves of CL vs. α plotted, which is as shown in the figure 1.

Table 2: Experimental data obtained on a wing without flap

α	C_L	C_D	C_M
-2	0.40901	0.023671	-0.13854
0	0.51931	0.019212	-0.14354
4	0.66843	0.038338	-0.15499
8	0.84128	0.06986	-0.16236
10	0.86359	0.073197	-0.13184
12	1.0734	0.144363	-0.13318
16	0.66963	0.198953	-0.1616
20	0.66115	0.239644	-0.15527

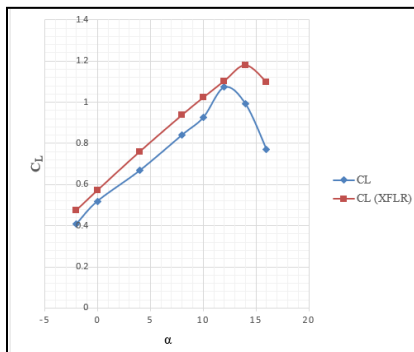


Figure 1: Experimental data obtained on a wing without flap

3.2. ANALYSIS OF S1223 WING WITH FLAP USING VINYL PLASTIC RUBBER

Further, the flap made of Vinyl Plastic Rubber of thickness 0.5 mm was attached to the wing such that it covers 80 % of the span at 0.7 x/c position.

The experiment on Selig S1223 wing by using Vinyl Plastic Rubber of thickness 0.5 mm as flexible material

was carried out at Reynolds no: 175000 and flow velocity of 12.2 m/s at different AOA stretching from -2 to 20 degrees. The investigational data attained from the force component balance is as described in table 3. The polar curves were obtained from the experimental data and are plotted as shown in the figures below.

Table 3: Experimental data obtained on a wing with Vinyl Plastic Rubber (0.5 mm)

α	C_L	C_D	C_M	C_L/C_D
-2	0.39041	0.035732	-7.907611	10.92598
0	0.505342	0.022698	-10.61555	22.26398
2	0.658653	0.022243	-11.8121	29.6113
4	0.700955	0.019024	-12.32755	36.8451
6	0.877787	0.041065	-14.43813	21.3758
8	0.876065	0.034887	-9.439348	-4.1E-22
12	0.881323	0.075236	-10.39862	11.71405
16	0.878851	0.13512	-18.09056	6.504229
20	0.844312	0.147959	-19.20523	5.706393

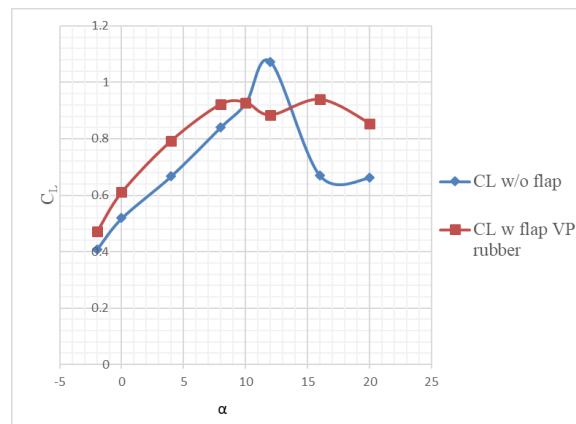


Figure 2: Comparison of Lift coefficient vs Angle of attack curve for wing with and without flap (Vinyl plastic rubber)

3.3. ANALYSIS OF S1223 WING WITH FLAP USING PVC SHEET HAVING THICKNESS OF 0.5 mm and 0.8 mm

The flap made of PVC sheets having thickness of 0.8 mm was attached to the wing such that it covers 80 % of the span at 0.8 x/c position. The experiment on Selig S1223 wing by using PVC sheet of thickness 0.8 mm as flexible material was carried out at Reynolds no: 175000 and

flow velocity of 12.2 m/s at different AOA stretching from -2 to 16 degrees.

Table 4: Experimental data obtained on a wing with PVC sheet flap (0.8 mm)

α	C_L	C_D	C_L/C_D
-2	0.46418	0.0319	14.5493
0	0.54156	0.02913	18.5908
4	0.76451	0.03814	20.0434
6	0.83876	0.04035	20.785
8	0.94294	0.03358	28.0821
10	1.0197	0.04284	23.8005
12	1.05878	0.07961	13.2998
14	0.96184	0.1017	9.45787
16	0.88097	0.19285	4.56816

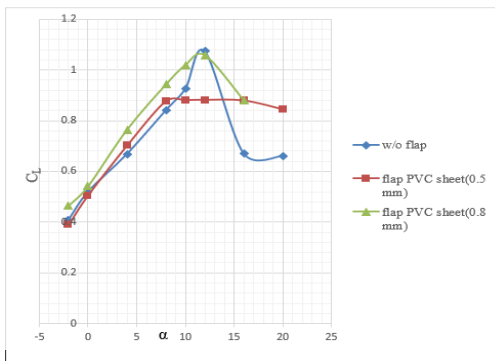


Figure 3: Comparison of CL vs. AOA curve for wing with and without flap

4. COMPARISON OF POLAR CURVES OF A WING WITH TRADITIONAL FLAP WITH WING HAVING FLEXIBLE FLAP

It was observed that at lower AOA the flexible flap stays attached with the airfoil. At post stall angles, the flap raises and attains an equilibrium position, which helps in increasing the lift of the wing. For wing without flexible flap, the lift in case of lower AOA is similar to that with flexible flaps, hence the lift remains unaffected by flexible flaps when it is at lower AOA. At high AOA, for a wing in the absence of the flexible flap, it can be seen that there is a stall at around 12 degrees. But with increasing AOA, the flap organizes at AOA of 14 degrees and recuperates some of the lift. With the help of flexible flaps they distract more airflow at the rare of the flaps initiating a tougher recirculation flow that is more

proficient in dragging the free stream flow down and generate more lift.

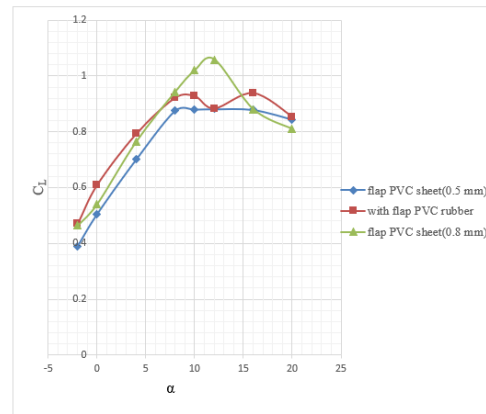


Figure 4: C_L vs Angle of attack curve for flaps with different materials

5. CONCLUSION

Experimental aerodynamic analysis on wings with flexible flaps has been conducted on finite wing of S1223 with flap materials Vinyl Plastic Rubber of thickness 0.5mm and vinyl plastic sheet of thickness 0.5 mm and 0.8 mm, covering 80% of wing span and $0.7x/c$ at Reynolds number 175000 and flow velocity of 12.2 m/s at different AOA and the result obtained gives us the following conclusions.

The flexible flaps have an upper hand in improving stall physiognomies and increasing the lift at greater AOA. By the use of flexible flaps, the overall lift is enhanced by 12%. The study with both the materials has led to satisfactory results, but when the materials are compared with each other, vinyl plastic rubber is more desired than PVC sheet as it has much better lift characteristics at higher AOA.

6. FUTURE SCOPE

The foremost drawback of a wing with traditional flaps is that it has reduced lift coefficient at higher AOA. This difficulty can be resolved to an extent by the incorporation of the flexible flaps to the wing. By the results obtained from the analyses, it is clear that the incorporation of flexible flaps has substantiated to be operative in augmenting the lift coefficient of the wing thereby, increasing the overall stall characteristics of the wing. By corrugation of flaps further, it may be possible to improve the efficiency further, thereby increasing the scope of the use of flexible flaps in the near future. With analytical and experimental, unsteady aerodynamic

analysis exact angle of inclination of flexible flap can be predicted.

REFERENCES

- [1] Anderson, John D., Jr.: “Fundamentals of Aerodynamics”, 5th ed., McGraw Hill Book Company, Boston 2005
- [2] Adaptive Compliant Trailing Edge Flight Experiment”, article published by NASA at < <https://www.nasa.gov/centers/armstrong/research/ACTE/index.html>>
- [3] “Popped rivets on Austral Air starboard flaps”, https://www.reddit.com/r/aviation/comments/3iq4rq/popped_rivets_on_atral_air_starboard_flaps/
- [4] C.H. John Wang, Jörg Schlüter, ‘Stall control with feathers: Self-activated flaps on finite wings at low Reynolds numbers’ C. R. Mecanique 340 (2012) 57–66

Conveyor Interlocking with Equipment, Data Acquisition and Automated Process Control System using RFID and IoT for Axle Assembly Line

^[1]Mamatha M, ^[2] Halesh M. R

^[1]Dept. of Electronics and Communication, JSS Science and Technology University, ^[2] Assistant Professor, Dept. of Electronics and Communication, JSS Science and Technology University

^[1] mamatha12j@gmail.com, ^[2]haleshmr@sjce.ac.in

Abstract:-- Simplification of engineering and efficient control of manufacturing process will result significant cost savings. The present project emphasis on the application of PLC's and IoT in the process monitoring, control and data capturing in production process. This concept is a kind of taking PLC as the control core of the conveyor which is used for assembly line for production and its sub equipments. PLC is used for conveyor interlocking with equipments and process data capturing using radio frequency identification (RFID). Working stations present on the conveyor have RFID in every stations and position of stations is monitored by the conveyor PLC. Model number of component present in the stations is automatically picked from the conveyor PLC with respect to position in that station by RFID. These collected data will be used for name plate engraving and test results obtained are dumped to edge server. Then it will be displayed on LED TV or take intelligent decisions automatically by using IOT. An another feature is Operators pull a cord or press a switch if there are upcoming or actual problems. Similarly, machines and processes can send a signal if something is wrong. The information flow regarding the status of the production system will be displayed on andon display. The main advantages of this project is traceability, digitalization.

Keywords: Programmable logic controllers (PLC), radio frequency identification, conveyor, edge server.

1. INTRODUCTION

Digitization plays a crucial role in automotive manufacturing. It equips the interior suppliers with necessary tools and helps them remain flexible and relevant in this modern era [1]. The industry 4.0 vision provides recommendations how companies can ease these challenges. With an increase in customer demand for value-added vehicles, the automotive suppliers are facing a problem in coping up with the changing preferences and requirements, while remaining operational and profitable. By digitizing automotive manufacturing will improve their competitiveness while setting a strong foundation for the future growth in a steadily evolving manufacturing landscape [4]. By doing automation that will results in higher productivity, reliability, availability, and increased performance and can decrease operating costs.

The conveyors are the basic important component of material handling. There are many types of conveyors that are used in industry like gravity conveyor, chain conveyor, belt conveyor, etc. The conveyor systems are used to transfer the objects and also to stop at predefined locations for some operation. Now the whole system is to be controlled, monitored and process data should be captured in order to have balanced system and accurate

data acquisition with all possible safety measures. For data capturing and data processing through wirelessly we are going for RFID Tags which has been a convenient method. RFID has many advantages they do not need to be within line of-sight of the reader to be tracked. Tags are attached to an object so that RFID can read data and also capture data stored on that tag [2]. It consists of many control components to achieve starting logic, stopping logic, tripping logic. Relays are used for protection purpose and other components are used as sensing components for its monitoring and protection purpose. Complexity occurs in the system due to hard wired circuits so future modification will become very difficult. The usage of electromagnetic relays, timers also creating major problem such as operational trouble such as start, consuming more time on fault tracing, stop increases, trip increase, increasing number of call duties, consumption more spares on circuit elements, inventory increases, cost of maintenance is more [3]. PLC method to regular the conveyor system is the solution for the above problems and desired results can be obtained. Sensing device like receiving conveyor position sensing, zero speed sensing are present in Conveyor system.

Industry 4.0 is an idea of smart factories where machines are augmented with web connectivity and connected to a system that can visualise the entire production chain and

make decisions on its own. The trend is towards automation and data exchange in manufacturing technologies which include cyber-physical systems (CPS), the Internet of things (IoT), the Industrial Internet of Things (IIOT), cloud computing and cognitive computing. Industry 4.0 is also referred to as the fourth industrial revolution.

An edge server is a type of edge device that provides an entry point into a network. Edge server will allow different networks to connect and share transit. The overall storage of this server is 500GB. There are three virtual machines in edge server. In these three virtual machines, the first one is for quality analysis, the second one for complete information about the production and the third for production storage.

II. INSTALLATIONS OF CONVEYOR AND ITS SUB EQUIPMENTS

A. Installation of conveyor belt

The below figure shows the conveyor belt installation carried out in the industry. Slat conveyors are used to transfer products from one location to another location [6]. This conveyor has 20 stations on it and in each station different work will be carried out on manufacturing product.



Fig.1. Installation of conveyor belt

B. Installation of Fixtures on conveyor and pull cord

Fixtures are mounted on the conveyor belt and each critical operations point has a pull cord. An electric pull switch is attached to a toggle type switch by pulling these switches ON/OFF operation can be done and these are used for stopping the conveyor during fault conditions like maintenance, quality etc [7]. There are total 42 fixtures in axle assembly line of this manufacturing industry.



Fig.2. Fixtures on conveyor and pull cord

C. Programmable logic controller

Programmable logic controller is a controller that will store instructions in programmable memory in order to implement logical functions such as timing, sequencing, counting and arithmetic functions in order to control machines and process[5].



Fig.3. Mitsubishi PLC (Q03UDV CPU)

D. Sealant dispenser

This equipment is used for pumping the sealant from the container to the dispensing gun.



Fig.4. Sealant dispenser gun

E. Nameplate engraving machine

This equipment is used for name plate engraving. It is used for printing the model number and company product description in a metal plate which is punched on the component for inventory purpose. This system will generate a unique code when ever matching is done between the products that has to be assembled on the conveyor, green signal will glow and information will be dumped to edge server[8]. If matching is not correct then it will give an error signal and it will halt the conveyor at that point for correction and an operator can override those commands if necessary.



Fig.5. Nameplate engraving machine

F. Air leak tester

Air leak testers are used to judge leaks by pressurizing (test pressure 125Kpa) the inside of sealed work by air and measuring the pressure change this type of air leak test

is used for leak check in an axle[9]. The figure shows the air leak testing equipment.



Fig.6. Air leak tester

G. DC Nut runner

This Equipment is used for tightening nuts of an axle. Nut runners and nut drivers are tools used for tightening of nuts.



Fig.7. DC Nut runner

III. METHODOLOGY

A conveyor system in axle assembly line is equipment that moves products from one place to another. Conveyors are especially useful in applications involving the transportation of heavy and light materials. Conveyor systems are used across wide range of industries due to the numerous benefits they provide. They can move loads of all sizes, shapes, and weights. The below figure shows the block diagram. This Conveyor has 20 work stations or fixtures where each fixture will have RFID Tag and Position of fixture is monitored by the conveyor PLC. The work stations are divided into three points A, B and C respectively and each have PLC which control, monitor and give feedback to main conveyor PLC for conveyor interlocking and process data capturing.

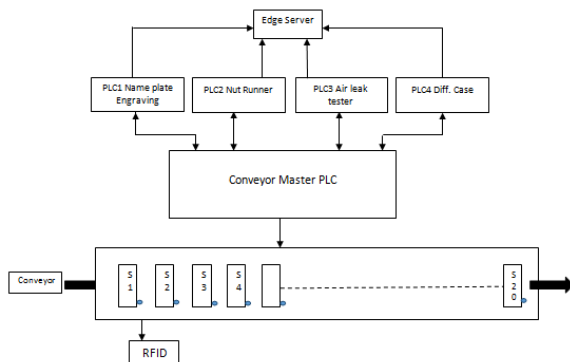


Fig.8. Block Diagram of proposed system

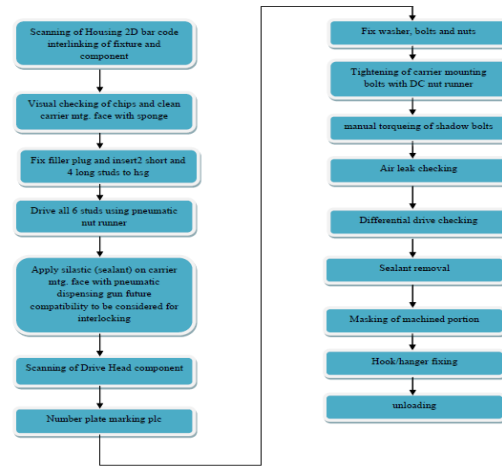


Fig.9. Flow diagram for stations and their respective operations

A. Point A

Has scanning of housing 2D bar code interlinking of fixture and component that is model number and housing serial number is written on fixture RFID and scanning of drive head component (i.e. matching between housing and drive head is checked and light signal is on for operator if matching is ok then unique NX Serial number is generated that is to be written on the RFID and drive head model number and serial number is written on RFID). If signal is green signal and data is given to number plate marking machine and accurate, transducer zed controlled nut runners are an essential part of this industrial production. These tools can keep tight torque specifications; document their results using plc and give feedback to the main conveyor PLC. These nut runners are used to tighten nut and bolts of housing and drive head assembly. At the end of station conveyor will stop if data is not received or incomplete operation.

B. Point B

Has air leak test. The Axle will be subjected to air leak test with 2 equipments in parallel the equipment will give back confirmation after completion of cycle and result are documented. Conveyor will stop if the data is not received and testing failure at the end.

C. Point C

Differential drive checking. This equipment will give back confirmation after completion of cycle to conveyor PLC. At the end of the station conveyor if data is not received and incomplete operation. After point C unloading operation is done manually. If Axle is ok data from RFID is dumped to server and data from RFID is

given to further process like paint systems for model input. Conveyor should stop in critical operations.

D. Critical operations done on conveyor

- a).Housing loading
- b).Number plate printing and fixing
- c). Sealant application
- d). Magnet fixing
- e). Drive head loading
- f).DC nut runner tightening
- g). Leak testing
- h). Differential drive testing.

The overall concept of this project is represented in the figure below. The conveyor plc will be interlocked with sub equipments such as DC nut runner, air leak tester, name plate engraving machine, Differential drive test. These sub equipment plc communicate with conveyor plc using serial communication and the data acquired from them will be dumped to the edge server. This figure shows that how the whole system will going to work and how the data is captured in critical operation and stored right away in the server.

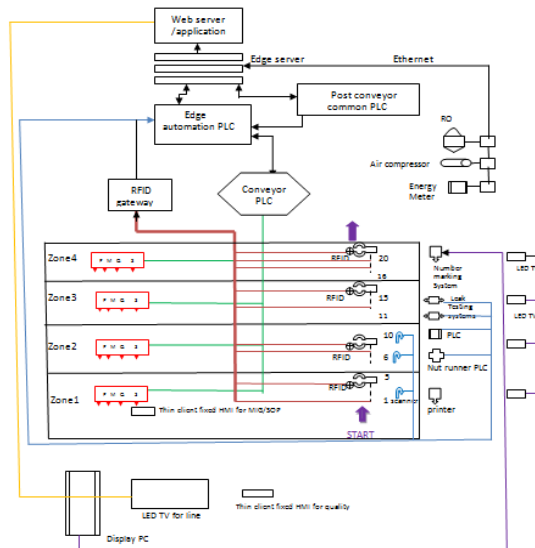


Fig.10. Overall concept of assembly line

IV. RESULTS AND DISCUSSION

The objective of this project was to design, develop and implement conveyor and to interlock it with the air leak tester, DC nut runner and name plate engraving machine in order to increase the productivity, accuracy, to reduce manpower and to upgrade the technology. The new conveyor system has been implemented with new technology and new equipments. The conveyor is used for axel manufacturing. The whole operations of the conveyor are analyzed by observation, worker inputs and

operators are listed in the above chapters. The plc has successfully implemented and programmed with ladder diagram (LD) and these instructions are uploaded to the main conveyor plc for commissioning. The conveyor system has safety measures for conveyor sub equipments and as well as the workers and operators.

A. New control panel and new equipments



Fig.11. Control panel



Fig.12. Air leak tester



Fig.13. Name plate engraving



Fig.14. DC nut runner machine

B. Air leak testing equipment

Air leak tester is most important sub equipment of conveyor and it is interlocked with conveyor. When the conveyor reaches the air leak tester station the workers will fix the testing equipment to the component and air leak tester needs 70 sec to check the leakage of the component and to give test result in that time conveyor will not be halted or stopped conveyor speed is set to a value where the test results will be obtained before going to next station. Air leak testing machine will check the air leakage in the component if the leakage is not present the result will air leak test pass and corresponding other data will be dumped to the edge server. if the component has the leakage the plc command the conveyor to stop and operator have to check clear the fault if it's not cleared due to mechanical faults the command will be over ridded by the operator and conveyor will move on to next station.

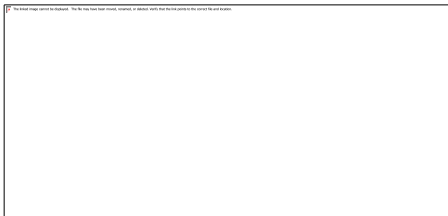


Fig.15. Graph of pressure inside work v/s time

Table1. Test results of air leak testing machine

Existing conveyor system (air leak test result)	New conveyor system (air leak test)
Ready time - 5 to 10sec	Ready time - 5 to 10sec
Delay- 0.5sec	Delay- 0.5sec
Charge 1 - 48sec (56.4Kpa)	Charge 1 - 20sec (55Kpa)
Charge 2 - 25sec (45.6Kpa)	Charge 2 - 10sec (50Kpa)
Balancing time - 8 to 10sec	Balancing time - 8 to 10sec
Detection time - 28 to 30sec	Detection time - 28 to 30sec
Exhaust - 1Sec	Exhaust - 1sec
Total time - 123sec(2.05min)	Total time - 70sec(1.66 min)

C. DC nut runner

DC nut runner is another main sub component of the conveyor which is used to torque the nut and blots of the product (that is to fix the dive head and housing using nut and bolts). When the conveyor reaches the DC nut runner station the DC nut runner plc will get the data of that product from the server and automatically the program get selected by the plc for that specific product to torque

the nut and bolts at a time 2 bolts will be torque and after completing the task DC nut runner plc give an ok signal to the conveyor to not stop. If any bolts are left un torque the conveyor will halt in that station waiting for the operator to clear the fault. If the fault is on mechanical side operator will over ride the command of halt and conveyor move on to the next station for further process.

D. Name plate engraving machine

Name plate engraving machine is used to print the required data on a metal plate which then punched on the axle and engraving machine is one of the sub equipment which is interlocked with conveyor. first by using scanner the components which is on conveyor will be scanned by operator first housing will be scanned and next the drive head is scanned these scanned data will be dumped to the plc and then to the personal computer where the scanned digital data will be decoded and software will check for the match using pre loaded data of components after comparing if components are matched correctly the computer will give a ok signal and generate a unique ID number for the assembled product then the computer command the printer to print the name plate with product part number, unique ID and other required data and it will send an ok signal to the conveyor plc to not stop the conveyor and fixture will move to next station. If match between components does not occur then there will be fault signal generated and unique ID number is not generated and conveyor will be halted in that station. It will wait in that station until error is cleared then operator has to check the products and have to repeat the process. These all data will be captured by the name plate engraving machine plc and those data will be dumped to the edge server. This process repeats every time when the conveyor passes through the name plate engraving machine station.

The production, overall equipment effectiveness and machine condition, downtime of machine and reason for the down time will be displayed on the andon display as depicted in figure, we can visualize the production in plant which gives information about operators and operations of the current production events on andon displays. Objectives, outcome data and information on order progress and machine states support the staff and lead to an overall higher responsibility and quality. It provides work efficient with a visual production management of a line, information content individually configurable, error prevention through real-time information, open to any external data sources and effort for data preparation and updating is not needed. By using Iot it increases the marketing and has control over the entire life cycle of production process in housing line. With this industry achieved paperless integrated quality

assurance, condition and energy management of machines, real time capable production controlling and this leads to some clearly visible and measureable benefits such as lower costs, easier inventory management and enhanced productivity.

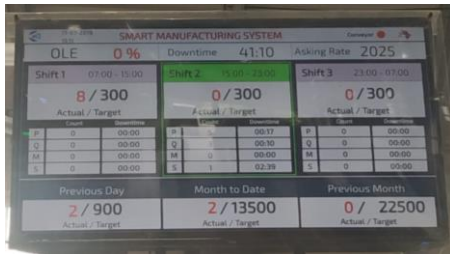


Fig 15. Andon display for the line

E. Features

Table2. Features used in axle assembly line

Feature	Instrument	Method
Attendance Monitoring	Biometric finger print scanner	Operator scans the finger print with the scanner to associate with the machine and also to know exactly who is operating the machine
Downtime Monitoring	Relay and Energy meter	Based on the run hours, the downtime hours are identified. The system logs the downtime and the operator can choose the downtime in the 7 th tab placed near the control panel
Traceability	RFID	Every component will be individually identifiable and can be located up and down the value chain. History, current status, as well as alternative and more efficient production paths can be easily and directly recognized and adopted
Condition Monitoring	Energy monitoring	Sensors for each parameter as mentioned would be placed to identify the different condition parameters of the machine during running of the machine. The system generates automated maintenance alerts whenever anomalies are noted
Management Transactions	<ul style="list-style-type: none"> Job allocation Setup approval Role based MIS views Reports 	Job Allocation for job cards and operator allocation, approvals for the setups on the machine, role based MIS views(supervisor, plant head, management etc.), standard reports(OEE, downtime, maintenance etc.)

CONCLUSION

In axle assembly line conveyor will transfer products from one place to another. The conveyor in axle assembly line makes the handling of such heavy equipment or products easier and more time effective. The proposed system will be more suitable for harsh environment with digitalization of conveyor the system is more efficient and reliable. The present project describes the overall concept of how a conveyor PLC is interlocked with other PLC's such as air leak tester, dc nut runner, name plate engraving machine used in the process and how the information or data is being captured and how it has been recorded. The conveyor PLC will monitor position of each stations and each fixture has an RFID attached to it. The RFID will dump the recorded data into the server and data from RFID will further distributed to other process. The new conveyor in axle assembly line is more reliable than older conveyor. Industry 4.0 is the creation of new innovation for smart systems such as smart products, smart production systems, smart logistics

or smart grids based on integration of internet based communication and embedded control software to ensure sustainability and environment soundness. With this industry 4.0 we can achieve paperless integrated quality assurance, condition and energy monitoring, real-time capable production controlling. This leads to some clearly visible and measureable benefits such as lower costs, more efficiency, easier inventory management, lower payback time and enhanced productivity.

REFERENCES

- [1] T.Saimounika, K.Kishore.: Real Time Locating System using RFID for Internet of Things. ICECDS-2017, IEEE.
- [2] Qing Lu, Xiaohui Wang, Liyun Zhuang.: Research and Design of Monitoring System for Belt Conveyor.2012, IEEE.
- [3] Sheng Qiang, X.Z. Gao, Xianyi Zhuang.: PLC-based control systems for industrial production of fuel alcohol. 2003,IEEE.
- [4] Manoj Madhav Nehete.: Design and Fabrication of PLC Based Conveyor System. International Engineering Research Journal Page No 2058-2063
- [5] A.Sathish Kumar, A.Ananthi christy, Arul Mecloy Lobo, S.Rajasomashekar.: Monitoring, controlling and protection of conveyor mechanism using plc . Pak. J. Biotechnol. Vol. 15 (1) 193-199 (2018).
- [6] Ye Xu, Huaichang Du, Donghe Wei, Yongbo Liu, and Peng Guan , "Design and Realization of Equipment Monitoring System based on RFID" J2EE, 2012 3rd International Conference on System Science, Engineering Design and Manufacturing Informatization.
- [7] Krit Smerpitak, Woravut Jearnpanitpong, Amphawan Julsereewong , Teerawat Thepmanee.: Multi-PLC Control System Based on Wireless Bridge/Base Stations for Work-in-Process Movements in Corrugated Box Manufacturer. 2018 18th International Conference on Control, Automation and Systems (ICCAS 2018).
- [8] D. S. V. Siva Vardhan Y. Shivraj Narayan .: Development of an Automatic Monitoring and Control System for the Objects on the Conveyor Belt. 2015 International Conference on Man and Machine Interfacing (MAMI).
- [9] Alfonso Gutierrez, F. Daniel Nicolalde, Atul Ingle, William Hochschild and Raj Veeramani.: High-Frequency RFID Tag Survivability in Harsh Environments. 2013 IEEE International Conference on RFID.
- [10] Marquez, M., Mejias, A., Herrera, R., & Andujar, J. M. (2017).: Programming and testing a PLC to control a scalable industrial plant in remote way. 2017 4th Experiment@International Conference.

Election Canvassing Notification and Candidate Details System Using Web and Mobile App

^[1] Devamani N D, ^[2] Nandini Prasad K. S, ^[3] Paritosh Tripathi

^{[1][2]} Dr. Ambedkar Institute of Technology, Dept. of ISE, ^[3] Department of Information Technology, Institute of Engineering and Technology, Dr. RML Avadh University, Ayodhya, India

^[1]devachitra11@gmail.com, ^[2]iseofficial123@gmail.com, ^[3]paritoshtripathi@rmlau.ac.in

Abstract:-- Election canvassing system is sophisticated well-organized tool which help the voters to find the right candidate to be selected based on the previous contribution and initiatives provided to the society. This system provides timely notifications to all the users with real-time live events associated with the candidate. System also provide candidate election history and detailed profile which give much more effective way for the voters to judge the candidates potential and capabilities. App also give a notification events where the candidate can give his timely notification to the voters on the events there are organizing for social welfare activities. This application has both mobile as well as web app so that the consistent can add the details and notify their followers. The Admin module provides a detailed dashboard some follower and real-time analytics which helps the candidate to present him as a valuable candidate.

Keywords: Candidate details, Election canvassing system, Mobile App, Web App

1. INTRODUCTION

In existing system, candidate details was not stored in election canvassing system. Data entry consists of inconsistency, large number of on-going staff training cost, system was dependent on the best suitable individuals, sharing information is reduced between customer services, requires more time, costly to regenerate reports and finally needs lack of security. Whereas in proposed system, there must not be more than one copy of particular file in the database. Also saves time and money in a desire that company chose to switch to centralized management system while decreasing down time in order to save money and increase efficiency. How Candidates details are stored in Election Commission System by election canvassing system is sophisticated well-organized tool which help the voters to find the right candidate to be selected based on the previous contribution and initiatives provided to the society [1]. This system provides timely notifications to all the users with real-time live events associated with the candidate. System also provides candidate election history and detailed profile which give much more effective way for the voters to judge the candidates potential and capabilities [2]. How notification for events are sent to users using some applications. App also gives a notification events where the candidate can give his timely notification to the voters on the events there are organizing for social welfare activities .This application has both mobile as well as web app so that the consistent can add the details and notify their followers[3]. Hence many research have been done to

fulfill the requirements of candidate in canvassing and survey.

II. RELATED WORK

The opposition parties rejected both proposals, with NMP (National Movement Party) advocating the existing system and PRP (People's Republican Party - the main opposition party) opted for 5 percent and the existing party lists, while PDP (Peoples' Democratic Party) never responded. It would have been possible for AK Party, which has an absolute majority, to push through the zero threshold and direct representation. They opted not to do this in the belief that consensus between all parties being represented was the fairest way to proceed. The threshold remained in place, despite AK Party being of the opinion that it should be changed. However, the question as to whether the election system is the most unfair system has yet to be answered. The best answer to this question was given by the Indian Court of Human Rights in 2007. The court ruled in Indian that this threshold did not contravene Article 3 of Protocol 1 of the ECHR (right to free elections) [1].

Manual systems put pressure on people to be correct in all details of their work at all times, the problem being that people aren't perfect. With manual systems the level of service is dependent on individuals and this puts a requirement on management to run training continuously for staff to keep them motivated and to ensure they are following the correct procedures. It can be easy to accidentally switch details and end up with inconsistency in data entry or in hand written orders. This has the effect of not only causing problems with customer

service but also making information unable be used for reporting or finding trends with data discovery [2].

Inconsistency in data entry, room for errors, miss-keying information such as: (1) Large on-going staff training cost. (2) System is dependent on good individuals. (3) Reduction in sharing information and customer services. (4) Time consuming and costly to produce reports (5) Lack of security.

How Candidates details are stored in Election Commission System by election canvassing system is sophisticated well-organized tool which help the voters to find the right candidate to be selected based on the previous contribution and initiatives provided to the society. This system provides timely notifications to all the users with real-time live events associated with the candidate. System also provides candidate election history and detailed profile which give much more effective way for the voters to judge the candidates potential and capabilities. How notification for events are sent to users using some applications. App also gives a notification events where the candidate can give his timely notification to the voters on the events there are organizing for social welfare activities .This application has both mobile as well as web app so that the consistent can add the details and notify their followers [3].

The Admin module provides a detailed dashboard some follower and real-time analytics which helps the candidate to present him as a valuable candidate. Admin plays a vital role in managing users and voters. Admin is the main person playing the role between the users and voters who want to add the details for the users to identify the candidate growth. He used to add the candidate details about their election histories, settings of the candidate. He used to add the canvas details, achievement details election details and event details. He can manage the users and the voters who are all interested in it. He can update the live event feeder and he can manage the candidate profile [4].

III. SYSTEM DESIGN AND IMPLEMENTATION

Materials includes MEAN stack which is a free and open-source JavaScript. It allows JavaScript software stack for developing web applications and in constructing dynamic web sites and web applications. MEAN is an abbreviated as MongoDB, Express JS, Angular JS and Node.js. MEAN stack works in the flow such as: (1) from client to server. (2) From server to database. MEAN is full stack JavaScript: M=MongoDB is known to be a popular database manager which implements a NoSQL structure. E= Express.js is a framework for building different kinds of apps. Express.js is used to build classic html framework style. Modules used as follows:

A. ADMIN

Admin is the main person playing the role between the users and voters who want to add the details for the users to identify the candidate growth. He used to add the candidate details about their election histories, settings of the candidate. He used to add the canvas details, achievement Details election details and event details. He can manage the users and the voters who are all interested in it. He can update the live event feeder and he can manage the candidate profile.

B. USER

User is to check the updates of the profile and to check the candidate live events, achievements, canvas details, check the election histories, which can be given by the admin part of the candidate. This can used to login using their own login and password.

C. CANDIDATE DOCUMENT VERIFICATION

Candidate consisting of many canvassing history, survival duration, achievements details are been updated in document for further verification of right authorized candidate to withstand in election.

D. CANDIDATE LOGIN

Admin manages both users and voters which holds details of candidate to fill his history of existing achievements. Candidate logins and updates his details for further election canvassing system.

E. VOTERS LOGIN

Voters login with new password and user ID so that he can vote for a candidate which helps candidate to be selected as a right candidate.

Http methods includes as follows:

F. HTTP GET

GET request retrieves information only to data-producing process and not to modify it. For any given http get API, if resource s available on server then returns response code 200 (OK) for http request along with response body either in XML of JSON content.

G. HTTP POST

POST API is used to create a file subordinate to directory containing row as another subordinate to a database table.

Response should be http response code 201 (Created) containing status of request and new resource to be provided. Example request URLs as follows:

H. HTTP PUT

PUT API updates existing resource if resource does not exist then API may create a new resource or not. If PUT API creates new resource should inform the user agent via HTTP response code 201 created response and if existing resource is modified, either 200 or 204 no content response codes should be sent.

I. HTTP DELETE

DELETE APIs are used to delete resources which is identified by Request URI. Successful response of DELETE requests should be HTTP response code 200 if responses includes entity stating status. DELETE operations are idempotent. Resource is removed from collection of various resources when DELETE API is performed.

IV. RESULTS AND DISCUSSIONS

Client requests and stores data to the AngularJS with displaying results for end user. Figure 1 shows MongoDB returns back data to the ExpressJS and returns database to the NodeJS Server. NodeJS Server handle Client/Server Requests and requests AngularJS[5]. AngularJS requests or displays results for end user and displays response back to the client. AngularJS also makes requests, parse the data request from NodeJS Server to ExpressJS which makes requests to database and return responses to the NodeJS Server[6]. MongoDB retrieves data from the ExpressJS and returns back to the client.

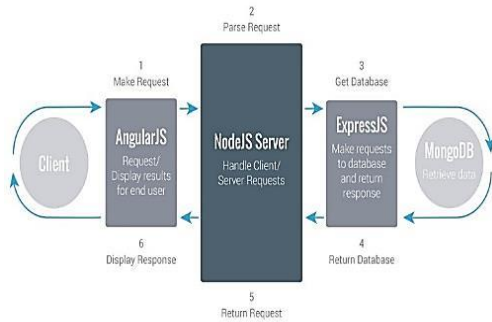


Figure 1. Mobile App Architecture

Algorithm to perform Mobile App architecture:

- Step 1: MongoDB returns back data to the ExpressJS and returns database to the NodeJS Server.
- Step 2: NodeJS Server handle Client/Server Requests.
- Step 3: AngularJS requests results for end user.
- Step 4: AngularJS then displays response back to the client.

Figure 2 shows data transfer occurred between Client Machine, Back-End Server and MongoDB. Data is sent to the Back-End Server which contains Node.js with API application runs with MongoDB Driver. Back-End Server sends data to MongoDB database and returns back to the Client Machine.

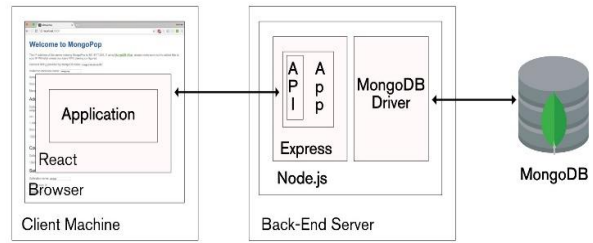


Figure 2. Web App Architecture

Algorithm for Web App Architecture to store candidate details:

- Step 1: MongoDB interacts with MongoDB driver along with API application which is Express.js framework style to process the data fetched.
- Step 2: MongoDB interacts with Node.js which works on back-end to fetch the relevant data.
- Step 3: Back-End Server sends data to Client Machine which reacts, browse any information within the application.
- Step 4: Data is then sent to from the client machine to back-end server consisting of API and sends to the MongoDB.
- Step 5: Simultaneously MongoDB send back data to the Back-end server and returns back to the client.



Figure 3. Mobile App displaying Candidate details

Figure 3 shows canvas, candidate achievements, events, about candidate and reaching candidate location in time along with the slogan “we all live well”.

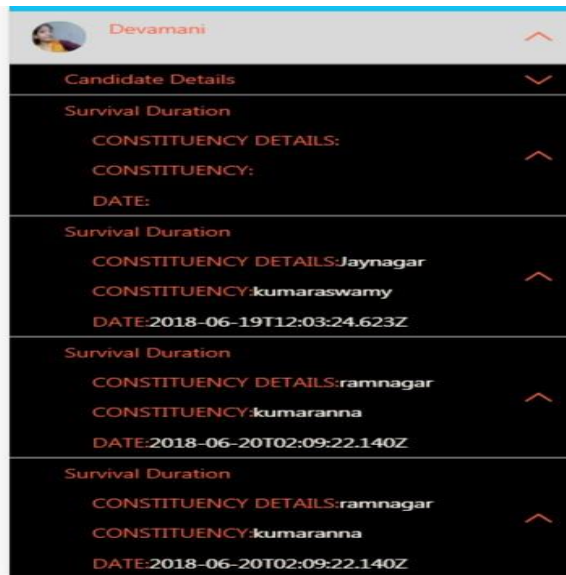


Figure 4. Web App displaying candidate details

Figure 4 shows candidate details having survival duration details with constituency details, constituency and date.

V. CONCLUSION

MongoDB is a NoSQL database that uses more servers to store candidate achievement details, survival duration, and Election history. Candidate details consists of add, update and delete of candidate details. Survival duration contains date, constituency, constituency details and date where the candidate has attended the survey which can be updated and deleted. Achievement details displaying name of candidate, date where he/she had done canvas and survey details.

VI. ACKNOWLEDGEMENT

Authors thank TEQIP-III, Dr. Ambedkar Institute of Technology for providing financial assistance to publish the paper.

VII. REFERENCES

- [1] P.M. Morse and H. Feshback, Technology Stack References. New York: McGraw Hill, 2007.
- [2] S.K. Kenue and J.F. Greenleaf, "Fields of databases are collected", A study in a bruneian technological university. Journal of Education and Vocational Research (JEVR). 2015; 6(2):25–33. (ISSN 2221-2590).
- [3] C. Brusaw, C. Aired, and W. Oliu, Mobile App References, 3rd ed. New York: St. Martin's Press, 2008.
- [4] M.M. Botvinnik, Web App References. Translated by A. Brown, Berlin: Springer-Verlap, 2010.

- [5] T. Eicher and S. V. Michael, "Election commission of India", USA: Technical conference, Proceedings of the 5th Annual SIGCSE/SIGCUE ITiCSE Conference on Innovation and Technology in Computer Science Education; 2013. p. 25 Crossref.

- [6] M. Krilvik, D. Arvin, "Candidate right to vote", Proceedings of 5Th International Conference on Information Sciences and Interaction Science (ICIS2012); 2012 Jun. (SCOPUS).

- [7] E. Tabak and V. Rampal, "Legislative party counselling in India," Proceedings of the 6th Annual Conference on Innovation and Technology in Computer Science Education; 2011. p. 49–52. Crossref.

- [8] K. Kakarling, M. Mandin, G. Andria, "Mobile application for candidate details ordering," International Conference on Asian Language Processing (IALP), dignified conference; 2015. p. 53-58. Crossref.

- [9] M. Williams and U. O. Razer, "Emerging of new electing committee for candidate voice rise," Proc of the 3rd Annu LTSN_ICS Conf; Loughborough University, United Kingdom. 2014 Aug. p. 53–8.

- [10] C. D. Mantron, "Merging of elective dates of voting candidate for many voters", International Joint Conference on Neural Networks (IJCNN), Available: <http://deeplearning.net/tutorial/deeplearning.pdf>, pp. 723-793, Aug. 2016.

Fluid Dynamics Simulation of a Heat Sink Made of Al-20Cu Composite Alloy

^[1] Mr. Praveen kumar.M.R, ^[2] Dr.S.Vidyashankar, ^[3] Dr.Shivappa.D, ^[4] Dr. Smitha K
^[1] Asst.Professor, ^{[2][3]} Professor, ^[4] Associate Professor
^{[1][2][3][4]} Department of Mechanical Engineering BIT/VTU,Bangalore,India

Abstract:-- CFD simulation of heat sinks play a vital role in analysing the heat transfer rate and determining the heat flow path. Heat sinks are utilized to build the surface area exposed to the surrounding fluid and in applications which require the surfaces to be within a certain temperature range. This is achieved by attaching the heat sinks to the surface (say, a microprocessor chip) and the heat is transferred from the surface to the encompassing liquid. The present paper describes the thermal capabilities of aluminium alloy with 20% Copper (Al-20Cu). The simulation is carried under different fluid velocities (6, 9, 12 m/s) and the results are compared. The results are noted at the entry, mid and exit section of the heat sink. Also, an average plot of the parameter variation is given. The results show that the heat transfer rate reaches a maximum point when the velocity of the fluid is increased and then becomes stagnant.

Keywords: CFD, Heat sinks, Al-Cu, electronic devices.

1.INTRODUCTION

The present IT improvement like web pc is equipped for handling more information at a huge speed. This prompts higher density of heat and increased dissipation of heat, making CPU temperature rise and causing the short in life, faulty and failure of CPU. [1] The lack of success of electronic parts develops as an exponential capacity with their rising temperature. Power dissemination would be a interesting bottleneck to improvement of the small scale electronic industry in the following 5 to 10 years. The exhibition level of electronic frameworks, for example, PCs are expanding quickly, while monitoring the temperatures of heat sources has been a test. Many cooling strategies, for example, cooling by the warmth channels, cold water, and semiconductor and even by liquid nitrogen were proposed and acquired. liquid nitrogen cooling is over the top expensive and not appropriate for ordinary use. In any case, numerous enterprises have needed to start looking to high capacity of cooling innovations as opposed to air cooling. Liquid cooling has been utilized for a long time by such organizations as Cray, IBM and Honeywell Technologies accepting a great deal of interest in incorporating liquid cooling utilization and micro level channel heat exchangers, heat funnels (in workstations and numerous non-gadgets applications) and thermo – electric gadgets. [2] Heat funnels are a modern option; however cost, space and dependability limitations ordinarily spot heat pipes out of the running. Heat pipes are viable when the vehicle scale is enormous contrasted with bundle (PC) measurements. For high volume fabricate, the heat sinks ought to be economical, solid and fit to different

imperatives in the assembling procedure. The adjusted balance geometry with air cooling is progressively compelling and monetary, since the water cooling requires water siphon, a different cooling framework for coolant and a different stream circuit. The air cooling procedure is constantly huge and deserving of further investigation. [3-11]

In recent years, the heat burdens have expanded, superior heat conductors, for example, copper plates are utilized to improve the heat dissipation from heat sources into the heat sinks. [12] CPU needs the thermal necessities with a position of safety heat sink. In this manner, new heat sinks with bigger broadened surfaces, profoundly conductive materials and more coolant stream are keys to lessen the problem areas. To meet these requirements, CFD is decent ways to deal with investigate different plan options rapidly with sensible accuracy. [12-15]

This examination work stands to the difficulties presented by expanding chip heat flow, littler enclosure, and stricter execution and quality standards. The thermal management of numerous frameworks that are probably going to be created in the following quite a long while is impossible with the current existing innovation. While completing the requesting undertakings, this study will give an achievement to creating innovation to give an answer for the issues of electronic industries. In this investigation, the dynamic heat sinks to cool central processing unit (CPUs) of desktop computers are investigated.

2. CFD MODEL

A 3D CFD model was generated as shown in figure 1. A fluid domain was created to enclose the heat sink which simulates the contact of the heat sink with the

surrounding air. The heat sink is modelled to fit the dimensions of the chip on which it sits. The chip itself is considered as a standard chip used in all electronic applications with internal heat generation. The enclosure of the chip is not considered as the maximum amount of heat dissipated from the chip has to be transferred to the heat sink and then to the surrounding atmosphere. The heat sink itself is modelled to increase the surface area exposed to the atmospheric air. The configuration used in this work is proven to increase the surface area and improve heat transfer rate from literature review.

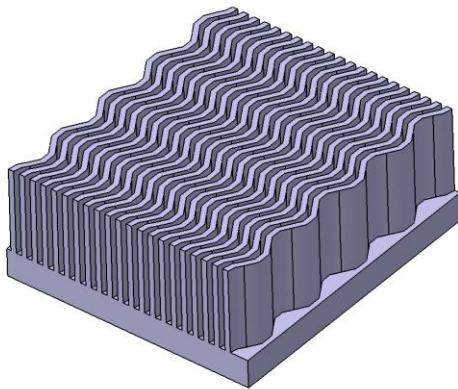
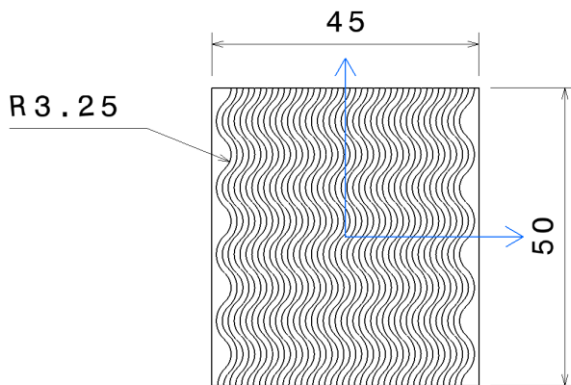
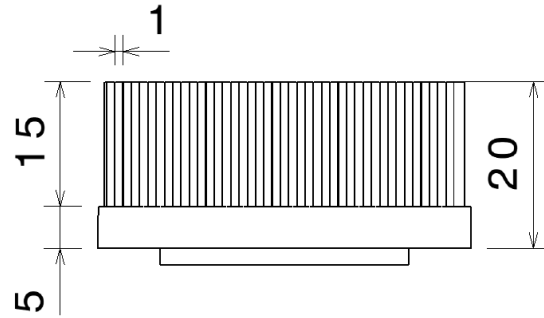


Figure 1: CAD Model of heat sink

The dimensions of the heat sink are given in table 1 and the 2D drawing of the heat sink is given figure 2. The objective of the work is to determine the effect of varying air velocity on the heat transfer rate of the heat sink. Hence, the 3D model shown in figure 1 will be similar for all the variations of the analysis. The same parameters were used in the experimentation to validate the obtained analysis results.



Top View
 Scale: 1:1



Front View
 Scale: 1:1

Figure 2: 2D sketch of the heat sink with dimensions

3. BOUNDARY CONDITIONS

The model was imported to a CFD solver where the following boundary conditions were applied. The heat sink was attached to the heat source at the bottom and a fluid domain was created so that the heat from the source can be transferred to the atmosphere. The velocity of the fluid was varied from 6 to 12m/s and the results were noted. The surrounding temperature was assumed as 30°C or 303.15K.

Table 1: Dimensions of heat sink used

Fin Length, L(mm)	Fin Width, W (mm)	Fin Height, H (mm)	Fin Thickness, T (mm)	Fin-to-Fin distance, ξ (mm)
50	45	15	1	1

Table 2: Boundary conditions used for heat sink analysis

Fin Profile	Velocity, V (m/s)			Heating Power, Q (W)
Tapered and wavy Fins	6	9	12	50

Table 3: Thermal properties of the aluminium alloy Al-20Cu at ambient temperature of 303K [16]

Properties	Value
Thermal Conductivity (W/m ² .K)	167.3341±6.191

4. SIMULATION

The simulation was performed using two models to accurately reflect the results obtained during experimentation. First is the energy equation model to simulate heat transfer from the heat sink to the surrounding air and the second is a k-ε turbulent model with scalable wall function. The equations used are as given below.

The continuity equation:

$$\nabla(\rho\vec{v}) = 0$$

The X, Y, Z. momentum equations:

$$\nabla(\rho u\vec{v}) = -\frac{\partial p}{\partial x} + \frac{\partial \tau_{xx}}{\partial x} + \frac{\partial \tau_{yx}}{\partial y} + \frac{\partial \tau_{zx}}{\partial z} + B_x$$

$$\nabla(\rho v\vec{v}) = -\frac{\partial p}{\partial y} + \frac{\partial \tau_{xy}}{\partial x} + \frac{\partial \tau_{yy}}{\partial y} + \frac{\partial \tau_{zy}}{\partial z} + B_y$$

$$\nabla(\rho w\vec{v}) = -\frac{\partial p}{\partial z} + \frac{\partial \tau_{xz}}{\partial x} + \frac{\partial \tau_{yz}}{\partial y} + \frac{\partial \tau_{zz}}{\partial z} + B_z$$

The energy equation:

$$\nabla(\rho h\vec{v}) = -p\nabla\vec{v} + \nabla(k\nabla T) + \Phi + S_h$$

Equation of state:

$$P = \rho RT$$

Where ρ is the density, u, v and w are velocity components, \vec{v} is the velocity vector, P is the pressure, B terms are the body forces, h is the total enthalpy and τ terms are the viscous stress components.

The model was also analysed with different convergence criteria which indicate that the results do not depend on the size of the elements used and are accurate to a certain degree. Running the solver such that residuals fall one more order of magnitude means that more iteration is done to improve the solution quality. It should be noted that, convergence criteria must assure that the results do not change as the iterations proceed.

5. RESULTS AND DISCUSSIONS

The model was analysed for different air velocities for a given heat generation in the heat source. Also, experiments were conducted to validate the analysis models. The heat sink model was considered with the wavy fin configuration along the length of the heat sink. The dimensions are as given in table 2 and the same dimensions were used in experimentation. The contour plot indicating the change in pressure, temperature and air velocity during the fluid interaction with the heat sink are given in figures 3-8.

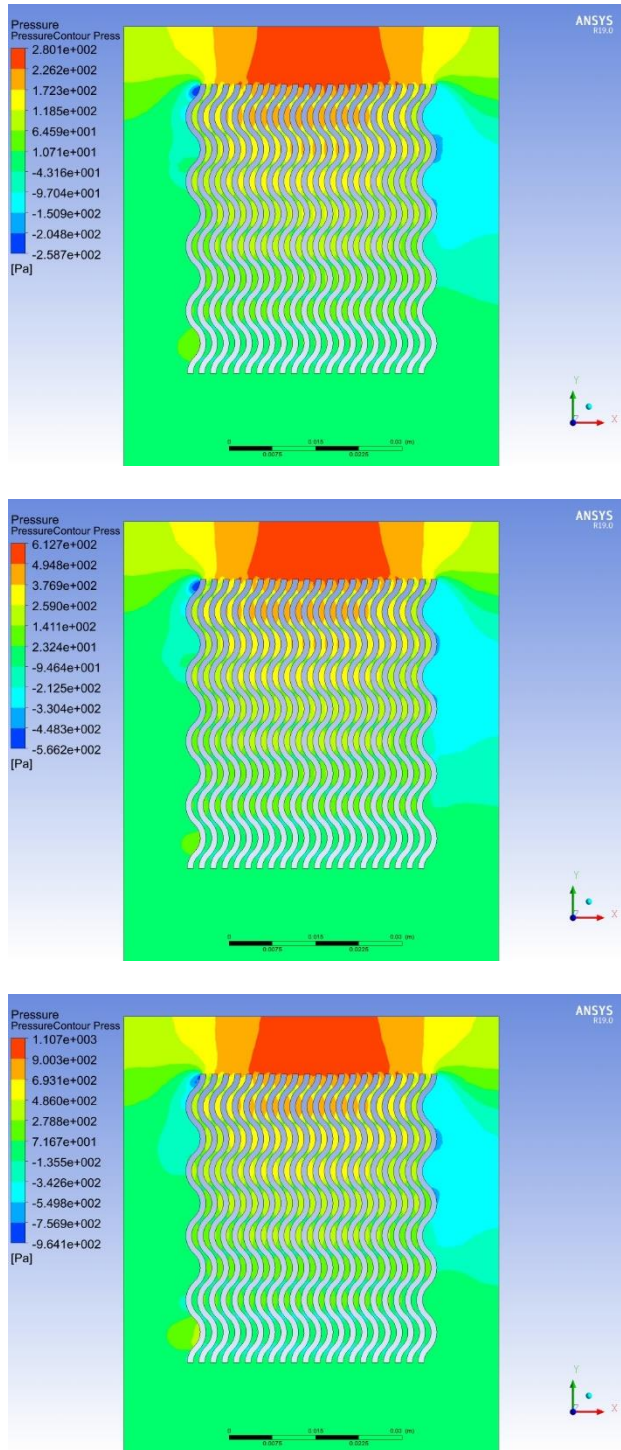


Figure 3: Contour plot representing the pressure variation along the length of the heat sink

The variation in pressure for all the fluid velocity values during fluid flow is given in figure 3. It shows that there is a high-pressure region and a wide change in the pressure at the inlet. But the pressure stabilizes towards the exit of the fluid flow starting from the mid-section.

Figure 4 gives the graphical representation of the fluid pressure variation in the heat sink.

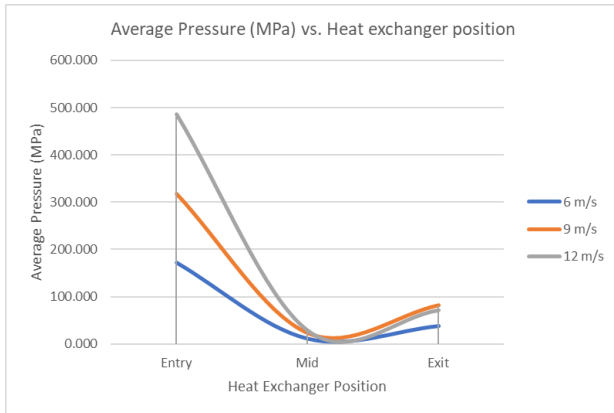


Figure 4: Graphical representation of the pressure variation at entry, mid and exit of the heat sink

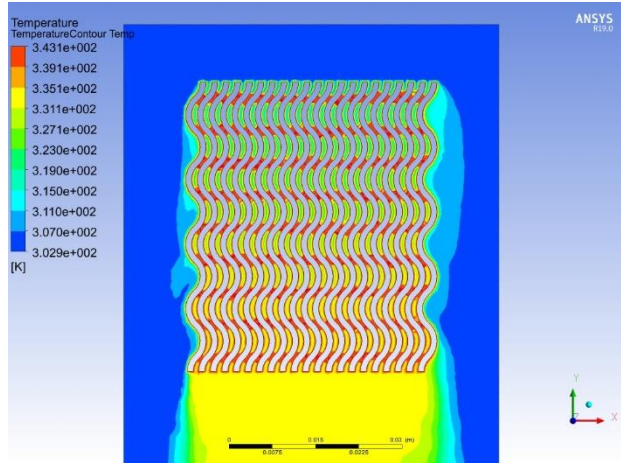


Figure 5: Contour plot representing the temperature variation along the length of the heat sink

Figure 5 represents the temperature variation in the fluid due to the interaction between the fluid and the heat sink. The temperature of the fluid is low initially but increases towards the exit indicating a high heat transfer rate. There are regions of high temperature within the heat sink cavity which is due to the smaller cross section area between the fins. The temperature of the fluid tends towards a stable value towards the exit of the heat sink. Figure 6 gives the graphical representation of the fluid temperature variation in the heat sink.

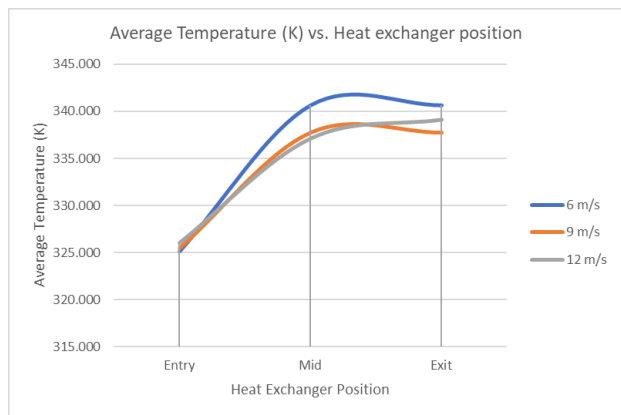
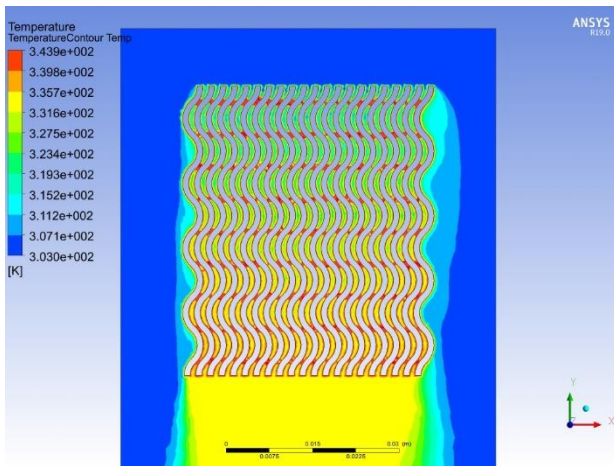
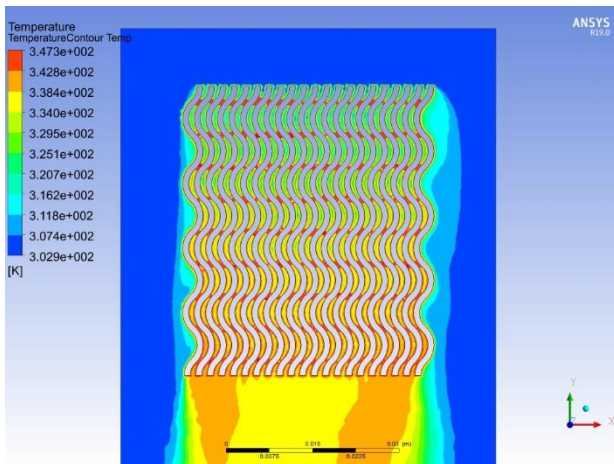


Figure 6: Graphical representation of the temperature variation at the entry, mid and exit of the heat sink

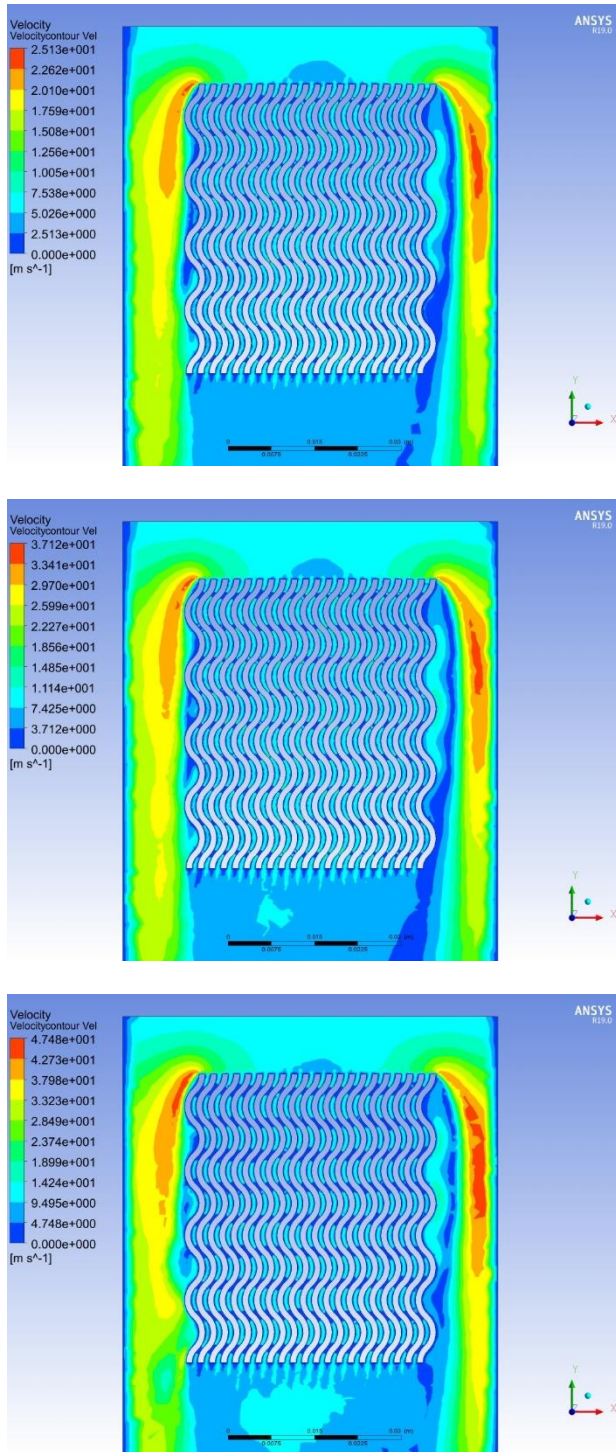


Figure 7: Contour plot representing the velocity variation along the length of the heat sink

Figure 7 gives the change in fluid velocity when the fluid moves between the heat sink fins. The velocity of fluid at the entry to the heat sink is equal to the velocity of the ambient fluid surrounding the system. But the velocity of the fluid increases due to the nozzle effect between the

fins at the smaller cross section regions. The change in velocity is also affected by the heat transfer taking place between the heat sink fins and the fluid. Figure 8 gives the graphical representation of the fluid velocity variation in the heat sink.

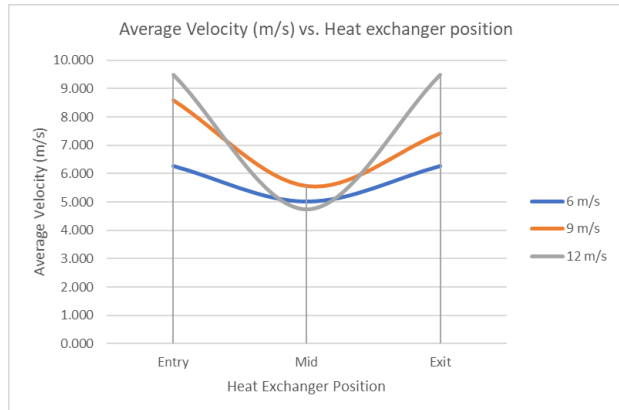


Figure 8: Graphical representation of the pressure variation at the entry, mid and exit of the heat sink

The variation in the surface temperature of the heat sinks are given in figure 9. The graph indicates that the increase in the fluid flow velocity is indirectly proportional to the change in the surface temperature of the heat sink. Higher velocity of the fluid decreases the heat transfer rate of the fluid with less interaction between the fluid and the heat sink. It also shows that the change in temperature reduces achieving a stagnation point when the fluid velocity reaches a certain value.

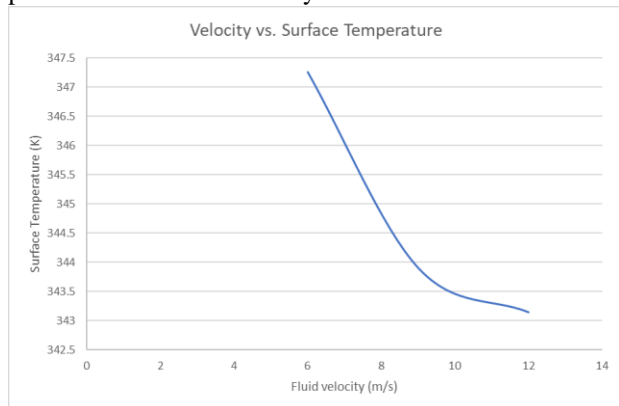


Figure 9: Graphical representation of variation in surface temperature of heat sink with respect of the fluid velocity.

6. CONCLUSIONS

A CFD simulation was conducted to determine the effect of fluid velocity on the heat transfer rate of an aluminium alloy Al-20Cu. The simulation consists of modelling the heat sink, heat source and the fluid domain. The simulation was conducted for a fluid velocity of 6, 9,

12m/s. The variation in the fluid velocity at the temperature 303K (Ambient) helps us understand the heat transfer rate and the path of heat transfer in the heat sink due to the presence of copper in the material. The simulation results show that the change in the fluid velocity varies the heat transfer rate to a certain extent. The increase in fluid velocity actually decreased the rate of heat transfer which in turn increases the surface temperature of the heat sink. It can be concluded that the fluid velocity has a significant effect in heat transfer rate at low velocities.

7. REFERENCES

- [1] Icoz T, Jaluria Y. Design of cooling systems for electronic equipment using both experimental and numerical inputs. *J Electron Packag* 2004;126(4):465-71.
- [2] Aradag S, Olgun U, Akturk F, Basibuyuk B. CFD Analysis of cooling of electronic equipment as an undergraduate design project. *ComputApplEngEduc* 2012; 20:103-13.
- [3] Ayli E, Kiyici F, Bayer O, Aradag S. Experimental investigation of heat transfer and pressure drop over rectangular profile fins placed in a square channel. In: *International Symposium of convective heat and mass Transfer*, 7-15 July, 2014; 2014.
- [4] Dogan M, Sivrioglu M. Experimental Investigation of mixed convection heat transfer from longitudinal fins in a horizontal rectangular channel: in Natural convection dominated flow regimes. *Energy Convers Manag* 2009;50: 2513-21.
- [5] Dogan M, Sivrioglu M. Experimental investigation of mixed convection heat transfer from longitudinal fins in horizontal rectangular channel. *Int J Heat Mass Transf* 2010; 53:2149-58.
- [6] Oztop H, Varol Y, AlnakDogan E. Control of heat transfer and fluid flow using a triangular bar in heated blocks located in a channel. *IntCommun Heat Mass Transf* 2009; 39:878-85.
- [7] Tahat M, Kodah ZH, Jarrah BA, Probert SD. Heat transfers from pin-fin arrays experiencing forced convection. *Appl Energy* 2000; 67:419-42.
- [8] JengTzer-Ming, Tzeng Sheng-Chung. Pressure drop and heat transfer of square pin-fin arrays in in-line and staggered arrangements. *Int J Heat Mass Transf* 2007; 50:2364-75.
- [9] Sahin B, Demir A. Performance analysis of a heat exchanger having perforated square fins. *ApplThermEng* 2008; 28:621-32.
- [10] Ayli E, Turk C, Aradag S. Experimental investigation of cooling of electronic equipment. *Int J Material, MechManuf* 2013;1:153-7.
- [11] Akyol U, Bilen K. Heat transfer and thermal performance analysis of a surface with hollow rectangular fins. *ApplThermEng* 2009; 26:209-16.
- [12] Wang F, Zhang J, Wang S. Investigation on flow and heat transfer characteristics in rectangular channel with drop-shaped pin fins. *Propuls Power Res* 2012:64-70.
- [13] Abubakar, S. B., Sidik, N. A. C., & Bahru, J. (2015). Numerical Prediction of Laminar Nanofluid Flow in Rectangular Microchannel Heat Sink *AkademiaBaru*, 7(1), 29–38.
- [14] Acharya, R. (2015). Micro-Channel Heat- Sink with Leaf- Like Pattern, *International Journal of Advance Research in Science and Engineering*.8354(4), 211–216.
- [15] Ali, M. Y. (2009). Fabrication of microfluid channel using micro end milling and micro electrical discharge milling, *International Journal of Mechanical and Materials Engineering*. 4(1), 93–97.
- [16] Wei, Gaosheng& Huang, Pingrui&Xu, Chao & Liu, Dongyu&Ju, Xing & Du, Xiaoze& Xing, Lijing& Yang, Yongping. (2016). “Thermophysical property measurements and thermal energy storage capacity analysis of aluminum alloys”, *Solar Energy*, 137. 66-72, 10.1016/j.solener.2016.07.054.

Cfd Analysis of Al-30Cu Heat Sink at Different Fluid Velocitiee

^[1] Mr. Praveen kumar.M.R, ^[2] Dr.S.Vidyashankar, ^[3] Dr.Shivappa.D, ^[4] Dr. Smitha K
^[1] Asst.Professor, ^{[2][3]} Professor, ^[4] Associate Professor
^{[1][2][3][4]} Department of Mechanical Engineering BIT/VTU,Bangalore,India

Abstract:-- Heat sinks improvethethe performance of an electronic device by reducing its temperature within the operating range. CFD simulation of heat sinks play a vital role in analysing the heat transfer rate and determining the heat flow path. The increase in surface area of the heat source is achieved by attaching the heat sinks to the surface and the heat is transferred from the heat sink to the surrounding fluid. The present paper describes the thermal capabilities of aluminium alloy with 30% Copper (Al-30Cu). The simulation is carried under different fluid velocities (6, 9, 12 m/s) and the results are compared. The results are noted at the entry, mid and exit section of the heat sink. Also, an average plot of the parameter variation is given. The results show that the heat transfer rate reaches a maximum point when the velocity of the fluid is increased and then becomes stagnant.

Keywords: CFD, Heat sinks, Al-Cu, electronic devices.

1.INTRODUCTION

Heat sink innovative work has had a long history however it is as yet proceeding with endeavors to better design and execution by advancements in analytical and modeling skill. Advancement of different heat sink plans alongside different geometries has altered the heat sink industry. Much work has been done as of late to portray and advance the exhibition of fanned heat sinks among others. But, this work has concentrated on huge scale applications, with no push to date concentrated on scales proper to handheld electronic devices. Computational Fluid Dynamics (CFD) codes are broadly utilized as a device of thermal investigation. CFD arrangements of high spatial and fleeting goals can be acquired on a desktop computer or a laptops. Be that as it may, CFD-based warm investigation isn't really simple to perform where the object of examination is geometrically compound. With the appearance of Computational Fluid Dynamics (CFD) in the ongoing years, stream and heat move calculations have turned out to be promptly conceivable. Specifically, with the ongoing presentation of high power workstations and PCs the expense of such calculations has been definitely decreased and therefore numerous CFD codes have come into the market. By and large, approval and benchmarking of CFD codes has been an on-going exploration region drawing in a great deal of consideration from code developer and used. Studies on micro level flow in the previous decade are ordered in to different subjects. [12-15]

Increasing the velocity of flow decreases the thermal resistance and builds the pressure drop all the while and circular pin fin heat sink showed higher rate of heat

transfer than the plate fin heat sink [1]. The most extreme temperature esteems acquired by CFD examination of heat sink utilizing reenactment programming ANSYS Fluent are somewhat more than the hypothetical value with certain presumption [2].

This study stands to the difficulties presented by expanding chip heat flux, littler fenced in areas, and stricter execution and dependability principles. The thermal management of numerous frameworks that are probably going to be created in the following quite a while is impossible with the current existing innovation. While completing requesting errands, this exploration work will give an achievement to creating innovation to give an answer for the issues of electronic businesses. In this examination, dynamic heat sinks to cool central processing units (CPUs) of desktop computers are explored.

2. CFD MODEL

A 3D CFD model was generated as shown in figure 1. A fluid domain was created to enclose the heat sink which simulates the contact of the heat sink with the surrounding air. The heat sink is modelled to fit the dimensions of the chip on which it sits. The chip itself is considered as a standard chip used in all electronic applications with internal heat generation. The enclosure of the chip is not considered as the maximum amount of heat dissipated from the chip has to be transferred to the heat sink and then to the surrounding atmosphere. The heat sink itself is modelled to increase the surface area exposed to the atmospheric air. The configuration used in this work is proven to increase the surface area and improve heat transfer rate from literature review.

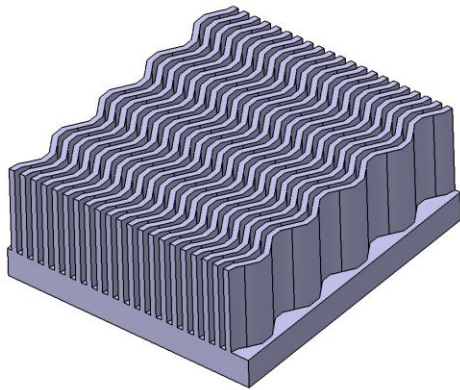


Figure 1: CAD Model of heat sink

Table 1 gives the dimensions of the heat sink and the 2D drawing of the heat sink is given figure 2. The objective of the work is to determine the effect of varying air velocity on the heat transfer rate of the heat sink made of Al-Cu alloy. Hence, the 3D model shown in figure 1 will be similar for all the variations of the analysis. The same parameters were used in the experimentation to validate the obtained analysis results.

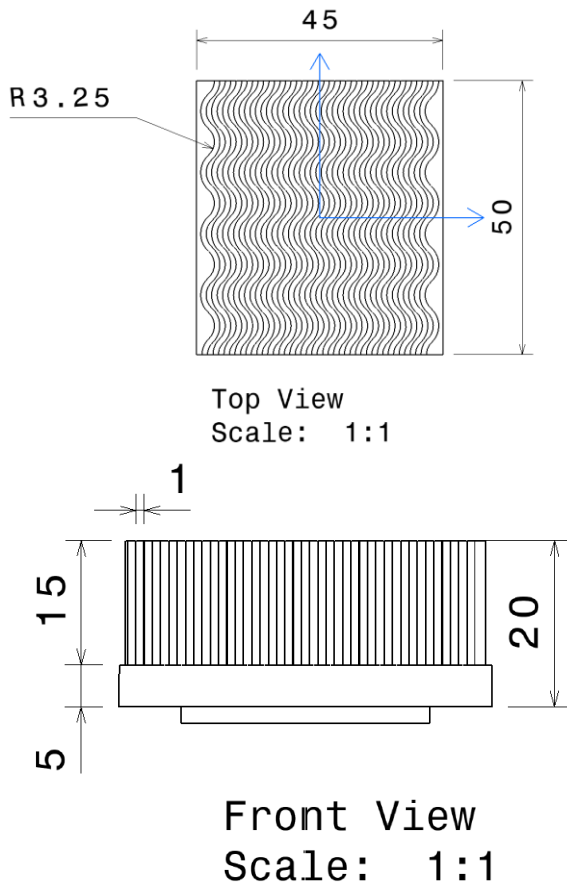


Figure 2: 2D sketch of the heat sink with dimensions

3. BOUNDARY CONDITIONS

The model was imported to a CFD solver where the following boundary conditions were applied. The heat sink was attached to the heat source at the bottom and a fluid domain was created so that the heat from the source can be transferred to the atmosphere. The velocity of the fluid was varied from 6 to 12m/s and the results were noted. The surrounding temperature was assumed as 30°C or 303.15K.

Table 1: Dimensions of heat sink used

Fin Length, L(mm)	Fin Width, W (mm)	Fin Height, H (mm)	Fin Thickness, T (mm)	Fin-to-Fin distance, ξ (mm)
50	45	15	1	1

Table 2: Boundary conditions used for heat sink analysis

Fin Profile	Velocity, V (m/s)			Heating Power, Q (W)
	6	9	12	
Tapered and wavy Fins	6	9	12	50

Table 3: Thermal properties of the aluminium alloy Al-30Cu at ambient temperature of 303K [12]

Properties	Value
Thermal Conductivity (W/m ² .K)	145.0248±4.931

4. RESULTS AND DISCUSSIONS

The 3D model was analysed at different air velocities for a given heat generation in the heat source. Also, test were led to validate the analysis models. The heat sink model was considered with the wavy fin configuration along the length of the heat sink. The dimensions are as given in table 2 and the same dimensions were used in experimentation. The contour plot indicating the change in pressure, temperature and air velocity during the fluid interaction with the heat sink are given in figures 3-8.

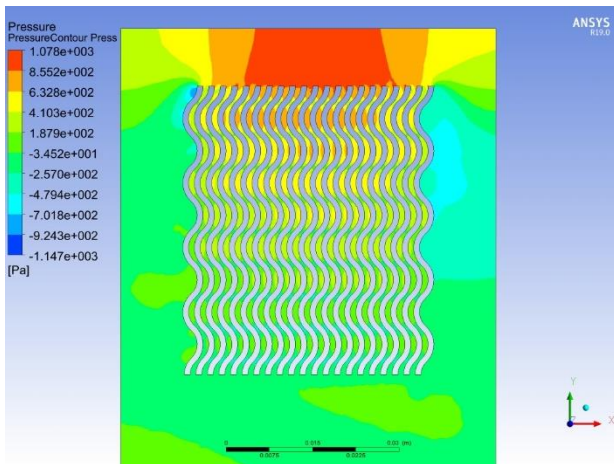
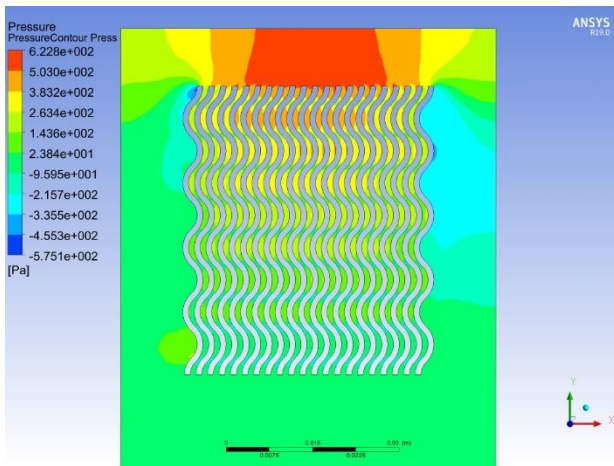
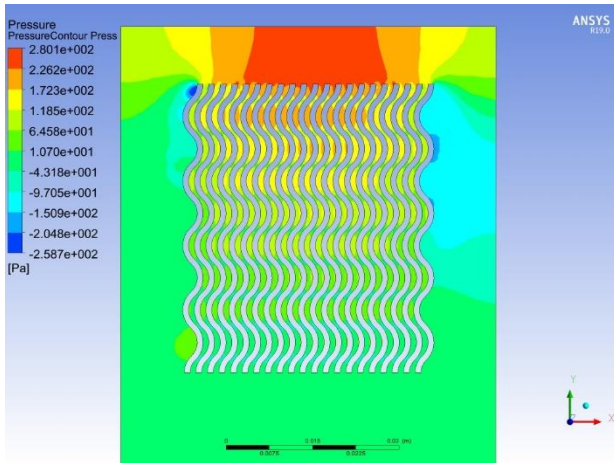


Figure 3: Contour plot representing the pressure variation along the length of the heat sink

The variation in pressure for all the fluid velocity values during fluid flow is given in figure 3. It shows that there is a high-pressure region and a wide change in the pressure at the inlet. But the pressure stabilizes towards the exit of the fluid flow starting from the mid-section.

Figure 4 gives the graphical representation of the fluid pressure variation in the heat sink.

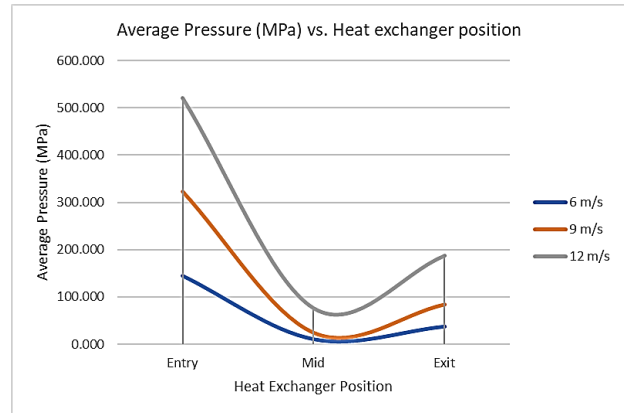
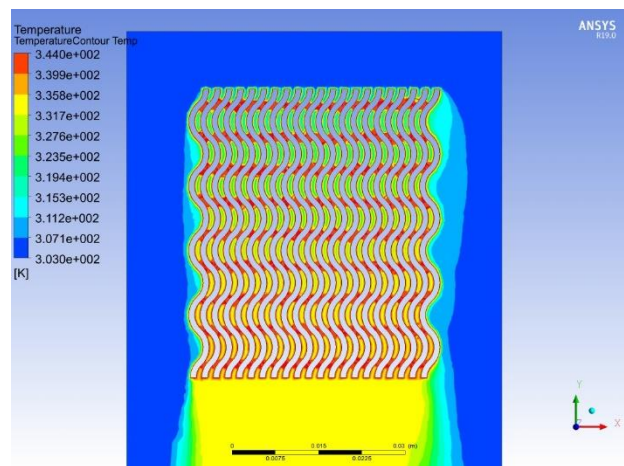
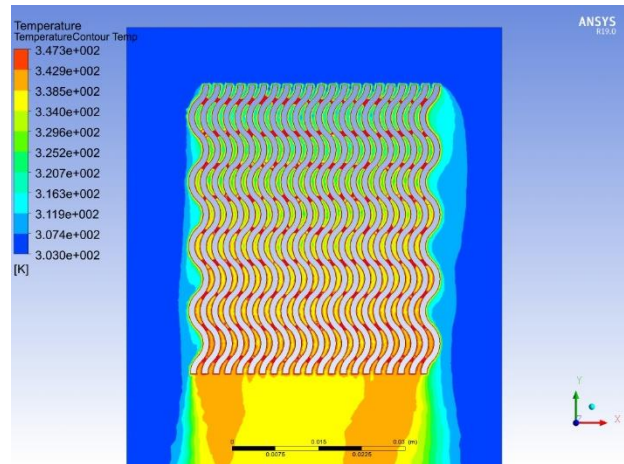


Figure 4: Graphical representation of the pressure variation at the entry, mid and exit of the heat sink



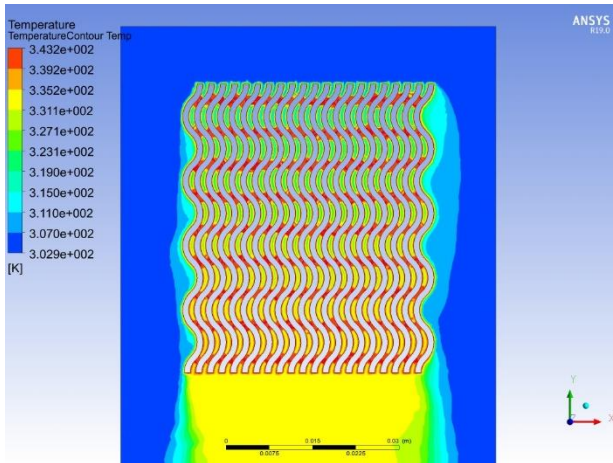


Figure 5: Contour plot representing the temperature variation along the length of the heat sink

Figure 5 represents the temperature variation in the fluid due to the interaction between the fluid and the heat sink. The temperature of the fluid is low initially but increases towards the exit indicating a high heat transfer rate. There are regions of high temperature within the heat sink cavity which is due to the smaller cross section area between the fins. The temperature of the fluid tends towards a stable value towards the exit of the heat sink. Figure 6 gives the graphical representation of the fluid temperature variation in the heat sink.

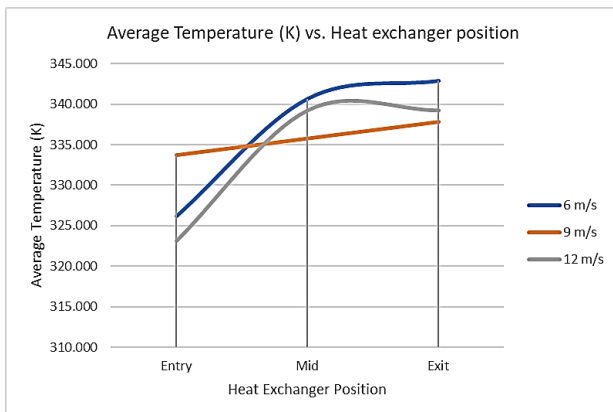


Figure 6: Graphical representation of the temperature variation at the entry, mid and exit of the heat sink

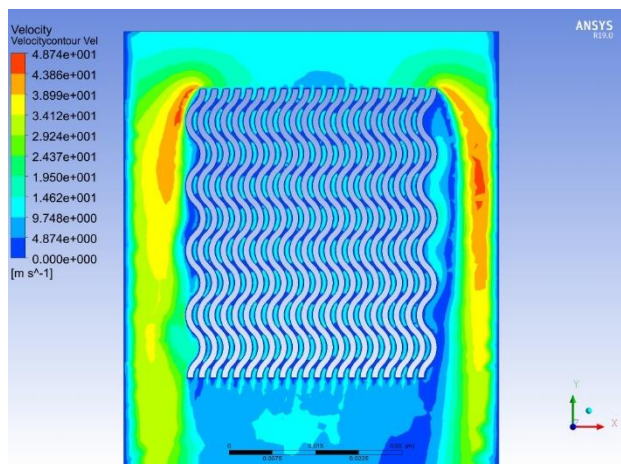
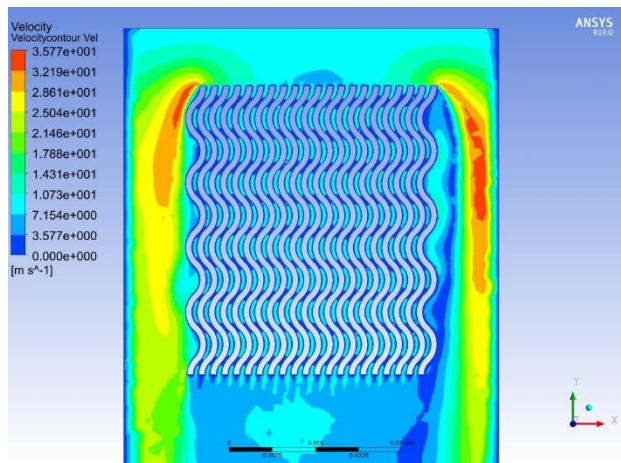
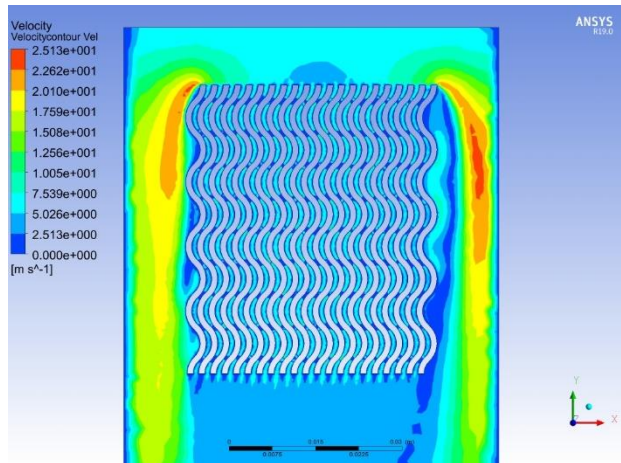


Figure 7: Contour plot representing the velocity variation along the length of the heat sink

Figure 7 gives the change in fluid velocity when the fluid moves between the heat sink fins. The velocity of fluid at the entry to the heat sink is equal to the velocity of the ambient fluid surrounding the system. But the velocity of

the fluid increases due to the nozzle effect between the fins at the smaller cross section regions. The change in velocity is also affected by the heat transfer taking place between the heat sink fins and the fluid. Figure 8 gives the graphical representation of the fluid velocity variation in the heat sink.

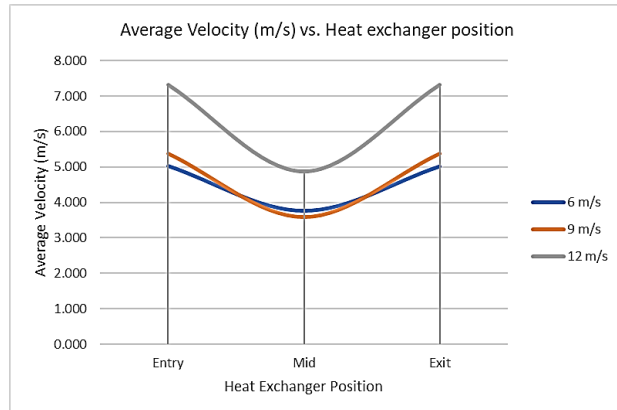


Figure 8: Graphical representation of the pressure variation at the entry, mid and exit of the heat sink

The variation in the surface temperature of the heat sinks are given in figure 9. The graph indicates that the increase in the fluid flow velocity is indirectly proportional to the change in the surface temperature of the heat sink. Higher velocity of the fluid decreases the heat transfer rate of the fluid with less interaction between the fluid and the heat sink. It also shows that the change in temperature reduces achieving a stagnation point when the fluid velocity reaches a certain value.

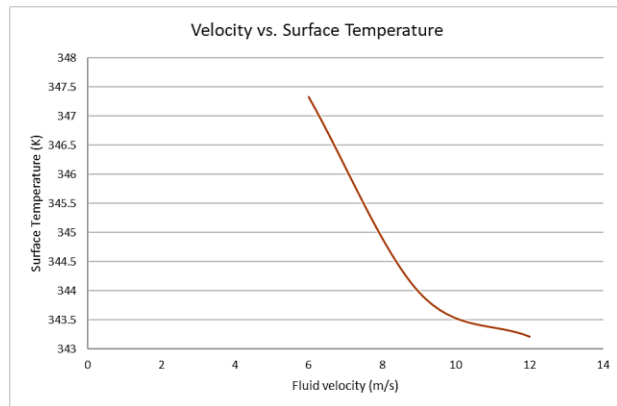


Figure 9: Graphical representation of variation in surface temperature of heat sink with respect of the fluid velocity.

5. CONCLUSIONS

A Fluid dynamics analysis was conducted on a heat sink made of Al-30Cu alloy under different fluid velocities.

The model was created with a wavy fin configuration and the model was surrounded by a fluid domain. The base of the heat sink was attached to a heat source which generates about 50W of heat. These boundary conditions coupled with the varying fluid velocities give us an accurate account of the interaction between the fluid and the heat sink. The objective was to determine the effect of increasing the percentage of copper in the alloy on the heat transfer rate. The results indicate that the increase in the percentage of copper improves the heat carrying capacity of the heat sink but to a small extent. Higher fluid velocities have a higher effect on heat transfer than a large increase in the percentage of the copper in the alloy.

6. REFERENCES

- [1] Mohammad Saraireh, Computational Fluid Dynamics Simulation of Plate Fin and Circular Pin Fin Heat Sinks, Jordan Journal of Mechanical and Industrial Engineering Volume 10 Number 2, June.2016.
- [2] S. Jeevaraj, Heat Transfer Analysis of Heat Sink by Computational Fluid Dynamics (CFD), International Journal on Emerging Technologies (Special Issue on NCRET-2015), 6(2), 2015.
- [3] AgnihotraSarma O, A Ramakrishna, CFD Analysis of Splayed Pin Fin Heat Sink for Electronic Cooling, International Journal of Engineering Research & Technology (IJERT) Vol. 1 Issue 10, December- 2012
- [4] Anuj Kumar, Amit Dhiman, Laszlo Baranyi, CFD analysis of power-law flow and heat transfer around a confined semi-circular cylinder, International Journal of Heat and mass Transfer 82 (2015) 159-169.
- [5] Deepak Gupta, Momin Nausheen, A.D. Dhale, CFD Analysis & Simulation of Pin Fin for Optimum Cooling of MotherBoard, IJEDR, Volume 2, Issue 2, 2014 2321-9939.
- [6] Qu, W. and Mudawar, I. 2002, Experimental and numerical study of pressure drop and heat transfer in a single-phase micro-channel heat sink. International Journal of Heat and Mass Transfer. 45, 2549 – 2565
- [7] T. Therisa, B. Srinivas and A. Ramakrishna, Analysis of Hybrid Structured and Perforated Pin Fin Heat Sink in Inline and Staggered Flow, International Journal of Science Engineering and Advance Technology, IJSEAT, Vol. 2, Issue 4, April-2014
- [8] R. Hagote, S. K. Dahake, Enhancement of Natural Convection Heat Transfer Coefficient by Using V-Fin Array, International Journal of Engineering Research and General Science, Vol-3, Issue-2, April 2015.

- [9] Bhramara P., T. K. K. Reddy, K. Prashanth Reddy, CFD Analysis of Desk Top Heat Sink. Journal of Enhanced Heat Transfer, 15(3) 1–12, 2008.
- [10] Park, Park-Kyoun Oh, Hyo-Jae Lim, The application of the CFD and Kriging method to an optimization of heat sink, International Journal of Heat and Mass Transfer 49 3439–3447, 2006.
- [11] Yue-Tzu Yang, Huan-Sen Peng, Numerical study of pin-fin heat sink with un-uniform fin height design, Int. J. Heat Mass Transfer, 2008, 51 (19-20), pp. 4788-4796.
- [12] Wei, Gaosheng & Huang, Pingrui & Xu, Chao & Liu, Dongyu & Ju, Xing & Du, Xiaoze & Xing, Lijing & Yang, Yongping. (2016). “Thermophysical property measurements and thermal energy storage capacity analysis of aluminum alloys”, Solar Energy, 137. 66-72, 10.1016/j.solener.2016.07.054.

Optimal and Computationally Efficient Priority-Based Routing and Wavelength Allocation Strategy Supporting QoS for High-Speed Transport Networks

^[1]Tarun Gupta, ^[2]Amit Kumar Garg
^[1]Ph.D. Scholar, ^[2]Professor
^{[1][2]}DCRUST University, ECE Department, Haryana, India
^[1]tarungupta2605@gmail.com, ^[2]garg_amit03@yahoo.co.in

Abstract:-- One of major optical network problem is to route and to assign the wavelength efficiently because of its wavelength reuse characteristics and information transparency. By utilizing the trade-off scheme between the blocking probability and setup time of the requested route, priority-based RWA (PRWA) approaches has been studied for WDM networks by introducing a priority criterion which depends on calculation of hop counts and volume of the traffic. The simulation result shows that PRWA technique reduces both the blocking probability (approx. 20%) as compare with non-priority based RWA scheme and the average end to end delay near about (10 msec.) as compare with Adaptive routing (AR) at various traffic load conditions. This approach also results in cost-effectiveness as well as reduction in the complexity of the network in comparison to earlier reported techniques.

Keywords: WDM, Blocking probability, Priority queue, NSFNET, Routing and wavelength assignment.

1.INTRODUCTION

An optical network utilizing the concept of wavelength division multiplexing (WDM) which promises of providing the larger bandwidth demand for various challenging applications by allocating the bulk communication bandwidth of a fiber (approx.50Tb/s) into number of transmission channels with bandwidths (approx.10Gb/s) suitable with the electronic processing speeds of the destination users.

In all optical networks where, optical path is established between the wavelength routing nodes on all the available links is generally referred as Lightpath which is primarily essential for any network architecture and their constructive establishment is important to assign routes to the requested lightpath and to provide wavelengths on all available connections in order to maximize the performance metrics. This is basically the concept of RWA issues [2]. This problem enhances the efficiency of wavelength-routed optical networks where number of users can be adjusted and only a few users require to be rejected during congestion periods by the designed network.

Additionally, efficient assignment of wavelength is equally important in any communication model and it must be assigned in such a way that any two lightpaths which shares the common physical link not to use the same wavelength at any cost [1]. Furthermore, in

networks where conversion of wavelength [9] is absent or ignore, the concept of wavelength continuity constraint comes into the picture where same wavelength must be used for the available connections of the requested light paths.

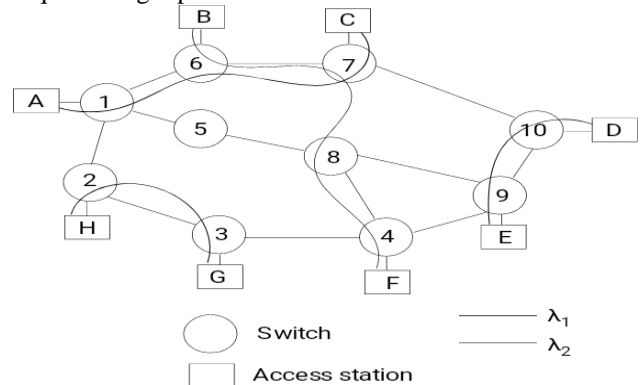


Fig. 1: Wavelength routed WDM network.

The above figure represents the lightpaths establishment between (s-d) pairs by using two different wavelengths in an optical network. Here because of its wavelength continuity constraint, same wavelength must be used on each lightpath on all the available hops from source to destination path. Table 1 shows the lightpaths establishment between all the available s-d pairs.

Table 1: Summary of lightpaths establishment

Source-Destination	Available wavelengths	Established lightpath
A-C	λ_1	A-1-6-7-C
B-F	λ_2	B-6-7-8-4-F
H-G	λ_1	H-2-3-G
D-E	λ_1	D-10-9-E

The fiber link requests (H-G), (D-E) due to its reuse characteristics utilize the same wavelength which has been used by fiber link (A-C) i.e. λ_1 . But the link requests (B-F) uses the other wavelength (λ_2), because (A-C) and (B-F) uses the common link (6-7).

This research discusses most of the possible scenarios of prioritizing the link requests to improve the system performance and in order to achieve, requested lightpath is categorized in several groups based on priority which depends on number of hops count a request requires and capacity of the traffic [4-5]. This paper proposed RWA algorithm priority-based to minimize the blocking ratio and average setup time in the designed topology. The output of proposed PRWA approach than differentiate with the existing NPRWA schemes.

The remaining work is categorized as follows. Related work outlines in section 2. Section 3 proposed PRWA approach and discussed in detail by using some examples. In section 4, outcomes of suggested scheme have been demonstrated. Lastly, concludes the research paper in section 5.

2. RELATED WORK

Currently there are several suggested approaches which have been acquired such as greedy, evolutionary, fuzzy logic to solve the routing and wavelength assignment problem. D. Mishra presented various dynamic routing problems and differentiate it with the outcomes of the existing or similar algorithms where different approaches such as metaheuristic, fuzzy [11] showcase the grade of transmission aware algorithm. Y. Dong et al. [16] modeled a path length-based optimization algorithm assuming physical impairments, traffic grooming functionality and using the metaheuristic approach. Furthermore, Y. Dong et al. [19] discussed routing, wavelength assignment problem by introducing the dynamic functions which highlights path length-based optimization for all optical networks. Presenting the ant-based heuristics, M. Dell' Orco [17] studied discrete time model which estimates the time of travel based on the flow of traffic. In addition, Y.S. Kaviani et al. [20] presented a logical approach where issues related to hop count and RWA propagation delay can be optimized.

Further, D. Sousa [18] discussed other associated RWA problem by using evolutionary, IL programming algorithms.

Two conventional approach of routing and wavelength assignment have been discussed, static and dynamic RWA based on specific scenarios [3]. N. Charbonneau [12] proposed static routing assignment issues by using some heuristics approach. A.G. Rahbar [13] studied a literature review where the more focus given on dynamic impairment schemes. Additionally, the method associated with link characteristic is suggested by ignoring the statistical multiplexing effects which leads to face some crucial application limitations. A.N. Khan [14] studied a routing-based strategy to design or construct the large size networks where more s-d pairs are active parallelly.

To reduce the blocking ratio in all optical network, P. Rajalakshmi et al. [15] proposed a dynamic wavelength-based reassignment algorithms where continuous wavelength route is demanding and in order to fulfill, already established path needs to be reassigned to the other wavelengths which results to serves newer lightpaths for the same network configuration by considering minimal overlap schemes. In the proposed scheme, route for each established lightpath remains the same which means only the wavelength reassignment is performed.

In recent years, idea of prioritization has been integrated with RWA scheme for minimizing the blocking problems on WDM networks. D.M. Shanan et al. [10] proposed an offline wavelength assignment based on priority where each traffic connection has been evaluated at source nodes in respect of the volume of the traffic enters and based on that prioritization of the wavelength can be accomplished. However, this proposed scheme not considering the other parameters like which type of traffic enters and number of hops count it requires and due to this the proposed scheme not met the expectation beyond a certain range.

The significant work accomplished on the existing researches but still few RWA related research seen where one can consider blocking probability and average setup time as a tradeoff approach to suitable with dynamic network state [6]. To overcome the challenges related with transmission speed and quality with the dynamically changed network requests, this paper researches a priority based RWA strategy by adding a value which depends on calculation of hops count and volume of the traffic of the requested connection for wavelength routed networks.

3. PROPOSED PRWA APPROACH

To minimize the blocking probability in optical networks, PRWA scheme suggested where link requests are handled based on the priority order as per RWA approach. The calculation of the priority of each link request depends on the below two scenarios: (i) requested path either connects the s-d pair via direct path or indirect one (ii) capacity of the traffic. Considering these scenarios, higher priority would be given to the link request having direct path requests instead of link requests having indirect path [5]. Once the path is determined whether direct or indirect then the priority of the requests is structured in the descending order as per the volume of traffic and the goal is to minimize the BP and to improve the capacity utilization of a designed optical network.

In absence of wavelength conversion [9], the wavelength continuity constraint concept used where same wavelength must be used on available connections of the requested lightpath, but this may lead to a state where link requests cannot be maturated because of unavailability of the required wavelengths, although the other wavelengths may be available for the designed network at that given point of time. Thus, if the link requests are calculated based on the priority order, blocking of link requests can be minimized to a large extent which enhances the outcomes of the simulated network.

The framework of suggested approach is shown in Fig. 2. First link requests arrive at the edge node of the network based on Poisson process which is random in nature. Then to evaluate their priority position the link requests can be passed through the Priority Queue [5]. Once the priority is assigned, link requests are served within the holding time (tH). Holding time is the average time a request waits in the priority queue before being served. If the request is not maturated within that period, it is considered as a blocked request. To understand the significance of the proposed work along with its brief algorithm are discussed as below.

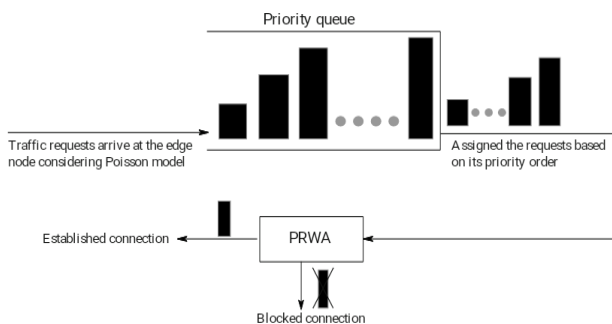


Fig. 2: PRWA Framework

Here, in Fig. 3 constructed a NSFnet topology contains 6 nodes, 9 two-way fibre links and all link consists of wavelengths (λ_1 and λ_2). In Table 2, five lightpath requests considered based on volume of the traffic. Once the algorithm is applied to the designed topology, ordered sets of lightpath requests are formed in two groups (LR1 and LR2) in such a way that LR1 = {lr1,5, lr1,6, lr1,2} and LR2 = {lr1,4, lr1,3}. In Table 3, lightpath request is established based on the priority of the request.

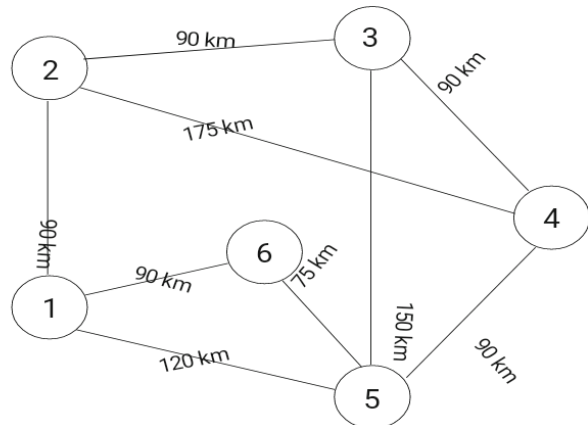


Fig. 3: 6-nodes NSFNET topology

Lightpath requests	Traffic (Kbps)
lr 1,4	1,20,000
lr 1,2	10,000
lr 1,5	1,30,000
lr 1,6	40,000
lr 1,3	1,00,000

Table 2: Lightpath requests vs volume of traffic

Groomed connection requests	Priority order
lr 1,5	1 st
lr 1,6	2 nd
lr 1,2	3 rd
lr 1,4	4 th
lr 1,3	5 th

Table 3: Connection requests vs prioritization

4. PERFORMANCE ANALYSIS

To examine the outcomes of RWA algorithms in respect of BP, considers First-Fit (FF) WA approach as its offers lesser blocking probability and lower evaluation complexity among all existing schemes [1].

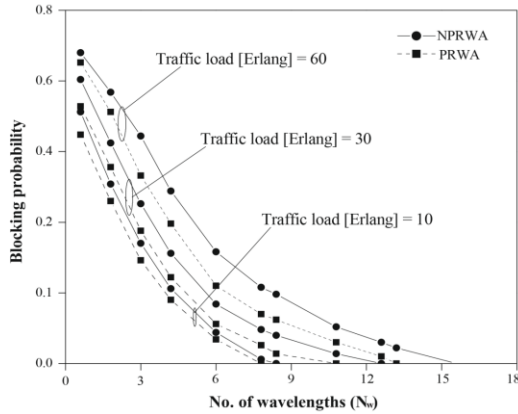


Fig. 4: Blocking probability vs NW on priority and non-priority based schemes by using different traffic load.

Fig. 4 shows BP vs number of wavelengths (NW) considering the Priority and non-priority based RWA approaches for different traffic load by using NSFNET topology. It is clearly seen from the simulation results that by implementing the suggested scheme, there is a reduction appears in BP (approx. 20%) as compare with non-priority based RWA scheme at various traffic load conditions. The result also shows as the traffic load increases, rate of increase in blocking probability is higher.

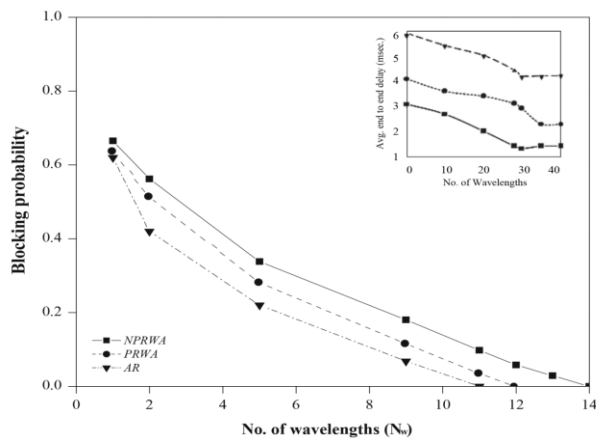


Fig. 5: Blocking probability vs NW on various RWA algorithms in NSFNET topology.

Fig. 5 shows BP versus no. of wavelengths for various RWA algorithms like NPRWA, PRWA, AR (Adaptive Routing) [7-8]. The result reveals that the BP reduces when there is increase in available wavelengths because of more lightpaths have been setup, but in all available algorithms rate of reduction in BP in case of AR is more than other existing routing algorithms and its due to the fact that in this routing algorithm all the best possible

paths are considered between s-d pair based upon the link-state information. Furthermore, simulation result reveals that BP for proposed PRWA is (approx. 20%) less than the existing NPRWA [5] although it's comparatively high in comparison of AR. But on the other hand it can also be observed, on AR higher average setup time (approx. 10msec.) requires as compared to PRWA and other existing algorithms and its mainly due to AR algorithm considers all the best possible paths and as count of the routes increases, average end to end delay increases as well (which is shown in the inner graph of above figure).

5. CONCLUSION

The paper examined priority-based RWA approach to minimize the blocking ratio in all optical networks. The priority-based establishment of lightpath request is evaluated which depends on the fact whether the requested path in between source-destination pair is the single hop link or multi-hop path and secondly the capacity of the requested traffic. Once the priority is assigned, the proposed scheme serves the optical path requests accordingly. The outcome reveals that BP using the proposed approach is less than that of using the non-priority based RWA approach. Adaptive routing (AR) using First-Fit approach provides the better results in respect of BP, but meanwhile setup time requires for AR is much higher in comparison with the discussed scheme. The proposed scheme provides the trade-off between the two-performance metrics which will enhance the overall system productivity in respect of blocking probability and the average end to end delay of the requested route.

REFERENCES

[1] P.H.G. Bezerra, A.J.F. Cardoso, C.R.L. Frances, Performance evaluation of algorithms for wavelength assignment in optical WDM networks, IJCSNS vol. 10, no. 1, pp. 130–136, 2010.
 [2] B.C. Chatterjee, N. Sarma, P.P. Sahu, Review and performance analysis on routing and wavelength assignment approaches for optical networks, IETE Tech. Rev. vol. 30, no. 1, pp. 12–23, 2013.
 [3] Neal Charbonneau. Static Routing and Wavelength Assignment for Multicast Advance Reservation in All-Optical Wavelength-Routed WDM Networks. In IEEE/ACM Transactions on Networking (TON) vol. 20, no. 1, pp. 15-20, 2012.
 [4] H.-P. Schwefel, L. Lipsky, Impact of self-similar On/Off traffic on delay in stationary queuing models, Performance Evaluation, vol. 43, no. 4, pp. 203–221, March 2001.

- [5] B.C. Chatterjee, N. Sharma, P.P. Sahu, A heuristic priority-based wave-length assignment scheme for optical networks, *Optik* vol. 123, no. 17, pp. 1505–1510, 2012.
- [6] D. Banerjee, B. Mukherjee, Wavelength-routed optical networks: Linear formulation, resource budget trade-offs and a reconfiguration study, *IEEE/ACM Transactions on Networking*, vol. 8, no. 9, pp. 598–607, Oct. 2000.
- [7] E. Karasan and E. Ayanoglu, “Effects of Wavelength Routing and Selection Algorithms on Wavelength Conversion Gain in WDM Optical Networks,” *IEEE/ACM Transactions on Networking*, vol. 6, no. 2, pp. 186-193, April 2008.
- [8] Asuman E. Ozdaglar and Dimitri P. Bertsekas Routing and Wavelength Assignment in Optical Networks. In *Networking*, *IEEE/ACM Transactions*, vol. 11, no. 2, pp. 220-230, 2003.
- [9] G Shen, T.H Cheng, S.K Bose, C Lu, T.Y Chai, H.M.M Hosseini. Approximate analysis of limited-range wavelength conversion all-optical WDM networks. In *Computer Communications*; vol. 24, no. 10, pp. 126-130, 2001.
- [10] Shan, D.M., Chua, K.C., Phung, M.H., Mohan, G.: Priority-based offline wavelength assignment in OBS networks. *IEEE Trans. Communications*: vol. 56, no. 10, pp. 1694-1704, 2008.
- [11] D. Mishra and U. Bhanja, “FWM Aware Fuzzy Dynamic Routing and Wavelength Assignment in Transparent Optical Networks”, *International Journal of Electrical, Electronic and Communication Engineering*, vol. 9, issue 8, pp. 981-990, 2015.
- [12] N. Charbonneau and V.M. Vokkarane, “Static Routing and Wavelength Assignment for Multicast Advance Reservation in All-Optical Wavelength-Routed WDM Networks”, *IEEE/ACM TRANSACTIONS ON NETWORKING*, vol. 20, issue 1, pp. 1-14, 2012.
- [13] A.G. Rahbar, “Review of Dynamic Impairment-Aware Routing and Wavelength Assignment Techniques in All-Optical Wavelength Routed Networks”, *IEEE COMMUNICATIONS SURVEYS & TUTORIALS*, vol. 14, issue 4, pp. 1065-1089, 2012.
- [14] A.N. Khan and P. Saengudomlert, “Design based routing and wavelength assignment in WDM networks using link-based multiplexing gain”, *Optical Switching and Networking*, vol. 15, no. 10, pp. 111-120, 2015.
- [15] Rajalakshmi, P., Jhunjhunwala, A. Wavelength reassignment algorithms for all-optical WDM backbone networks. *Opt. Switch. Networks*, vol. 4, no. 3, pp. 147–156, 2007.
- [16] X. Wang, M. Brandt-Pearce, and S. Subramaniam, “Distributed grooming, routing, and path length-based wavelength assignment for dynamic optical networks using ant colony optimization”, *IEEE/OSA Journal of Optical Communications and Networking*, vol. 6, issue 6, pp. 578-589, 2014.
- [17] M. Dell' Orco, M. Marinelli, and M.A. Silgu, “Bee Colony Optimization for innovative travel time estimation, based on a mesoscopic traffic assignment model”, *Transportation Research Part C: Emerging Technologies*, vol. 66, issue 2, pp. 48-60, 2016.
- [18] A. de Sousa, C.B. Lopes, and P. Monteiro, “Lightpath Admission Control in Dynamic Optical Transport Networks”, *Electronic Notes in Discrete Mathematics*, vol. 52, issue 8, pp. 205-212, 2016.
- [19] Y. Dong, S. Zhao, H. dan Ran, Y. Li, and Z. Zhu, “Routing and wavelength assignment in a satellite optical network based on ant colony optimization with the small window strategy”, *IEEE/OSA Journal of Optical Communications and Networking*, vol. 7, issue 10, pp. 995-1000, 2015.
- [20] Y.S. Kavian, A. Rashedi, A. Mahani, and Z. Ghassemlooy, “Routing and wavelength assignment in optical networks using Artificial Bee Colony algorithm”, *Optik - International Journal for Light and Electron Optics*, vol. 124, issue 12, pp. 1243-1249, 2013.

Real Time Communication between Nodes using LoRaWAN for emergency alert in Elevator

^[1] Anupriya, ^[2] Dr. C Rama Krishna, ^[3] Ajay Kumar
^{[1][2][3]} NITTTR Chandigarh
^[1]anupriya1329@gmail.com, ^[2] rkc_97@yahoo.in, ^[3] ajaygodara12@gmail.com

Abstract:-- From the last many decades, elevator is used for transportation of goods or people vertically in downward and upward direction in organization or residential buildings. Due to this, elevator must ensure all the safety standards and requirements before use. In case of power failure, system behaves differently and there is a need to come up with a solution that provides a platform which motivates us to strengthen the system precaution measures to increase the trust of individuals. We provide a solution where a real time communication between end node and Raspberry Pi based gateway via LoRaWAN protocol would take place. End node provides emergency information to the remote control for immediate rescue procedure.

Keywords: LoRaWAN, Internet of thing, safety

Effect of Exhaust Gas Recirculation on combustion and emission characteristics of direct injection - diesel engine fueled with biodiesel: A review

^[1] S.Asha, ^[2] T.suresh

^[1] Department of Mechanical Engineering, college of Engg - Guindy.

^[2] Research Scholar, Department of Mechanical Engineering, Kumaraguru college of Technology. Tamil Nadu India

^[1] suresh.vel40@gmail.com

Abstract:-- In the current scenario, one of the daunting issue the world has been facing immensely is environmental degradation. As there is a gradual depletion of the oil reserves in the recent timeline has created a sense of awareness among the global leaders to combat and develop coping strategies for alternative fuels. India is one of the fastest growing economy that relies greatly on the importation of oil reserves. Among the various fuel resources, diesel poses as the main transportation for India, seeking for a suitable alternative over diesel as there is an urgent need. The interests towards bio-diesel have increased a lot, the main issue in the reduction of NOx emission. Exhaust gas recirculation (EGR) remains effective in reducing NOx exhausted from diesel engines as they reduce flame temperature and oxygen concentration of the combustion chamber. Also, the emission reduction of NOx techniques involving, utilizing fuel for blends of biodiesel-diesel mixtures and EGR method in Compression ignition engine is discussed in detail in this paper. The characteristic emission from various biodiesel-diesel blends also discussed and summarized from EGR method, which is found to be quite efficient. Reduction of NOx emission to over 25-75% from EGR method, as EGR rate ranging within 5-25% optimized from biodiesel fuelled engine. This technique also facilitates towards reducing harmful and highly prone compounds like carbon monoxide, smoke as well as hydrocarbons. This could be achieved via controlling the overall combustion peak in temperature from the combustion chamber as well as from the oxygen content of the fuel. For predominant cases, emissions of NOx are reduced using compromising brake thermal efficiency (BTE) as well as from brake specific fuel consumption (BSFC).

Keywords: Biodiesel, Exhaust gas recirculation (EGR), Engine performance, Exhaust Emission
